Studying the Immunomodulatory Role of Blood Induced *Anopheles* Heme Peroxidase HPX15 and Mosquito Larvicidal Properties of *Agave angustifolia*

THESIS

Submitted in partial fulfillment
of the requirements for the degree of
DOCTOR OF PHILOSOPHY

By

MITHILESH KAJLA

Under the Supervision of

Prof. Sanjeev Kumar

BIRLA INSTITUTE OF TECHNOLOGY AND SCIENCE, PILANI
2016

BIRLA INSTITUTE OF TECHNOLOGY AND SCIENCE, PILANI

CERTIFICATE

This is to certify that the thesis entitled **Studying the Immunomodulatory Role of Blood Induced *Anopheles* Heme Peroxidase HPX15 and Mosquito Larvicidal Properties of *Agave angustifolia*** and submitted by **Mithilesh Kajla** ID No **2009PHXF410P** for award of Ph.D. degree of the institute embodies original work done by her under my supervision.

Signature (Supervisor):

Name (Supervisor) : **SANJEEV KUMAR**

Designation : **Associate Professor, Department of Biological Sciences**

: **Associate Dean, SRCD, BITS-Pilani**

Date:

Dedicated to my Mummy-Papa,
my Husband and my sister Pooja

ACKNOWLEDGEMENTS

First of all I thank GOD, for listening to me in the times of need and showering his blessings to help me achieve my targets.

I would like to pay my gratitude to my Supervisor Prof. Sanjeev Kumar, Associate Professor, Department of Biological sciences, BITS, Pilani and Associate Dean, Sponsored Research and Consulting Division (SRCD), BITS, Pilani. It has been an honor to be his first Ph.D. student. He has taught me, both consciously and unconsciously, how good experimental Vector Biology is done. I appreciate all his contributions of time, ideas, and funding to make my Ph.D. experience productive and stimulating. The joy and enthusiasm he has for his research was contagious and motivational for me, even during tough times in the Ph.D. pursuit. I am also thankful for the excellent example he has provided as a successful Scientist and Professor. I shall forever be indebted to him for guiding me patiently, always understanding my limitations, and yet motivating me to accomplish the goals I set for this study.

I express my gratitude to Prof. Souvik Bhattacharyya, Vice Chancellor, BITS, Pilani

and Prof. V S Rao, Prof. B N Jain and Prof. L K Maheshware, former Vice Chancellor, BITS, Pilani for providing me the very pleasant , enjoyable environment and facilities to pursue PhD.

I also wish to thank Prof. M M S Anand, Registrar, BITS, Pilani, Director: Prof. A. K. Sarkar, BITS, Pilani, G Raghurama, former Director, Prof. Sanjay Kumar Verma, Dean, Academic Research Division (ARD), Prof. S C Sivasubramanian, Dean, Administration Division, Prof. Sanjeev Kumar, Associate Dean, Sponsored Research and Consulting Division (SRCD), Prof. Hemant Kumar Jadav, Associate Dean, Academic Research Division (ARD), Prof. N V Muralidhar Rao, Unit Chief, Centralized Purchases Unit

(CPU), Prof B. K. Rout, Associate Dean , Academic Registration and Counseling (ARCD), Prof. Kumar Neeraj Sachdev, Associate Dean, Student Welfare Division (SWD) for their support and willing guidance extended throughout the research work.

My gratitude is due to Prof. Rajesh Mehrotra, Head of the Department, Department of Biological Sciences, BITS, Pilani for his invaluable suggestions and ever willing support offered to me throughout my study period. I am thankful to former HOD, department of biological sciences, BITS-Pilani Prof. Jitendra Panwar, Prof. Shibashish Choudhary and Prof. A K Das for their support and guidance.

I thank profusely the Doctoral research committee, Prof. Jitendra Panwar, Covenor, Department of Biological Sciences, BITS, Pilani and my DAC members- Prof. Lalita Gupta and Prof. Vishal Saxena, who reviewed the programs periodically and provided useful suggestions. I would like to thank all the faculty members of Department of Biological Sciences, BITS, Pilani Prof. A K Das, Dr. Shibashish Choudhary, Dr. Shilpi Garg, Dr. P. N. Jha, Dr. Sandhya Mehrotra, Dr. Sandhya Marathe, Dr. Pankaj Kumar Sharma, Dr. Sudeshna Mukherjee, Dr. Rajdeep Chowdhary, Dr. Uma S. Dubey, Dr. Vani B., Dr. Ashish Runthala and Dr. Manoj Kannan.

I would also like to thank Dr. Sushil Kumar Yadav, In-charge, Central Animal Facility, BITS, Pilani for providing me animals for my research work.

I would like to acknowledge Prof. S. K. Verma, Dean, and Prof. Hemant R. Jadav, Associate Dean, Academic Research Division, BITS, Pilani for their constant help and advice at all stages of my PhD work. I also thank Mahipal ji and Raghuveer ji, office staff of ARD, BITS Pilani, who rendered a lot of help in organizing various forms of paper work related to my PhD work.

I gratefully acknowledge the funding sources that made my Ph.D. work possible. I was funded by the UGC- BSR fellowship for my PhD tenure. My work was also supported by

the Department of Science and Technology (DST) for research funding and Department of Biotechnology (DBT) for proving International Travel Support.

I am grateful to Dr. Asif Mohmmad, Scientist, ICGEB for providing *Plasmodium berghei*-ANKA strain, Dr. Agam Singh, Scientist, NII, New Delhi for providing *Plasmodium berghei* GFP strain, Dr. Rajnikant Dixit, Scinetist, NIMR, New Delhi for providing S7 primers and Dr. S.K. Gakhar, Vice-Chancellor, Chaudhary Bansi Lal University and his student Dr. Ashwani Kumar for providing *Anopheles culicifacies* strain.

Bioscience office in-charge Mr. Kamlesh Soni, Lab assistant Subhash ji, Ajay ji, and staff Mukesh ji, Naresh ji, Parmeshwar Ji, Manoj, store in-charge Mahendar ji who are highly acknowledged.

I thank my fellow labmates- Parik Kakani, Tania Pal Choudhury, Kuldeep Gupta, Rini Dhawan, Vikas, Pinky, and Tripti for the stimulating discussions, for the sleepless nights we were working together before deadlines, and for all the fun we have had during lab work. I want to thank all lab members.

I would also like to acknowledge my seniors and colleagues of the Department of Biological Sciences, BITS, Pilani, Dr. Deepak Pakalapathi, Dr. Amit Kumar Subudhi, Dr. Naveen Jain, Boopathi PA, Dr. Purva Lohan, Dr. Garima gupta, Dr. Shaifali, Dr. Prakash Kumari, Dr. Sachi Singh, Swarna Kanchan, Senthil, Arpit, Gagan, Isha, Zarna, Gurpreet, Panchsheela, Parva, Divya, Vandana, Manohar, Ramandeep, Jyothi, Rajnish for all their support. I owe my special thanks to Divya, Anya, Naveen, Ujjwal, Kurchi, Yamna, Swati, for their involvement as project students during my research work.

My time at BITS was made enjoyable in large part due to the many friends that became a part of my life, namely Parik Kakani, Tania Pal Choudhury, Dr. Garima Balwani, Dr. Vibhu, Deepali Gupta, Shrikant Sharma Sir, Prashant sir.

Lastly, I would like to thank my family for all their love and encouragement. For my parents, who raised me with a love of science and supported me in all my pursuits. My mother Mrs. Bimla Devi in the first place is the person who put in me the fundamentals of character, showing me the joy of intellectual pursuit ever since my birth. She is the one who sincerely raised me with her caring and gentle love. This thesis would not be possible unless I express my deepest and heartfelt gratitude to my Papa Mr. Madan Singh. He was the person who encouraged me all the time during my PhD tenure. I seek the blessing of my loving grandma who always adored me as her favorite grandchild. I wouldn't have been able to pursue my PhD without the support and loving memories of my sister late Pooja Kajla. I cannot forget mentioning my dear sister Poonam for her immense support, love and affection.

Words fail to express my appreciation to my husband Mr. Vijay Meel for being a loving, supportive, encouraging, and patient husband whose dedication, love and persistent confidence in me, took a major part of my load, off my shoulder. Hence, I would also thank my Mother In-law, Father In-law and other family members for letting me, be a part of their family and providing me mental support time to time.

Finally, I would also like to thank everybody who was important for the successful realization of this thesis, and express my apologies that I could not mention personally one by one.

Thank you.

Mithilesh Kajla,

BITS Pilani

ABSTRACT

Malaria is a major health problem in tropical and subtropical regions of the world. This deadly disease is caused by *Plasmodium,* which completes its asexual cycle in human host and sexual cycle in female *Anopheles* mosquitoes. Several species of *Anopheles* mosquito transmit the human malaria parasite while *A. stephensi* and *A. culicifacies* are major malaria vectors in India.

In order to fight against malaria, several control measures are in progress however, the emergence of drug-resistant parasites and insecticide resistance in mosquito vectors are major hurdles in this area. Alternative malaria control strategies include the blocking of *Plasmodium* development inside the mosquito host and hence termed as transmission blocking approaches. In addition, the control of disease vectors with the help of biological agents or bioproducts is also a newly emerging area.

The transmission blocking approaches demand to understand the molecular interaction of *Plasmodium* with the mosquito immune system and identifying those mosquito molecules that exclusively regulate *Plasmodium* development. Our study, characterized a heme peroxidase HPX15 from Indian malaria vectors, and identified that it plays a crucial role in determining *Plasmodium* development inside the mosquito host. At starting of the study, we obtained partial (1075 bp) as well as full length (1794 bp) clones of *A. stephensi* HPX15 gene. Phylogenetic analysis of these clones revealed that HPX15 orthologs are present in the genome of eighteen worldwide-distributed species of *Anopheles* mosquito including *A. culicifacies* (Indian malaria vector) and *A. gambiae* (African malaria vector). However, HPX15 orthologs are not present in human, nematodes or other related arthropods such as, *Drosophila*, *Aedes* and *Culex* mosquitoes. Interestingly, all the anopheline HPX15 orthologs are highly conserved and share 65-99% amino acids identity. Thus, we defined HPX15 as a unique anopheline lineage-specific and evolutionary conserved heme peroxidase.

The HPX15 ortholog in African malaria vector *A. gambiae* has been reported to perform tyrosine crosslinking of a mucin layer in the midgut. This mucin layer acts like a physical barrier to protect naturally-acquired midgut bacteria and *Plasmodium* against mosquito innate immunity. Silencing of HPX15 gene in *A. gambiae* induced midgut immunity and drastically suppressed *Plasmodium* and bacteria development. Due to the conserved and distinctive nature of HPX15, we proposed that this molecule might be playing a similar role in other anophelines and thus, can be exploited as a common target for designing transmission-blocking strategies.

Our analysis of HPX15 characteristics in *A. stephensi* revealed that the expression of this gene is highly induced in the uninfected blood fed or *Plasmodium* infected midguts. The protein is secreted into the midgut lumen and exhibits other properties similar to *A. gambiae* HPX15. These findings revealed that *A. stephensi* HPX15 is also performing the same function as discussed above in case of *A. gambiae*. Our gene silencing strategies revealed that *A. stephensi* HPX15 modulates midgut immunity against bacteria and *Plasmodium*. We found that midgut Toll and Imd, the classical immune pathways, are induced after the bacterial feeding. However, in the HPX15 silenced midguts, the same bacteria did not induce the classical immune pathways rather it elicited an early induction of nitric oxide synthase (NOS) gene, an effector molecule of STAT pathway and also reported to be the negative regulator of *Plasmodium* development. These findings reveal that in the absence of midgut immune barrier, bacteria manipulate the mosquito midgut immunity and this can be easily explored to regulate the vectorial capacity of *Anopheles* mosquito and controlling *Plasmodium* development and subsequent transmission to the human host.

In addition, the silencing of *A. stephensi* HPX15 also exhibited the expected results on *Plasmodium* development. We found that the number of *Plasmodium* oocysts, a stage of parasite development, was drastically reduced through the activation of nitric oxide synthase (NOS). These findings indicated that the disruption of HPX15 mediated mucin barrier exposes the midgut bacteria or *Plasmodium* to the mosquito innate immunity and thus, this molecule might serve as a universal target to manipulate mosquito immunity and arresting *Plasmodium* development inside the vector host. It will generate new frontiers in the field of malaria research and disease control.

As we mentioned before that the biocontrol of vector population is also a beneficial approach in the field. We identified that the secondary metabolites, called phytoinsectisides, in a xerophytic plant *Agave angustifolia* effectively kills larvae from three major genera of human disease vectors *Aedes*, *Anopheles* and *Culex*. The plant extract exhibited a dose dependent lethality against mosquito larvae. This larvicidal activity of *Agave angustifolia* is heat resistant, modulated by the environmental temperature and independent of the plants vegetative growth. Interestingly, the dry powder of *Agave* also exhibits stronger larvicidal activity, which makes this plant a leading candidate to control mosquito population in nature.

Contents Page No.

List of Figures

Figure No.	Figure Legend	Page No.

Figure No.	Figure Legend	Page No.

Figure No.	Figure Legend	Page No.

List of Tables

Abbreviations

A.	*Anopheles*
HPX	Heme peroxidase
As	*Anopheles stephensi*
Ag	*Anopheles gambiae*
Ac	*Anopheles culicifacies*
PBS	Phosphate buffer saline
FBS	Fetal Bovine serum
PCR	Ploymerase chain reaction
qPCR	Quantative PCR
gDNA	Genomic DNA
cDNA	complementary DNA
mRNA	Messenger RNA
rRNA	Ribosomal RNA
NaCl	Sodium chloride
Tris-Cl	Tris(hydroxylmethyl)aminomethane-Hydrochloride
kDa	Kilo Dalton
AA	Amino acids
bp	Base pair
dsRNA	Double stranded RNA
h	Hours
ul	Micro litre
ug	Micro gram
nl	Nano litre
ng	Nano gram
ml	Milli litre
mM	Milli molar
^{0}C	degree Celsius
RT	Room temperature

Chapter 1

Introduction and Review of Literature

Some portion of this chapter has been published in:

Biochemistry & Physiology: Open Access

Kajla et al., Biochem Physiol 2015, 4:4
http://dx.doi.org/10.4172/2168-9652.1000182

Review Article Open Access

A Fine-Tuned Management between Physiology and Immunity Maintains the Gut Microbiota in Insects

Mithilesh Kajla, Kuldeep Gupta, Lalita Gupta and Sanjeev Kumar*

Molecular Parasitology and Vector Biology Laboratory, Department of Biological Sciences, Birla Institute of Technology and Science (BITS), Pilani Campus, Pilani 333031, Rajasthan, India

1.1 Malaria is a severe vector-borne parasitic disease

Malaria is a vector-borne devastating disease caused by protozoan parasites *Plasmodium,* which is transmitted by the female *Anopheles* mosquito. The disease in humans is caused by four major species of *Plasmodium*; *P. falciparum, P. vivax, P. ovale* and *P. malariae.* Human infections with *P. knowlesi,* a malaria parasite that normally infects monkeys, have also been described in virtually all Southeast Asian countries and the species is now considered as the fifth causal organism for human malaria (White, 2008; Cox-Singh and Singh, 2008). In endemic regions, co-infection of humans with more than one *Plasmodium* species is also reported (Mehlotra et al., 2000).

Malaria got global attention due to the health risks associated with the disease in a large portion of the world. According to the WHO World Malaria Report 2015, 214 million cases of malaria occurred and the disease led to 438,000 deaths world widely. Globally in 97 countries, approximately 3.2 billion people are at risk of being infected with malaria and 1.2 billion are at high risk (>1 in 1000 chance of getting malaria in a year) (**Figure 1.1**). This data indicates the importance of malaria in human health.

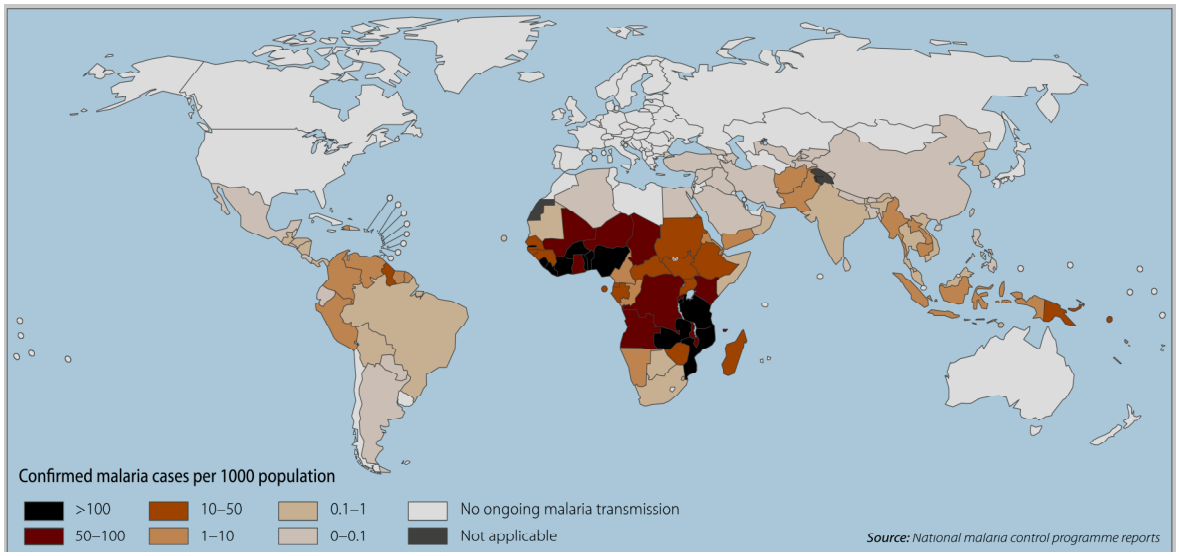

Figure 1.1: Worldwide distribution of malaria (WHO Malaria Report, 2014).

Tropical countries, including India are at the risk of malaria, as well as other vector-borne diseases. Specifically, in India the close vicinity and population density of host and vector augment the chances of malaria transmission and disease endemicity. Malaria is a major health problem in rural as well as tribal areas of the 16 Indian states, including seven northeastern states and nine states of central India (National Vector Borne Disease Control Program, 2014). Malaria endemic areas in India are depicted in **Figure 1.2.**

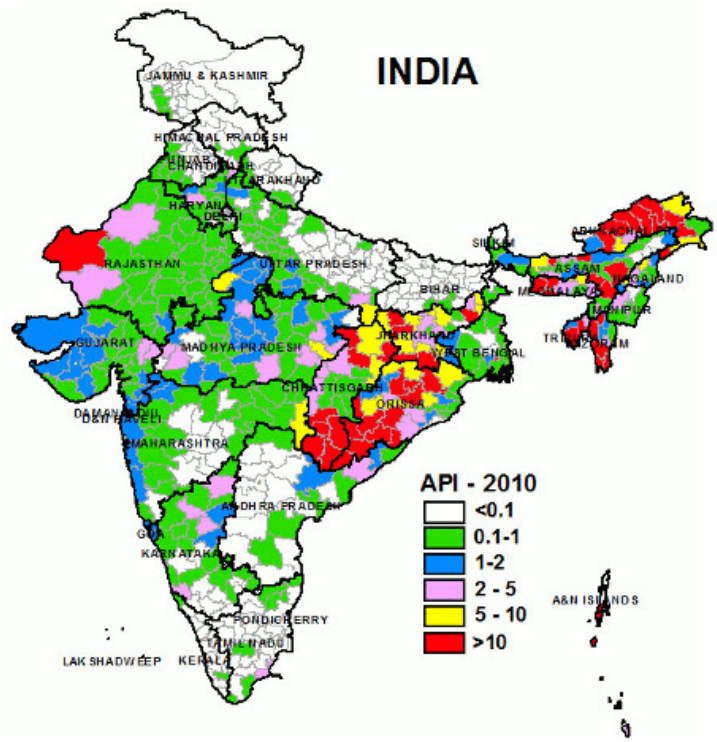

Figure 1.2: Malaria affected areas in India. Annual parasite incidence (API= Total no. of positive slides for parasite in a year x 1000 / Total population) is shown by colored bars. (http://www.malariasite.com/malaria-india).

Plasmodium exhibits a complex life cycle, which alternates between the human host and the *Anopheles* mosquito (**Figure 1.3**). Infection is initiated through the bite of an infected female *Anopheles* mosquito and the release of sporozoites from the salivary gland into the blood stream during feeding (Matuschewski, 2006). The sporozoites are carried by the blood stream to the liver, within half an hour where they invade hepatocytes. In the hepatocytes, the sporozoites begin to multiply asexually and within 6-15 days produce thousands of merozoites that remain inside the host cell vesicles called merosomes. The merozoites are eventually released into the blood circulation where they invade red blood cells (**Figure 1.3**). Inside the RBCs, the parasites replicate mitotically within 48 h and progress through a set of stages such as ring, trophozoite and schizont. The RBC containing mature schizonts burst and release merozoites, which immediately invade new, uninfected red blood cells and the cycle continues leading to the clinical manifestations of the disease. Some of the schizonts are stimulated to release merozoites, which further develop into male and female gametocytes. The mature gametocytes circulate in the human's blood stream and the sexual cycle of *Plasmodium* starts when *Anopheles* mosquito ingests these male and female gametocytes during a blood meal from the malaria infected person.

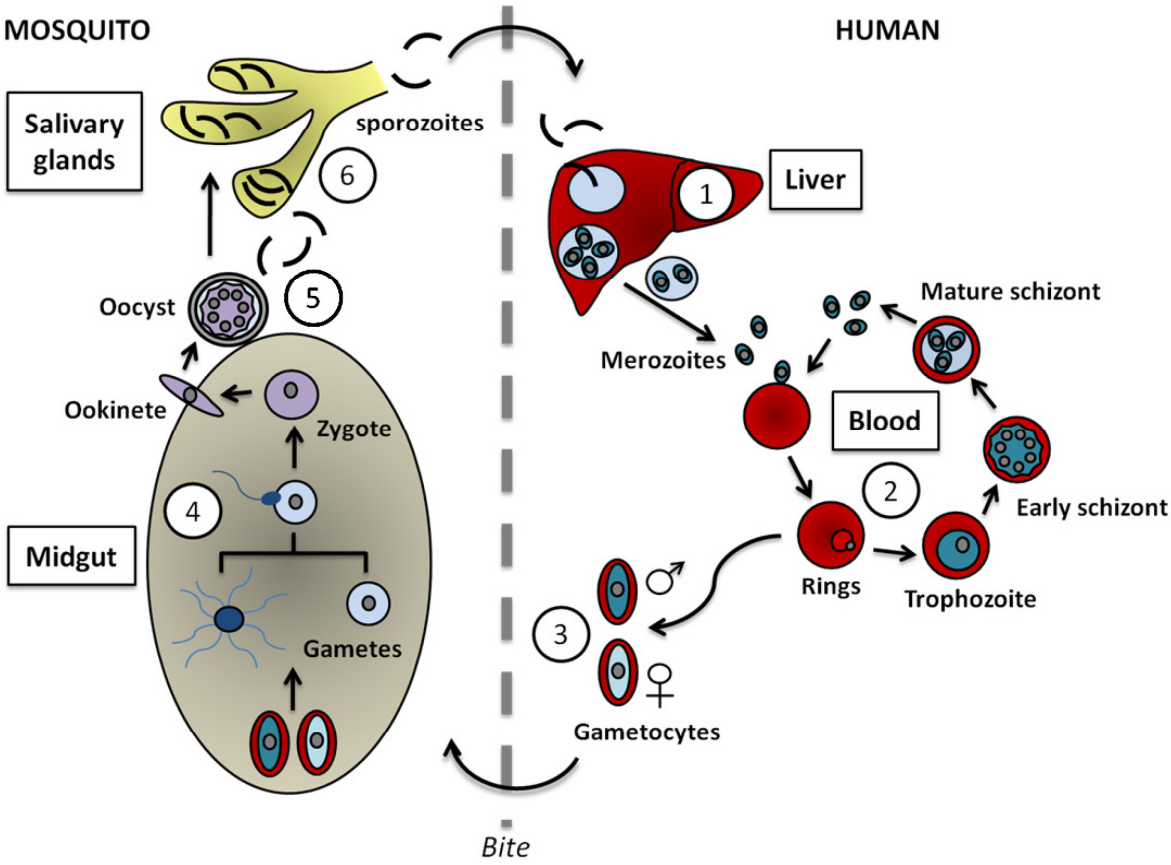

Figure 1.3: The Life cycle of the malaria parasite. The asexual life cycle of *Plasmodium* initiates when an infected female *Anopheles* mosquito bites a human being and injects sporozoites into the blood stream. **1) Liver stage**: These sporozoites then moved towards the liver, in hepatocytes *Plasmodium* starts its pre-erythrocytic cycle and produced number of merozoites. **2) Blood stage**: These merozoites were then released into the blood stream and invaded the RBCs and initiates the erythrocytic cycle. During this merozoites develop into early trophozoites. These trophozoites further develop into schizonts. They are then released from the RBC and immediately infect other RBCs. **3) Gametocyte stage:** in the continuation some of them the trophozoites differentiate into female and male gametocytes. Sexual cycle of *Plasmodium* starts when female *Anopheles* takes blood from infected human, along with blood it ingests mature gametocytes and **4) Mosquito midgut stage**: Soon after the ingestion of mature gametocytes undergo fertilization in the mosquito midgut. The zygote formed, which transforms into the motile ookinete. It traverses the midgut and develops into an oocyst. 5) **Mosquito hemocoel stage**: After maturation Oocyst then releases thousands of sporozoites into the hemocoel. **6) Mosquito salivary gland stage:** Sporozoites migrate to the salivary glands. This infected mosquito is ready to infect the next human host (Aminake and Pradel, 2013).

In the mosquito midgut gametocytes are activated by the drop in body temperature and mosquito derived xanthurenic acid (Billker et al., 1998; Garcia et al., 1998; Kuehn and Pradel, 2010). Gametocyte activation leads to the emergence of gametes from the enveloping erythrocyte (Sologub et al., 2011; Wirth and Pradel, 2012). During gametogenesis, the microgametocyte (male) and macrogametocyte (female) replicates and produces microgametes and macrogametes. The fusion of micro- and macro-gametes forms a zygote within 30 min post blood meal that develops into a

motile ookinete within the next 24 hours. The motile ookinete then traverses the midgut epithelium and settled down between epithelium and basal lamina to form an oocyst (Pradel, 2007). Oocyst matures and produces thousands of sporozoites that are released and invade the mosquito salivary glands. The life cycle of *Plasmodium* is completed when mosquito infects a healthy person following the subsequent blood meal.

1.2 Malaria Vectors and Mosquito life cycle

Female mosquitoes of the genus *Anopheles* are vectors of the malaria parasites. There are approximately 465 *Anopheles* species and approximately 70 of them can spread human malaria (Sinka et al., 2012). These anophelines are worldwide distributed as shown in **Figure 1.4** and transmit different species of *Plasmodium* depending on the region and the local environment (**Figure 1.4**).

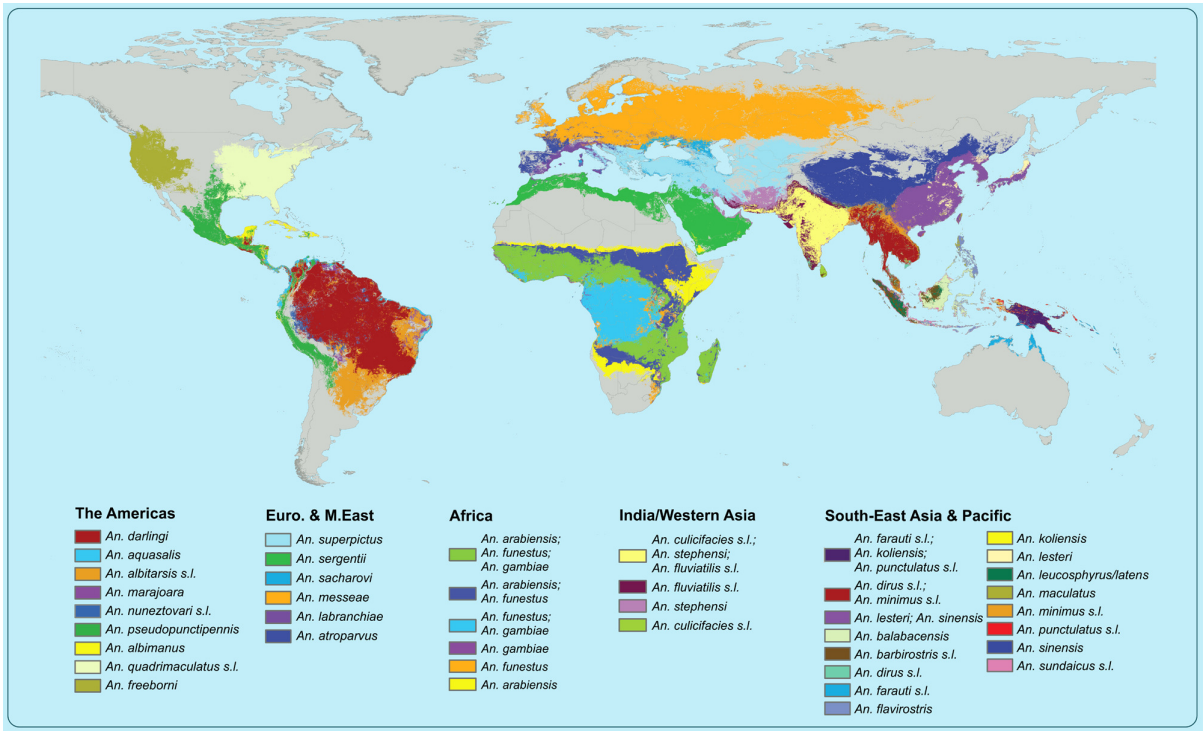

Figure 1.4: Global distribution of dominant malaria vectors (Sinka et al., 2012).

Anopheles gambiae and *Anopheles funestus* are the main vectors in Africa, where 90% of malaria-related deaths occur (Lindh et al., 2005). India is the tropical country, which has suitable climatic conditions to florist numerous mosquito fauna, that's why 58 *Anopheles* mosquito species are found in this region. Among them, *A. culicifacies, A. stephensi, A. fluviatilis, A. minimus, A. dirus* and *A. sundaicus* are Indian malaria vectors (Nagpal and Sharma, 1995). *A. culicifacies* and *A. stephensi* are major vector of rural and urban malaria, respectively (Subbarao, 1998). *A. culicifacies* is reported to have a

complex of five species named as A, B, C, D and E, which are present across India with distinct biological characteristics (Barik et al., 2009). *A. culicifacies* sibling species A, C, D and E are vectors for human malaria while species B is a non-vector (Subbarao et al., 1988). *A. stephensi* does not have species complex, but it is found in three ecological variants such as type form, intermediate form and variety *mysorensis* that were characterized on the basis of their egg morphometrics (Rao et al., 1938; Chakraborty et al., 1998). The 'type form' is an efficient vector of malaria in urban areas due to its anthropophilic (feeds on human host) nature while the '*mysorensis'* form is a poor vector due to its zoophilic nature. The 'intermediate form' is typically recorded in rural and peri-urban localities, and till date, its role in malaria transmission is not known (Chakraborty et al., 1998; Ghosh et al., 2008).

The *Anopheles* mosquito undergoes four main developmental stages during its life cycle, i.e. egg, larva, pupa, and adult (**Figure 1.5**). The first three stages (egg, larva and pupa) are aquatic and take about 5-14 days, for metamorphosis into an adult, depending on the species and the ambient temperature. Eggs are laid on water by females and they further develop into larvae within 2-3 days. *Anopheles* larva has four stages called instars, and then metamorphoses into pupae. At the end of each instar, the larvae molt, by shedding their exoskeleton and grow further. The larvae feed on algae, bacteria, and other microorganisms in the water surface micro layer (Wotton et al., 1997). The pupa then develops into adult within 2-3 days. Male *Anopheles* mosquitoes feed exclusively on sugar sources and therefore do not transmit the disease. Female mosquitoes also feed on sugar from different sources, however, need blood for development of their eggs.

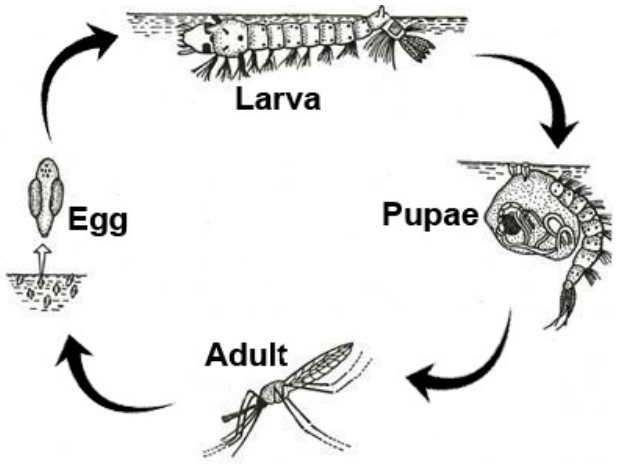

Figure 1.5: Mosquito life cycle (WHO, 1997, Vector Control Methods for Use by Individuals and Communities)

1.3 Malaria control strategies

The world pays a heavy toll to malaria in terms of human health. This warrants attention to develop effective methods for malaria prevention. Several strategies are in progress to control the human cycle of *Plasmodium* such as, synthesis of effective antimalarial

drugs and vaccines development. In addition, to control *Plasmodium* in mosquito host, the application of mosquitocidal compounds or targeting potent immune molecules of the vector are also important to break the life cycle of the parasite.

1.3.1 Limitations of malaria control strategies in human host

To kill *Plasmodium* inside the human host, the synthetic drug chloroquine (CQ) was the first drug of choice since 1950. However, the emergence of CQ resistance in *Plasmodium* reduced the efficacy of this drug and severely affected the initial efforts to control malaria (Payne, 1987). Further, CQ drug was replaced by a first-line drug sulfadoxine/pyrimethamine (SP) however, the resistance against SP also spread worldwide (Roper et al., 2003; Nair et al., 2003). The extensive use of antimalarial drugs leads the parasite to evolve resistance mechanisms (Klein, 2013; White, 2004). For successful elimination of malaria, it is necessary to stop the development of antimalarial drug resistance and therefore, WHO recommended the use of artemisinin-based combination therapies (ACTs). Moreover, in recent scenario the resistance against ACTs is also reported in Southeast Asia (Dondorp et al., 2009; Noedl et al., 2010; Phyo et al., 2012). In conclusion, presently there is no new drug against malaria that entered a phase II clinical trial and it might take more time before another potent drug is finally approved.

Currently no commercial vaccine for malaria is in the market, but RTS,S/AS01 is the most advanced malaria vaccine candidate that has undergone large-scale phase 3 evaluation in Africa. The RTS,S/AS01 malaria vaccine, which blocks the pre-erythrocytic (PE) stage of *P. falciparum*, induces humoral and cellular immune responses against the circumsporozoite (CS) protein present on the surface of sporozoites and liver stage schizonts (The RTS,S, 2014). This vaccine is effective with low efficacy (30–50%) and provides protection for up to 45 months, as demonstrated in a trial in Mozambique children in the 1–4 year old age bracket. The RTS,S vaccine shows encouraging results, but there is a need to improve the vaccine's efficacy, either by modifying adjuvant or combining it with new antigens. Thus, further research is demanded to develop better vaccines against *Plasmodium.*

There is the need to develop new strategies aimed to eradicate malaria. There is a demand to focus on developing vaccines, which target different developmental stages of *Plasmodium* life cycle, including transmission-blocking (TB) vaccines (TBVs). TBV can block the sexual stages of parasite development in the mosquito midgut, thus it will

lead to reduce the burden of disease and transmission among human population (Butler, 2009).

1.3.2 Malaria control strategies in vector

To control vector, global malaria eradication campaign of WHO (launched in 1955) executed, a plan to eradicate malaria in 10–15 years with the indoor residual spraying (IRS) of dichloro diphenyl trichloroethane (DDT). Later it was not effective due to the development of resistance in > 50 species of anopheline mosquitoes, including many major vectors of malaria (Hemingway and Ranson, 2000). Adverse effect of DDT on human health such as early pregnancy loss, fertility loss, leukemia, pancreatic cancer, breast cancer, neurons developmental shortage, diabetes and its non-biodegradability nature, make it inappropriate as mosquitocidal (Beard, 2006; Chen and Rogan, 2003; Cox et al., 2007; Eriksson and Talts, 2000). The use of non-biodegradable larvicidal is also causing some unfavorable effects like, killing of beneficial organisms and biological accumulation through the food chain that resulted in a negative impact on the ecological systems (Mrema et al., 2013). In addition, the poor human acceptance of insecticide spray and development of insecticide-resistant mosquitoes are also major threats in this area (Kelly-Hope et al., 2008; Yang and Liu, 2013). Secondary metabolites from plants (called natural phyto-mosquitocides) are better alternates for controlling mosquito populations. These metabolites are easily obtained at reasonable cost and their intrinsic biodegradable nature makes them the best suitable for this purpose (Ghosh et al., 2012).

Another strategy to regulate malaria is to block the development of *Plasmodium* inside the mosquito vector and therefore, called transmission blocking vaccine (TBV). For that, *Plasmodium*- or mosquito target-specific antibodies are developed in the human host and these antibodies suppress parasite development inside the mosquito when ingested with the infected blood meal. The antigens such as Pfs230, Pfs48/45 and Pfs25/Pfs28 present on the surface of the different stages of *Plasmodium* development in the mosquito have been successfully targeted through transmission blocking vaccines (Farrance et al., 2011; Pradel, 2007). However, this area further needs to understand the details of immune interactions between *Plasmodium* and mosquito immunity.

1.4 Immune regulation of *Plasmodium* in mosquito

The malaria parasite, during its life cycle within *Anopheles* suffers severe losses (**Figure 1.6**). It may be as a result of parasite exposure to the innate immune defense of the vector. Mosquitoes, like other insects, are known to mount potent immune responses against invading bacteria, fungi, viruses and parasites (Lehane et al., 2004). Several evidences suggest that the mosquito is able to trigger a series of diverse defense

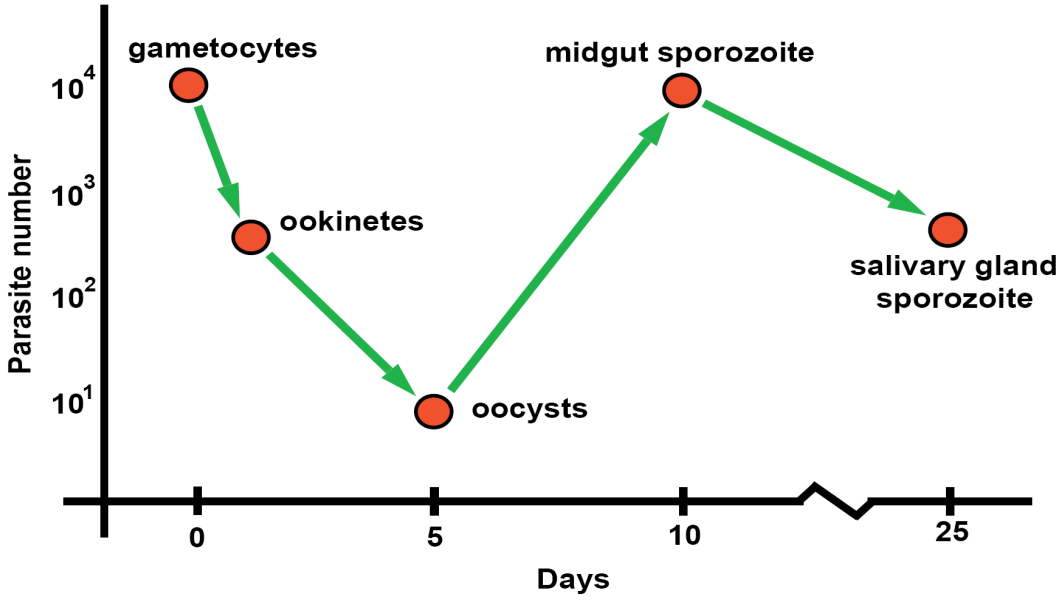

Figure 1.6: Parasite losses in the mosquito vector. The number of parasites successfully completing the sporogonic cycle is considerably affected by the host midgut environment. Parasite losses are often attributed to the mosquito defense mechanisms (Sinden, 1999).

reactions upon *Plasmodium* infection. These defense mechanisms are believed to account for the reduction of the parasite number.

1.4.1 Mosquito immune molecules and signaling pathways

Mosquitoes have innate immune defense. Innate immune molecules are rapidly active after encountering pathogens and have specificity against a particular immune elicitor. Studies carried out in African malaria vector *A. gambiae* revealed that the activation of innate immune molecules is mainly regulated by Toll, Immune Deficiency (Imd) and Janus kinase (JAK)-signal transducer and activator of transcription (STAT) pathways (Christophides et al., 2002; Meister et al., 2005; Lemaitre et al., 1996). The Toll pathway is primarily activated by Gram-positive bacteria, fungi, and viruses (Michel et al., 2001; Ramirez and Dimopoulos, 2010). The Imd (Immune deficiency) pathway is elicited by Gram-negative bacteria and *Plasmodium* (Lemaitre et al., 1995).

The recognition of pathogen-associated molecular patterns (PAMPs) activates the Toll and Imd pathways which lead to the nuclear translocation of the NF-κB

transcription factors Rel1 and Rel2, respectively. The negative regulators of these transcription factors in the cytoplasm are Cactus and Caspar, respectively. The activation of Toll and Imd pathways induce the transcription of numerous immune effector genes such as, Attacin, Cecropin, Defensin and Gambicin that are collectively known as antimicrobial peptides (AMPs) (Luna et al., 2006). Four AMPs- Attacin, Cecropin, Defensin and Gambicin are effective against Gram-positive as well as Gram-negative bacteria, yeast, fungi, and *Plasmodium*. Additionally, Imd pathway regulates a diverse set of anti-*Plasmodium* immune effectors such as APL1, TEP1, LRRD7 (APL2), FBN9, and LRIM1 (Meister et al., 2005; Riehle et al., 2008; Povelones et al., 2009; Blandin et al., 2004; Frolet et al., 2006; Garver et al., 2009 and 2012).

The JAK-STAT pathway mediates immune response against the malaria parasite through transcriptional activation of Nitric Oxide Synthase (NOS) gene, which leads to the production of highly reactive nitric oxide (NO), an antiplasmodial molecule. This pathway is negatively regulated by Suppressor of Cytokine Signaling (SOCS) and Protein Inhibitor of Activated STAT (PIAS) proteins. The transcription of SOCS gene is also induced by the STAT pathway that modulates STAT signaling by preventing STAT phosphorylation, while PIAS inhibits signaling by directly binding to STAT proteins and targeting them for degradation (Agaisse and Perrimon, 2004; Gupta et al., 2009). Previous knockout studies suggested that the JAK-STAT pathway regulates *Plasmodium* development in the African mosquito *A. gambiae* and Brazilian malaria vector *A. aquasalis* (Gupta et al., 2009; Bahia et al., 2011).

Although, gene silencing approaches identified several immune genes that effectively regulate *P. berghei* development, however, these genes are ineffective against human malaria parasites. For example, the silencing of LRIM1 gene in *A. gambiae* increased *P. berghei* infection and has no effect on *P. falciparum* infection. In addition, LRIM1 silencing has no effect in *A. stephensi-P. yoelii* system. This shows the compatibility of mosquitoes' immune system with different *Plasmodium* species (Jaramillo-Gutierrez et al., 2009). TEP1 mediated *P. berghei* lysis but remains ineffective against human malaria parasite *P. falciparum* (strain 3D7, NF54 and GB4) (Molina-Cruz et al., 2012). Thus, it demands the discovery of potential innate immune molecules, which have a broad spectrum of lethality against major species of human malaria parasites.

1.4.2 Role of gut microbial agents in physiology and immunity of mosquito

Natural gut microbiota play an important role in food digestion and nutrition (Dillon and Dillon, 2004). In addition, these endogenous bacteria also regulate the development and maturation of the mosquito gut innate immune system (Pumpuni et al., 1996). In mosquitoes, evidences suggest that bacteria *Serratia* and *Enterobacter* contain hemolytic enzymes and play a role in the blood digestion (Gaio et al., 2011). The bacterial species *Asaia bogorensis* is also found to provide vitamin supplements to *A. stephensi* mosquito (Crotti et al., 2010). The midgut bacteria of insects have been shown to play a vital role in preventing the development of pathogens. The midgut bacteria elicits basal innate immune responses through the expression of numerous anti-microbial peptides (AMPs) and other immune-specific genes that act as antagonist to the *Plasmodium* development and prime the mosquito against infection (Cirimotich et al., 2010). On the other hand, mosquitoes treated with antibiotics, which eliminate the most of the midgut microbiota, were more susceptible to *Plasmodium* infection as they did not show upregulation of these immune genes (Dong et al., 2009). Mosquitoes co-fed with bacteria and *P. falciparum* gametocytes triggered the upregulation of immune responses and resistance to infection. Gram-negative bacteria in *Anopheles* midgut reduced malaria parasite infection (Pumpuni et al., 1993 and 1996; Beier et al., 1994). Another study demonstrated that the conversion of *P. falciparum* ookinetes to oocysts number increased when anti-bacterial antibodies were generated against total midgut lysates (Noden et al., 2011). The mechanism by which midgut bacteria inhibit *Plasmodium* infection has been studied only to a limited extend and it has been suspected that midgut bacteria play a role either directly, by the production of various enzymes and toxins or indirectly by stimulating the mosquito's innate immune system to produce antimicrobial molecules against *Plasmodium* (Pumpuni et al., 1993; Azambuja et al., 2005; Dong et al., 2009). A recent report revealed that the isolation of an *Enterobacter* bacterium from wild mosquitoes in Zambia, and further co-infection of this bacterium in mosquito gut leads to the inhibition of *Plasmodium* development through the production of reactive oxygen species (Cirimotich et al., 2011a).

To maintain a fine balance between normal physiology and immunity, the gut immune system must distinguish commensal and pathogenic bacteria and avoiding the constitutive production of immune effectors, such as antimicrobial peptides (AMPs) and reactive oxygen species (ROS). Mosquitoes midgut synthesizes a peritrophic matrix (PM) in response to blood feeding, which serves as a shield to protect microvilli from

direct contact with ingested food and the abrasion caused by the food particles (Jacobs-Lorena and Oo, 1996). In other words, the PM compartmentalizes the gut environment where the food particles are enclosed by the matrix in endo-peritrophic space and leaving an ecto-peritrophic space between PM and midgut epithelium. Although peritrophic matrix acts like a barrier between the foreign food particles and gut epithelial immunity, however, the soluble elicitors released by the microbes present in the food may interact with the gut epithelium and can induce an immune response (Ahmed et al., 2002). Recent findings from Kumar et al., (2010) in *Anopheles gambiae* mosquitoes identified the presence of another barrier at the luminal surface of the midgut epithelium where mucins are cross-linked with the help of a heme peroxidases HPX15, also called Immunomodulatory peroxidase (IMPer). This barrier further compartmentalizes the ectoperitrophic space and reduces the possibility of interactions between microbial immune elicitors and midgut epithelium. The RNA interference (RNAi) mediated silencing of HPX15 gene induced an array of anti-bacterial immune markers, such as HPX8, cecropin, peptidoglycan recognition protein–S3 (PGRP-S3) and PGRP-LB. These immune genes collectively suppressed the bacterial load in the blood bolus. When the same experiment was carried in HPX15 silenced and antibiotics fed mosquitoes, these antibacterial immune markers were not induced (Kumar et al., 2010).

1.4.3 Role of heme peroxidase in the modulation of midgut immunity

Heme peroxidases are divided into two major families, namely the animal and non-animal heme peroxidases. Non-animal heme peroxidases include plant, bacterial, fungal and protest (Passardi et al., 2007). Animal heme peroxidases are present in vertebrate and invertebrate. In humans have role in antimicrobial and innate immune responses (Dunford, 1999; Klebanoff, 1970 and 1999; Wang and Slungaard, 2006).

A heme peroxidase HPX15 (AGAP013327) from *A. gambiae* has a potent role in modulation of gut immunity (Kumar et al., 2010). HPX15 forms a barrier between blood bolus and midgut epithelial cell by crosslinking tyrosine residue in mucin layer after blood feeding of mosquito *A. gambiae* and lessen the midgut permeability to immune activators, and thus protected the microbiota. This barrier also provides a safe environment for *Plasmodium* to develop in the midgut. After silencing of this gene in *A. gambiae, P. berghei* and *P. falciparum* oocyst number decreased via the induction of NOS, because barrier is broken and immune molecules are in direct contact with immune elicitors to mount an immune response. In this way HPX15 is modulating vector immune response (Kumar et al., 2010).

Gaps in Existing Research

The knowledge of gut immunity and immune active molecules (heme peroxidases) in Indian mosquitoes is least explored. Thus, understanding general mosquito gut immunity in major Indian malaria vectors is a prerequisite to develop malaria transmission blocking strategies. To achieve this goal first we have to identify potent mosquito gut molecules (heme peroxidases) which are specifically exhibiting a dynamic behavior (induction or suppression) in the presence of blood and/or microbial antigens. Further, manipulation of these molecules by using modern methodology will explore their role in the regulation of *Plasmodium* development.

Research Objectives

The objectives of this research work were to isolate, characterize heme peroxidase HPX15 from Indian malaria vector and to understand its role in regulation of *Plasmodium* and other blood-borne antigens. Along with, we also aimed to analyze the larvicidal activity of *Agave angustifolia* plant against mosquitoes.

The proposed research objectives are:

Objective 1: Characterization of blood-induced peroxidase in the mosquito gut epithelium.

Objective 2: To explore the role of blood induced peroxidase in anti-bacterial immunity.

Objective 3: To study the role of blood induced peroxidase in the modulation of gut immunity against *Plasmodium* using RNAi approach.

Objective 4: Biocontrol of human disease vectors.

Chapter 2

Materials and Methods

2.1 Rearing of mosquitoes

Anopheles stephensi, Aedes aegypti and *Culex quinquefaciatus* mosquitoes were reared in insectory at 28℃, 80% relative humidity (RH) and 12h light:dark cycle as described before (Kovendan et al., 2012). Larvae were fed on a 1:1 mixture of dog food (Pet Lover`s crunch milk biscuit, India) and fish food (Gold Tokyo, India). Adult mosquitoes were regularly allowed to take 10% sucrose solution. For colony propagation, four to five days old females were fed on anesthetized mice and their eggs were collected in moist conditions. The hatched larvae were floated in water to continue the life cycle as discussed above. The mice were maintained in the central animal facility and all the procedures were approved by the animal ethics committee. *A. culicifacies* sibling species A was reared in an insectory at Maharshi Dayanand University (MDU), Rohtak under the similar conditions as mentioned above. In addition, for rearing *A. culicifacies* the insectory was also equipped with simulated dusk and dawn system with a 14h light and 10h dark cycle as described before (Adak et al., 1999).

2.2 Designing of primers

2.2.1 Designing of *A. stephensi* heme peroxidase HPX15 degenerate and gene-specific primers

At the start of this study, genome sequences were not available thus, degenerate primers approach was used to clone *A. stephensi* HPX15 (ortholog of *A. gambiae* AgHPX15). Degenerate primers were designed based on the conserved regions of different insect peroxidase proteins as illustrated in **Figure 2.1**.

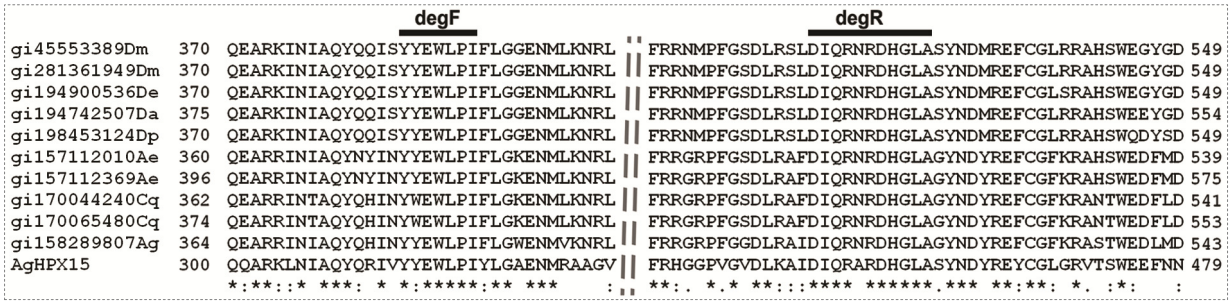

Figure 2.1: Designing of degenerate primers. Peroxidase protein sequences from different insects were aligned and degenerate forward (degF) and reverse (degR) primers were designed from the conserved amino acids regions as represented by thick black bars. The vertically inclined and broken gray bars indicate gaps created in the sequences for presentation purpose. Numbers on left and right sides represent starting and ending amino acids, respectively in the particular protein. gi numbers represent the protein ID. Abbreviation used Dm, *Drosophila melanogaster*; De, *D. erecta*; Da, *D. ananassae*; Dp, *D. pseudoobscura*; Ae, *Aedes aegypti*; Cq, *Culex qunquifaciatus*, Ag, *A. gambiae*.

The sequences of degenerate primers (**Table 2.1**) (5' to 3') were following:

Forward (degF): TACTRBGARTGGYTGCCVATY,

Reverse (degR): GCCARWCCRTGRTCVCGRKYRCGCTG. With the help of above deg primers 428 bp cDNA fragment was cloned (**Figure 3.1A**).

Later on, with the availability of *A. stephensi* genome (taxid: 30069), the AsHPX15 gene sequence was identified in contig 5285 (recently super contig KB665221, Ensembl gene identifier ASTE008179 in annotated genome) based on the nucleotide BLAST with the clone obtained by degenerate primers. The nucleotide sequence of this putative AsHPX15 gene was aligned with the known nucleotide sequence of AgHPX15 to design gene-specific primers AsHPX15 F2-R2 and AsHPX15 F3-R3 as illustrated in **Figure 3.2** (Chapter 3) and their sequences (5' to 3') are shown in **Table 2.1**.

We retrieved a partial cDNA clone of AsHPX15 (GenBank: KP223285) from the contig 5285 (recently super contig KB665221, Ensembl identifier ASTE008179 in annotated genome) of *A. stephensi* genome using HPX15 F3R3 primers as shown in **Table 2.1**. To sequence the full-length AsHPX15 gene, we predicted 1785 bp long cDNA from the contig 5285 with the help of GENSCAN software as before (Burge and Karlin, 1997). We aligned the predicted AsHPX15 cDNA with *A. gambiae* AgHPX15 (AGAP013327) cDNA and designed gene-specific primers F5R5 for full length cloning of the gene (**Figure 4.1A**). In addition, other sets of primer HPX15 F4-R4 (**Figure 4.1A** and **Table 2.1**) were also designed to confirm the identity of full-length clone. For tissue-specific gene expressions HPX15 F2-R2 primer set was used (**Table 2.1**).

2.2.2 Designing of *A. stephensi* gene-specific primers for immune genes and other heme peroxidase

Anopheles stephensi genome sequences were used to design primers for immune genes, Gram Negative bacteria Binding Protein (GNBP), Toll precursor, Gambicin and Thioester containing protein 1 (TEP1) as well as heme peroxidase HPX8 (**Table 2.1**). For GNBP primer designing, *Anopheles gambiae* GNBPB1, GNBPA1 (AGAP004455-PA) and putative GNBP (GenBank ID: AJ001042.1) sequences were used to perform BLAST against the genome sequence of *Anopheles stephensi*. As a result contig 47438 was obtained. This contig was aligned with AgGNBPB1 and putative AgGNBP. Primers were designed from the conserved region using primer 3 software.

Similarly for Toll precursor, *A. gambiae* Toll precursor (Choumet et al., 2007), which has match with Toll 5A, Toll 5B, Toll1A and Toll1B after the nucleotide BLAST with *Anopheles gambiae.* This Toll precursor sequence was used to retrieve *A. stephensi* contig 1897 after nucleotide BLAST with *A. stephensi* genome.

Table 2.1: List of *A. stephensi* primers. The sequences of the primers used to amplify the respective *A. stephensi* gene fragment are provided below.

Primer Set	Primer sequence (5′-3′)	cDNA template (bp)	gDNA template (bp)	Purpose	Referen-ces
DegHPX15 F DegHPX15 R	TACTRBGARTGGYTGCCVATY GCCARWCCRTGRTCVCGRKYRCGC TG	428	499	Cloning, Sequencing	Present study
HPX15 F2 HPX15 R2	GAGAAGCTTCGCACGAGATTA GAATGTCGATTGCTTTCAGGTC	329	400	Real time PCR, Sequencing	Present study
HPX15 F3 HPX15 R3	AGTGCAACAGCTTGCGTACC CCTTTAGTCCATGAGTGTTGTCA	1075	1146	Partial cDNA cloning & sequencing	Present study
HPX15 F4 HPX15 R4	CAAAGGATGATCCCGTTCTG CCGGTCTCCAGCATGTTTTG	530	530	Confirmation of clones & sequencing	Present study
HPX15 F5 HPX15 R5	ATGAAATCTATCGTCGGTTCAC CAAGGCCATCGGTTTAAATTC	1794	1941	To obtain Full length AsHPX15 clone and sequencing	Present study
SOCS F SOCS R	CGTCGTACGTCGTATTGCTC CGGAAGTACAATCGGTCGTT	241	306	Real time PCR	Dhawan et al., 2015
NOS F NOS R	ACATCAAGACGGAAATGGTTG ACAGACGTAGATGTGGGCCTT	250	382	-do-	Luckhart et al., 1998.
GNBP F GNBP R	GAGTTCCAGTGGTACACCAACA CTTCGGCAGCAACCAGAT	333	493	-do-	Present study
Toll prec F Toll prec R	ACCTGTCGGCGAATCCTTGG TCATCCTTGTGCGAGTACGA	358	358	-do-	Present study
Gambicin F Gambicin R	GTGCTGCTCTGTACGGCAGCCG CTTGCAGTCCTCACAGCTATTGAT	344	344	-do-	Present study
TEP1 F TEP1 R	GCTATCAAAATCAGATGCGCTATC ATCACAACCGCATGCTTCA	325	325	-do-	Present study
HPX8 F HPX8 R	GATCCTTTGCCGATGCGCTCAAT CAGTTCGGGCAGTTTATGTCGCAC	381bp	381bp	-do-	Present study
16S rRNA F 16S rRNA R	TCCTACGGGAGGCAGCAGT GGACTACCAGGGTATCTAATCCTGTT	467	467	-do-	Kumar et al., 2010
S7 F S7 R	GGTGTTCGGTTCCAAGGTGA GGTGGTCTGCTGGTTCTTATCC	487	600	PCR internal loading controls	Vijay et al., 2011

A. stephensi contig 1897 was aligned with *A. gambiae* Toll precursor, Toll5A, Toll5B, Toll1A and Toll1B using Clustal Omega and conserved region were chosen to design primer by primer3 software.

To design primers for *A. stephensi* gambicin, Thioester containing protein 1 (TEP1) and HPX8, *Anopheles gambiae* gambicin (GamM957_A), TEP1 (isolate A07-3114) and AgHPX8 (AGAP004038-PA) sequences from NCBI were retrieved and BLAST search was performed against *A. stephensi* genome. Nucleotide BLAST retrieved contig 6775, 5294 and 39256 respectively, for gambicin, TEP1 and HPX8. Obtained contig was aligned with respective retrieved *A. gambiae* gene and primers were designed from conserved region of *A. stephensi* and *A. gambiae* using Primer 3 software. Primer sequences for *A. stephensi* gambicin, TEP1 and HPX8 are shown in **Table 2.1**. Other primers for SOCS, NOS, 16S rRNA and S7 mentioned in **Table 2.1** were retrieved from mentioned references.

2.3 Malaria parasite *Plasmodium berghei* maintenance in lab

P. berghei (ANKA strain) was provided by Prof. Ashif Mohammad, Scientist, ICGEB, New Delhi, India), and a transgenic *P. berghei* PbGFP, expressing GFP at all developmental stages (Franke-Fayard et al., 2004) was a gift from Dr. Agam Prasad Singh, National Institute of Immunology, New Delhi, India. Both the *Plasmodium* strains were maintained in Swiss albino mice following the protocols (Dong et al., 2006; Dhawan et al., 2015). The parasitemia of the infected mice was determined from blood films stained with 1% Giemsa under a light microscope. For blood stage passages, 100-150 µl of blood from an infected mouse (parasitemia ~20%) was intraperitoneal injected into a healthy mouse. Parasitemia in mouse blood was determined and potential infectivity to mosquitoes was established using exflagellation assays as described before (Billker et al., 1997). In brief, 2 µl of tail blood were taken into heparinized pipette tips, immediately mixed with 10 µl of exflagellation buffer pH 8 (10mM Tris-Cl, 150mM NaCl and 10mM Glucose) and 10ul FBS (10%) placed on a microscope slide and covered with cover-slip. Further, observed under microscope. In all the experiments, mice with 5-7% parasitemia and exflagellation 2-3 per field under 40X objective were used for infecting mosquitoes.

2.4 Mosquito tissue collection

2.4.1 Tissue collection from mosquito different developmental stages and body compartments

Different developmental stages of *A. stephensi* such as, eggs, larvae (first to fourth instar), pupae, adult males and females were collected in RNAlater and stored at -80^{o}C. In some experiments *A. stephensi* and *A. culicifacies* females were allowed to feed on

an anesthetized mouse. After 24h of blood feeding, the midgut (Mg) and the rest of the body parts (carcass, CC) were collected from the pool of mosquitoes and stored at -80°C. Sugar fed midgut and carcass were also collected in a similar way that served as controls.

2.4.2 Infection of *A. stephensi* with bacteria and tissue collection

Escherichia coli (MTCC, no. 40) and *Micrococcus luteus* (MTCC no. 106) wild type bacterial strains were obtained from Microbial Type Culture Collection, Institute of Microbial Technology (IMTECH) Chandigarh, India. These two bacterial strains were individually grown in LB media following standard protocols (Gupta et al., 2009). Bacterial growth in LB medium was estimated by reading absorbance of the culture at 600 nm and 1500 µl from each culture (A_{600}=0.5) were mixed and centrifuged for 5 min at 5000 rpm. The supernatant was discarded, and the pellet was washed twice with 1X Ashburner's PBS pH 7.2 (3mM Sodium chloride, 7mM disodium hydrogen phosphate and 3mM sodium dihydrogen phosphate) and resuspended in 3 ml heparinized mouse blood to make the final concentration of 10^9cells/ml (finally $0.5x10^9$ cells of each bacterium per ml blood). *A. stephensi* adult female mosquitoes were allowed to feed on mouse blood supplemented with or without bacterial suspension through an artificial membrane feeder as before (Gupta et al., 2009). After blood feeding the midgut and carcass tissues were collected at different time point from fully engorged control and infected females in a similar way as given above. Sugar fed midguts and carcasses served as controls and were also collected in a similar way.

2.4.3 *P. berghei* infection in *A. stephensi* and tissue collection

Four to five days old and starved female mosquitoes were fed on anesthetized Swiss albino mouse infected with the wild type or GFP expressing *P. berghei.* After feeding the females were maintained at 21℃, which is a permissive temperature for *P. berghei* (Kumar et al., 2010; Dhawan et al., 2015). In some experiments, one day old female mosquitoes were injected with dsRNA and after 4 days were fed on infected mice as above. The adult mosquitoes were starved for 12 h prior to feeding to ensure engorgement. Sugar (SF), normal blood (BF) or *P. berghei* infected blood (Pb) fed midguts were dissected from a pool of mosquitoes (n=10) at different time points of feeding. The dissected midguts or carcass (rest of the body except midgut) were kept in RNAlater solution (Qiagen) and stored at -80℃. Sugar fed midguts and carcasses served as controls and were also collected in a similar way.

2.5 dsRNA synthesis

A 218-bp fragment of the lacZ gene (control) was amplified using the primers (5' to 3') F-GAGTCAGTGAGCGAGGAAGC and R-TATCCGCTCACAATTCCACA and cloned into the pCRII-TOPO vector (Gupta et al., 2010). To prepare dsAsHPX15 RNA, a 428-bp cDNA clone was used as template given chapter 3. This recombinant plasmid already had a T7 promoter site at M13F end. T7 promoter at the other end of fragment was incorporated by amplifying the cloned insert using the following primers: M13F-GTAAAACGACGGCCAGT and T7-M13R-CTCGAGTAATACGACTCACTATAGGGCAG GAAACAGCTATGAC. PCR amplification was carried out with 94℃ for 5 min, 40 cycles at 94℃ for 30 s, 55℃ for 30 s, 72℃ for 30 s and 72℃ for 10 min using M13 F and T7-M13R primers. Amplicons were extracted from gel with the QIA quick Gel Extraction Kit (cat no 28704, Qiagen, Valencia, CA, USA). PCR-purified amplicons tailed with T7 promoter sequences were used to synthesize dsRNAs (In vitro transcription) with the MEGAscript kit (Cat No. AM1626, Ambion, Austin). dsRNA was further purified using a Microcon YM-100 filter (Millipore) and finally concentrated to 3 µg/µl in DNase and RNase free water.

2.6 Effect of gene silencing on midgut bacteria

One to two days old female mosquitoes were injected with 69 nl of 3 µg/µl dsAsHPX15 (207 ng/mosquito) RNA into their thoraxes using a nanojector (Drummond, Broomall, PA, USA). Control mosquitoes were injected with dsLacZ in the same manner. Four days after injection, mosquitoes were allowed to feed on mouse blood supplemented with or without 10^9cells per ml bacteria *(E. coli* and *M. luteus).* Midgut and carcass tissues were collected at different time points as mentioned before. The efficiency of mosquito HPX15 silencing as well as its effect on midgut bacteria was calculated using quantitative PCR.

2.7 Effect of gene silencing on *Plasmodium* development

Female mosquitoes were injected with 69 nl of 3µg/µl dsAsHPX15 (silenced) or dsLacZ (control) RNA into their thoraxes as mentioned above. Four days after injection, mosquitoes were allowed to feed on blood containing *P. berghei* (Transgenic PbGFP) infected mice. The gene silencing efficiency of the method was analyzed in blood fed or *P. berghei* infected midguts through qPCR against the respective controls. Further to evaluate the effect of gene silencing on *Plasmodium* development, the females were fed

on a transgenic GFP-*P. berghei* infected mice four days post injection. The number of oocysts per midgut was determined after seven days post infection. For that, midguts were dissected in Ashburner's PBS (3mM Sodium chloride, 7mM disodium hydrogen phosphate and 3mM sodium dihydrogen phosphate PH 7.2), fixed for 15 min with 4% formaldehyde, washed thrice in PBS and mounted on glass slides in Vectashield mounting medium. The numbers of green fluorescent oocysts were counted in each midgut under a fluorescent microscope (Olympus).

2.8 RNA isolation and cDNA preparation

Total RNA was isolated from above mentioned tissue samples using RNAeasy mini kit from Qiagen (Cat no. 74104) with slight modification, 30 µl β-mercaptoethanol (2-ME) per 1 ml RLT buffer. First-strand cDNA was synthesized using Quantitech reverse transcription kit (Qiagen Cat no. 205311) following manufacturer's instructions.

2.9 PCR amplification, cloning and sequencing of AsHPX15 and AcHPX15 heme peroxidases

RT-PCR was performed with midgut and carcass cDNA of *A. stephensi* using above mentioned degHPX15 primers (**Table 2.1**). PCR with degenerate primers followed the first cycle at 94^{o}C for 3 min, 55^{o}C for 1 min, 72^{o}C for 3 min, 94^{o}C for 1 min, 42^{o}C for 1 min, 72^{o}C for 3 min. Then another cycle at 94^{o}C for 1 min, 52^{o}C for 1 min, 72^{o}C for 3 min was repeated 34 times with a final extension at 72^{o}C for 10 min. The resulting PCR product (428 bp, **Figure 3.1A** chapter 3) with degenerate primers was cloned into PCR2.1-TOPO TA vector (Invitrogen). The clone was sequenced in an automated sequencer at the commercial sequencing facility. The sequence identity was confirmed through Mega BLAST against the nucleotide sequence database at NCBI. Further, this degenerate clone nucleotide sequence was used to do BLAST against *A. stephensi* genome to identify AsHPX15 putative gene as discussed above.

The primer set HPX15F3R3 amplified ~1.1 kb PCR product from *A. stephensi or A. culicifacies* midgut cDNA templates and we termed them AsHPX15 and AcHPX15, respectively (**Figures 3.1B** and **3.1C** Chapter 3). Further, the sequence identity of AsHPX15 and AcHPX15 was confirmed and submitted to NCBI GenBank. The sequence accession numbers [GenBank: KP223285] for *A. stephensi* AsHPX15 and [GenBank: KP299257] for *A. culicifacies* AcHPX15 were obtained. The primer set F2R2 was used to confirm the identity of all these clones through PCR.

Twenty four hour blood fed *A. stephensi* female midgut cDNA templates were PCR amplified using AsHPX15 F5R5 primers set to get full length AsHPX15 clone. The PCR was initiated at 95°C for 5 min and then followed by 35 cycles at 95°C for 50 sec, 57°C for 50 sec and 72°C for 2 min. The final extension was carried at 72°C for 10 min. The PCR product was purified and sequenced in an automated sequencer at Eurofins genomics (www.eurofinsgenomics.eu). Due to the longer size of AsHPX15 full-length clone, different sets of primers (AsHPX15 F2R2, F4R4 and F5R5) were used for sequencing purpose (as mentioned in **Figure 4.1A** and **Table 2.1**). The sequence identity of full-length AsHPX15 cDNA clone was confirmed through Mega BLAST against the nucleotide sequences database and submitted to NCBI [GenBank: KT825861].

2.10 Analysis of conserved domains in AsHPX15 and AcHPX15 sequences

Signature domains in cloned AsHPX15 and AcHPX15 were identified using the Conserved Domain Database (CDD) search tool available online at NCBI (Marchler-Bauer et al., 2015). These results were validated after comparing them to the CDD results of *A. gambiae* heme peroxidase AgHPX15 and other anopheline peroxidases.

2.11 Selection of heme peroxidases for phylogenetic analysis and phylogenetic tree construction

The evolutionary relationship of cloned anopheline peroxidases (AsHPX15 and AcHPX15) was analyzed with selected 74 heme peroxidase protein sequences from various organisms (as shown in Chapter 3, **Table 3.1**). These sequences were downloaded from NCBI and VectorBase databases and their overhanging sequences were trimmed based on the predicted protein of AsHPX15 clone. Importantly, for these analyses, we selected heme peroxidase protein sequences from blood feeding (*Pediculus humanus, Aedes aegypti, A. gambiae* and *Culex quinquefasciatus*) as well as non blood feeding (*Tribolium castaneum, Apis mellifera* and *Drosophila melanogaster*) arthropods. In addition, *Caenorhabditis elegans, Arabidopsis thaliana* and *Homo sapiens* heme peroxidases were also included to understand their phylogenetic relationship and advancements during evolution. In some analyses, we also included non heme peroxidase protein sequences from *A. gambiae* (Chapter 3, **Table 3.1**).

To retrieve putative HPX15 peroxidases from additional 16 different anophelines, we performed BLAST of AsHPX15 clone against their (anopheline species) whole genome shotgun (WGS) sequences available at NCBI. The contig with best match was obtained and aligned with AsHPX15 clone by Clustal Omega algorithm to trim the overhanging regions. The predicted proteins for these trimmed sequences are mentioned in **Table 3.2** (Chapter 3). Peroxidases from other organisms were also trimmed in the same way. The phylogenetic tree was constructed using the full length or trimmed protein sequences of these peroxidases. The tree topology was same for full length as well as trimmed sequences thus, the results with trimmed sequences are presented.

Phylogenetic trees were constructed from selected peroxidases using the maximum likelihood (ML) and neighbor-joining (NJ) methods implemented in MEGA 5.2 program as described before (Saitou and Nei, 1987). We aligned all selected protein sequences by Clustal W algorithm in the MEGA 5.2 program as before (Tamura et al., 2011). Following criteria were selected for the phylogenetic analysis: 'WAG' option was selected as the model for amino acid substitution as this model best fits to our data. For gaps and missing data, we used 'all sites' option. The ML tree was generated using nearest neighbor interchange (NNI) tree search algorithm. Branching pattern reliability was tested for both ML and NJ tree by 1000 bootstrap replicates. The resulting phylogenetic tree was analyzed based on clusters and nodes formed. Because the topologies of phylogenetic tree obtained by ML and NJ methods were similar, therefore, only the ML tree for respective analyses is presented in this study.

2.12 Expression analysis of AsHPX15 and immune genes in different tissue samples using Real Time PCR

mRNA expression analysis of AsHPX15 and other immune genes were carried out through real time PCR using SYBRgreen supermix in an IQ5 multicolor real-time PCR detection system (Bio-Rad), where ribosomal protein subunit S7 gene was used as internal loading control for normalization as described before (Kumar et al., 2010; Salazar et al., 1993). The primer set HPX15 F2R2 was used and other immune genes primer pairs for q-PCR are mentioned in **Table 2.1**. PCR cycle parameters were an initial denaturation at 95℃ for 5 min, 40 cycles of 20s at 94℃, 30s at 57℃, and 50s at 72℃. Fluorescence readings were taken at 72℃ after each cycle. A final extension at 72℃ for 10 min was completed before deriving a melting curve, to confirm the identity of

PCR product. Fold values were calculated using $^{\Delta\Delta}$Ct method as described before (Livak and Schmittgen, 2001).

2.13 *In silico* analysis of AsHPX15 gene structure

5′ upstream sequences of AsHPX15 gene were analyzed by NNPP2.2 software to decipher the promoter region as mentioned before (Reese et al., 2001). In addition, the putative transcription binding sites in the 5′ regulatory region of this gene were determined by MetInspector and JASPAR software (Cartharius et al., 2005; Mathelier et al., 2013). For this analysis, the transcription binding sites from insect family were selected along with other default parameters. The putative signal peptide sequence at the N-terminal of AsHPX15 protein was predicted using SignalP software (Petersen et al., 2011). Protein 3D structure and putative substrate binding sites were analyzed using Phyre^2 and 3DLigandSite prediction server, respectively, as discussed before (Kelly and Sternberg, 2009; Wass et al., 2010).

2.14 Larvicidal activity of *Agave* leaf extracts

Agave angustifolia plants growing in the University campus (BITS-Pilani), roadsides in the nearby locations (geographical coordinates: 28° 22' 0" North, 75° 36' 0" East) or potted were used in this study (representative plants are shown in **Figure 7.1A** and **7.1B**). This plant is a wild weed and therefore, no permission was required for their usage. *Agave angustifolia* leaves, freshly excised from the plants, were used to prepare extracts in different organic solvents such as, hexane, acetone, ethanol or aqueous solvents as before (Bansal et al., 2012). Briefly, the leaves were washed in water, sliced as shows in **Figure 7.1C** (Chapter 7) and their flesh was finely triturated with the help of a mortal pestle to prepare a thick paste. Fifteen gm of the paste was transferred to a 50 ml centrifuge tube and 30 ml solvent, either acetone, ethanol, hexane or water was added to the paste and mixed properly. The tube was rocked for 2h at room temperature (RT), centrifuged at 2300x*g* for 10 min and debris-free supernatant was collected in a fresh tube.

Twenty five to forty 4th instar larvae of *A. aegypti*, *C. quinquefasciatus* or *A. stephensi* were allowed to float in water cups supplemented with various doses (20, 50, 100, 200 µg/ml) of the leaves extracts that were prepared in either of the solvent. The solvent alone was added in corresponding amounts to the sham treated controls. Percentage mortality of the larvae was calculated in each treatment against their respective controls at the stipulated time (12, 24 and 36h) and represented as mean ±

SD. The LD_{50} value was calculated by the probit analysis method as before (Kovendan et al., 2012). Quantitative measurement of the crude extract was carried after evaporating the solvents in speed vac. Each experiment was performed in triplicates and repeated at least thrice to confirm the findings.

2.15 Effect of environmental conditions on the regulation of larvicidal activity in *Agave* plants

To understand the effect of environmental temperature on induction of larvicidal activity in *Agave angustifolia*, we compared the larvicidal activity in plants those were maintained at different temperatures in semi-natural environments. For that, individually potted *Agave angustifolia* plants were kept at either 37°C or 4°C in plant growth chambers. Except the temperature, all other natural environmental conditions (light intensity ~1000 Lux, humidity 30-50% as present in the open environment at the time of study) for these plants were maintained same. After two days of incubation, the larvicidal activities in their leaf extracts were determined. The plants with similar vegetative growth and growing outside either in cold or hot weather, respectively served as controls for these experiments. Percentage mortality of larvae and statistical significance of the data was calculated as above.

2.16 Larvicidal activity in *Agave* dry leaf powder

For preparation of the dry powder, we took the fresh leaves and determined the larvicidal activity in their aqueous extract as mentioned above. *Agave angustifolia* leaves that exhibited strong larvicidal activity in their aqueous extracts were subjected to sun-, oven- or shade-drying process. The dried leaves were ground in a mixer and stored as powder in moisture-free conditions. After three months of shelf life at room temperature, 15 gm of powder was soaked in 30 ml water for 2h with continuous rocking. The tube was centrifuged at 2300x *g* for 10 min and powder-free supernatant was collected in a fresh tube. The powder-free extract or the powder itself, equivalent to the amount of fresh leaves, was analyzed for larvicidal activity as before. Percentage mortality of larvae and statistical significance of the data was calculated as above.

2.17 Analysis of secondary metabolites

Plant secondary metabolites such as flavonoids, phenols, alkaloids, phlobatannins, steroids, tannins, terpenoids and saponins in *Agave* extract were analyzed as described before (Edeoga et al., 2005). Briefly, the aqueous extracts of the leaves from the plants,

which were growing under different natural or semi natural environmental conditions, were bioassayed for these metabolites. For the resulting product, spectra were read at 400-700 nm. The relative levels of these metabolites are depicted as the absorbance maxima (A) in the visible range.

Analysis of alkaloids. 0.5 ml of aqueous extract was mixed with 1.5 ml of 10% acetic acid in ethanol and allowed to stand for 4h. The mix was filtered and the filtrate was concentrated to one fourth of the original volume (0.5 ml now) in a water bath at 80°C. Further, 0.025 ml of concentrated ammonium hydroxide was added and the orange color product was read in a spectrophotometer as mentioned above.

Analysis of phenols. 0. 2 ml of ammonium hydroxide solution and 0.5 ml of amyl alcohol was added to 0.5 ml of plant aqueous extract. The mixture was kept at room temperature for 30 min to react. The spectra were read for the final greenish-brown colored product as above.

Analysis of steroids. 0.5 ml ethanol was added to 0.5 ml aqueous extract and mixed properly. Further, 0.4 ml H_2S0_4 and then 0.4 ml of acetic anhydride was added with continuous mixing. The end product with greenish-blue color was read.

Analysis of phlobatannins. 0.5 ml aqueous extract was incubated at 80°C with 0.2 ml of 1% aqueous hydrochloric acid for 10 min. The red colored end product was read.

Analysis of flavonoids. 0.4 ml of the diluted ammonia solution was added to 0.5 ml aqueous extract. After mixing, 0.050 ml concentrated H_2S0_4 was added. The end yellowish product was read in spectrophotometer.

Analysis of saponins. 15 ml of 20% aqueous ethanol was added to the 5 gm of leaves paste and incubated at 55℃ for 5h with continuous shaking and after incubation, the mixture was filtered. The residue left after the filtration was re-extracted with 15 ml of 20% ethanol. The combined total filtrate (~30 ml) was reduced to 10 ml in a water bath at 90℃. 5 ml of diethyl ether was added to the concentrated filtrate and vortexed properly. After centrifugation the aqueous layer was separated and 15 ml of n-butanol was added to it. After vortexing it was centrifuged and the n-butanol layer was collected, washed twice with 5 ml of 5% sodium chloride. The butanol was evaporated in oven and the residual saponins were dissolved in methanol to read in a spectrophotometer.

2.18 Statistical analysis of the data

All the data were expressed as mean ± standard deviation. Statistical significance between test and respective controls was analyzed by Student's t-test or one-way ANOVA post Tukey's Multiple Comparison Test using GraphPad Prism 5.0 software

(Motulsky et al., 1999). The data with $P<0.05$ was considered significant. The sigma plot (SigmaPlot 10.0 Systat Software, San Jose, CA) and sigma STAT plus software (StatPlus v5, AnalystSoft Inc. statistical analysis program) were used to prepare graphs and performing the statistical analysis of data, respectively.

Chapter 3

Identification of an *Anopheles* lineage-specific unique heme peroxidase HPX15

The entire work presented in this chapter has been published in the journal *Phylogenetics and Evolutionary Biology*

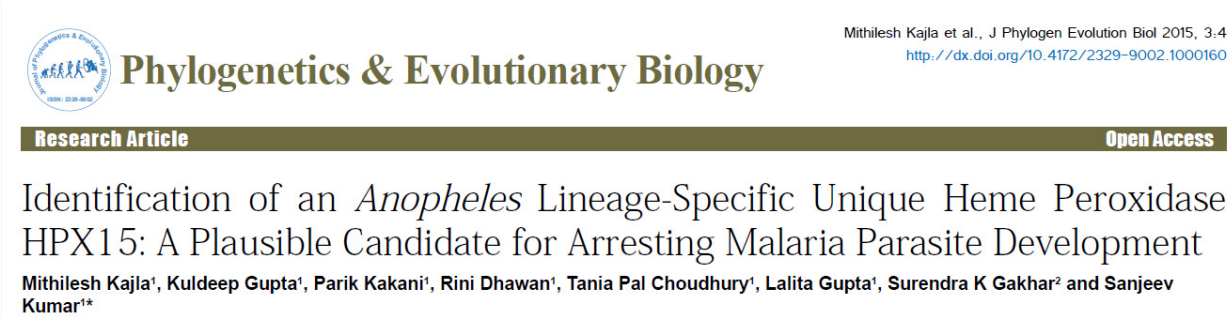

3.1 Abstract

Human malaria parasite *Plasmodium* is transmitted by several species of *Anopheles* mosquitoes. To control malaria, drug-resistant parasites and insecticide resistance in mosquito vectors are major hurdles. Thus, the manipulation of mosquito immunity is one of the ideal way to block *Plasmodium* development inside the insect host. This approach demands the identification of key mosquito molecules that regulate anti-plasmodial immunity. Previous findings revealed that the silencing of *Anopheles gambiae* heme peroxidase 15 (AgHPX15, AGAP013327) induced mosquito innate immunity and drastically suppressed the development of human and rodent malaria parasites. Further, we aimed to characterize HPX15 orthologs in Indian malaria vectors and other worldwide-distributed anophelines to understand the novelty of this molecule as a plausible target to block *Plasmodium* development. AgHPX15 orthologs were cloned from major Indian malaria vectors *A. stephensi* and *A. culicifacies* and their conserve domains were determined by the CDD search tool. The sequence homology and phylogenetic relationship of these clones with other heme peroxidases was analyzed using Mega5.2 software. We found that *A. stephensi* AsHPX15 and *A. culicifacies* AcHPX15 clones are close orthologs of *A. gambiae* AgHPX15. The phylogenetic relationship of these anopheline HPX15 with other animal and plant heme peroxidases revealed that they form a separate lineage-specific cluster and their orthologs are not found in human, nematodes or other related arthropods such as, *Drosophila*, *Aedes* and *Culex* mosquitoes. However, their putative orthologs are present in 16 other globally distributed anophelines and exhibit a highly conserved amino acids identity in the range of 70-99%. Based on these findings, we propose that the anopheline-specific and evolutionary conserved heme peroxidase HPX15 may serve as a unique target for designing transmission-blocking strategies to block *Plasmodium*-mosquito cycle. These findings will generate new frontiers in the field of malaria research and disease control.

3.2 Introduction

Heme peroxidases play an important role in insect development, immunity and are also extensively involved in the evolution and adaption to the environment (Shi et al., 2012). They catalyze tyrosine crosslinking in target proteins and this is a crucial process to stabilize extracellular matrices. This crosslinking is a fundamental feature of basal membranes and essential as an elemental mechanism of tissue biogenesis (Péterfi and Geiszt, 2014). In case of the mosquitoes similar mechanism of peroxidase-mediated

crosslinking is also reported in different organs at various stages of development for example, sclerotization of the cuticle and crosslinking during chorion hardening (Andersen, 2010; Kajla et al., 2015a; Kumar et al., 2010; Li and Li, 2006).

African malaria vector, *A. gambiae* has 18 heme peroxidases (HPXs), which have role in development and immunity in different stages of development and body compartments. Heme peroxidases HPX2 and HPX15 are major regulators of anti-*P. falciparum* immunity in *A. gambiae* (Kumar et al., 2010; Oliveira et al., 2012). *A. gambiae* heme peroxidase named AgHPX15 (AGAP013327) catalyzes protein cross-linking to form a physical barrier on the luminal surface of midgut epithelial cells. This barrier suppresses the recognition of blood bolus antigens by the mosquito immune system. The barrier-based mechanism maintains a 'low immunity' zone in this area to support the growth of endogenous bacteria in the blood fed midguts. *Plasmodium* takes the advantages of this situation to support its own development. Interestingly, the silencing of AgHPX15 gene suppressed the formation of midgut barrier and induced mosquito immunity against bacterial flora and *P. falciparum* (Kumar et al., 2010). Thus, AgHPX15 may be a 'potent candidate' that can be targeted to manipulate mosquito immunity to block *Plasmodium* development. In this study, we characterized AgHPX15 orthologs in major Indian malaria vectors, *A. stephensi* and *A. culicifacies* and analyzed their evolutionary relationships. Our results demonstrate that HPX15 is an *Anopheles* lineage-specific gene and evolutionary conserved among nineteen different species of *Anopheles* mosquitoes. These findings may help us to design common strategies for blocking the transmission of human malaria by targeting a key central molecule that regulates *Plasmodium* development.

3.3 Results

3.3.1 Characterization of AgHPX15 orthologs in *A. stephensi* and *A. culicifacies*

To identify AgHPX15 orthologs in major Indian malaria vectors (*A. stephensi* and *A. culicifacies*), we cloned HPX15 from these mosquito species. At the starting of this study *A. stephensi* genome sequences were not available, thus degenerate primers approach was used to clone HPX15 as discussed in Chapter 2 Materials and Methods and **Figure 2.1**. A PCR product of 428 bp from *A. stephensi* midgut cDNA was cloned and sequenced (**Figure 3.1A**). The nucleotide BLAST results revealed its closest match with *A. gambiae* AgHPX15 (77% identity and E value 6e-84). This clone was named degAsHPX15.

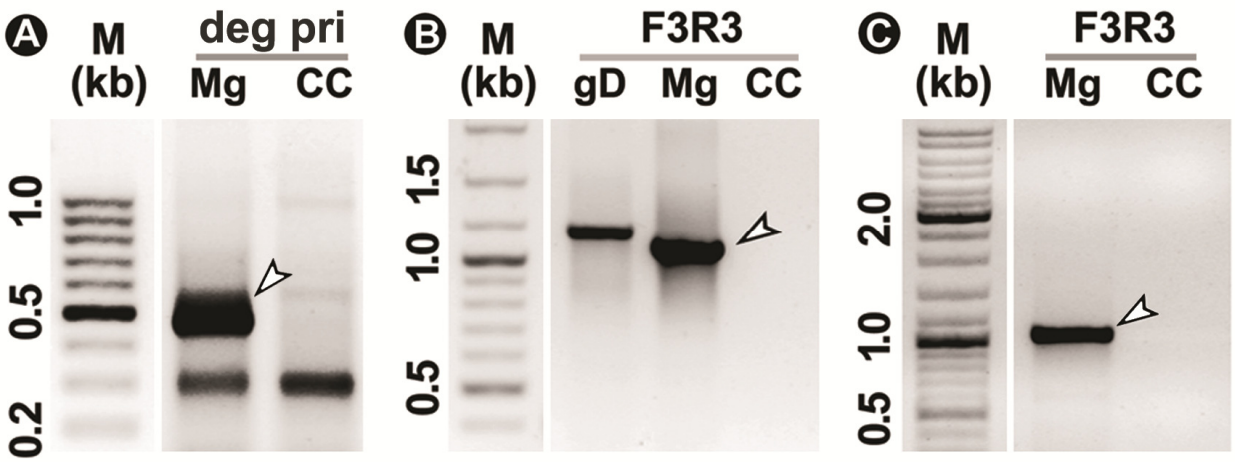

Figure 3.1: Cloning of HPX15 gene from Indian malaria vectors, *A. stephensi* and *A. culicifacies*. A) 24h post blood fed *A. stephensi* midgut (Mg) and carcass (CC) cDNA templates were PCR amplified using degenerate primers (deg pri) as depicted in **Figure 2.1**. These primers amplified a desired product of 428 bp from the midgut (Mg) cDNA. B) PCR amplification of *A. stephensi* midgut (Mg) and carcass (CC) cDNA using gene-specific primers (F3R3) as depicted in Figure 3.2. These primers amplified a single product of ~1100 bp exclusively from Mg cDNA. The genomic DNA (gD) template served as a control for the PCR reactions. C) *A. culicifacies* cDNA templates were PCR amplifies using F3R3 primers. The desired band of ~1100 bp is seen only in Mg cDNA. The leftmost lane in all the cases represents the standard DNA molecular marker (M) reference for identifying the size of amplified DNA fragments. Numbers on the left side indicate standard DNA size in kb. PCR products indicated by arrowheads were used for cloning and sequencing.

Later on the unannotated genome of *A. stephensi* (taxid: 30069) was available at NCBI. The nucleotide BLAST of degAsHPX15 and AgHPX15 against *A. stephensi* genome retrieved contig 5285 (recently super contig KB665221, Ensembl identifier ASTE008179 in annotated genome), which was used to design gene-specific primers (**Figure 3.2**). PCR with F3R3 primers amplified a fragment of ~1100 bp exclusively from *A. stephensi* midgut cDNA and no product was observed when carcass cDNA was used as template (**Figure 3.1B**). PCR with other primers F2R2 amplified a desired (329 bp) product and we used it to confirm the identity of our clones. We further continued with

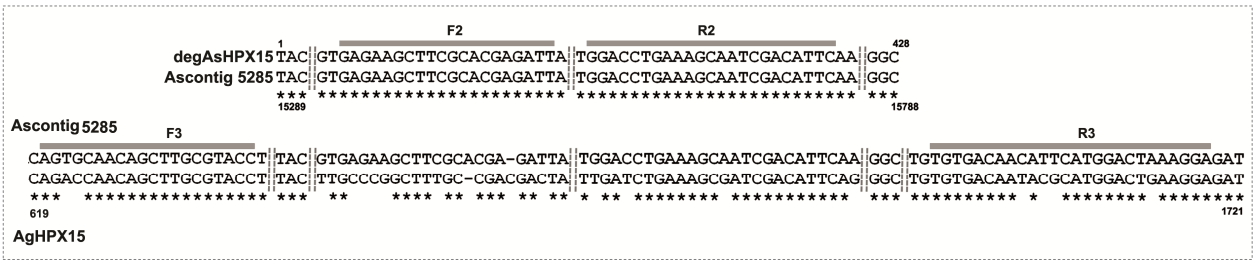

Figure 3.2: Designing of HPX15 gene-specific primers. The nucleotide sequence of *A. stephensi* putative HPX15 contig 5282 (recently super contig KB665221, Ensembl identifier ASTE008179 in annotated genome) was aligned either with the degenerate clone (degAsHPX15) or *A. gambiae* AgHPX15 gene. Primer pairs F2R2 and F3R3 are represented by thick black bars. The numbers on left and right sides indicate the nucleotide positions in the respective sequences. The vertically inclined gray bars indicate gaps created in the sequences for presentation purpose.

the larger (~1100 bp) PCR product obtained by F3R3 primers. This PCR product was sequenced (size 1075 bp), named as AsHPX15 and its sequence was submitted to NCBI [GenBank: KP223285]. The nucleotide or predicted protein BLAST of AsHPX15 identified its closest match to *A. gambiae* AgHPX15. NCBI nucleotide BLAST of obtained sequences disclosed 89% query coverage, 76% identity and E value 3e-168 with *A. gambiae* HPX15 (AgHPX15).

Interestingly, the *A. stephensi* AsHPX15 specific F3R3 primers also amplified a similar size PCR product when *A. culicifacies* midgut cDNA was used as template (**Figure 3.1C**). The obtained clone was named as AcHPX15 and its sequence (1077 bp) was submitted to NCBI [GenBank: KP299257]. NCBI nucleotide BLAST of AcHPX15 sequences revealed first hit as AgHPX15 with 81% query coverage, 77% identity and E value 0.0. Predicted proteins for AcHPX15 and AsHPX15 also have a close orthology to each other (79% identity and 86% similarity). These results revealed that AgHPX15, AsHPX15 and AcHPX15 are identical orthologs.

3.3.2 AgHPX15, AsHPX15 and AcHPX15 have identical domains

To understand details regarding the sequence identity, structure and functional relationships, AgHPX15, AsHPX15 and AcHPX15 proteins were subjected to conserved domain database (CDD) analysis. Results depicted in **Figure 3.3A** revealed that all these peroxidases exhibit characteristics, identity similar to the peroxinectin-like conserved domain of animal heme peroxidases superfamily. Peroxinectins are secreted as cell-adhesive and opsonic arthropod proteins that play crucial role in invertebrate immunity and interact with integrin family of transmembrane receptors (Sritunyalucksana et al., 2001). Human myeloperoxidase (MPO) is also a member of this vast family and interacts with integrins (Hampton et al., 1996; Persson et al., 2001). Animal heme peroxidases and related proteins superfamily contains a diverse group of enzymes, including peroxidases from metazoans and their members are also found in fungi, plants and bacteria (Dunford, 1999; Passardi et al., 2007). We also observed identical binding sites in the conserved domain of these three anopheline peroxidases. These sites are 10 heme binding, 14 putative substrate binding and 2 homodimer interface sites (**Figure 3.3B**).

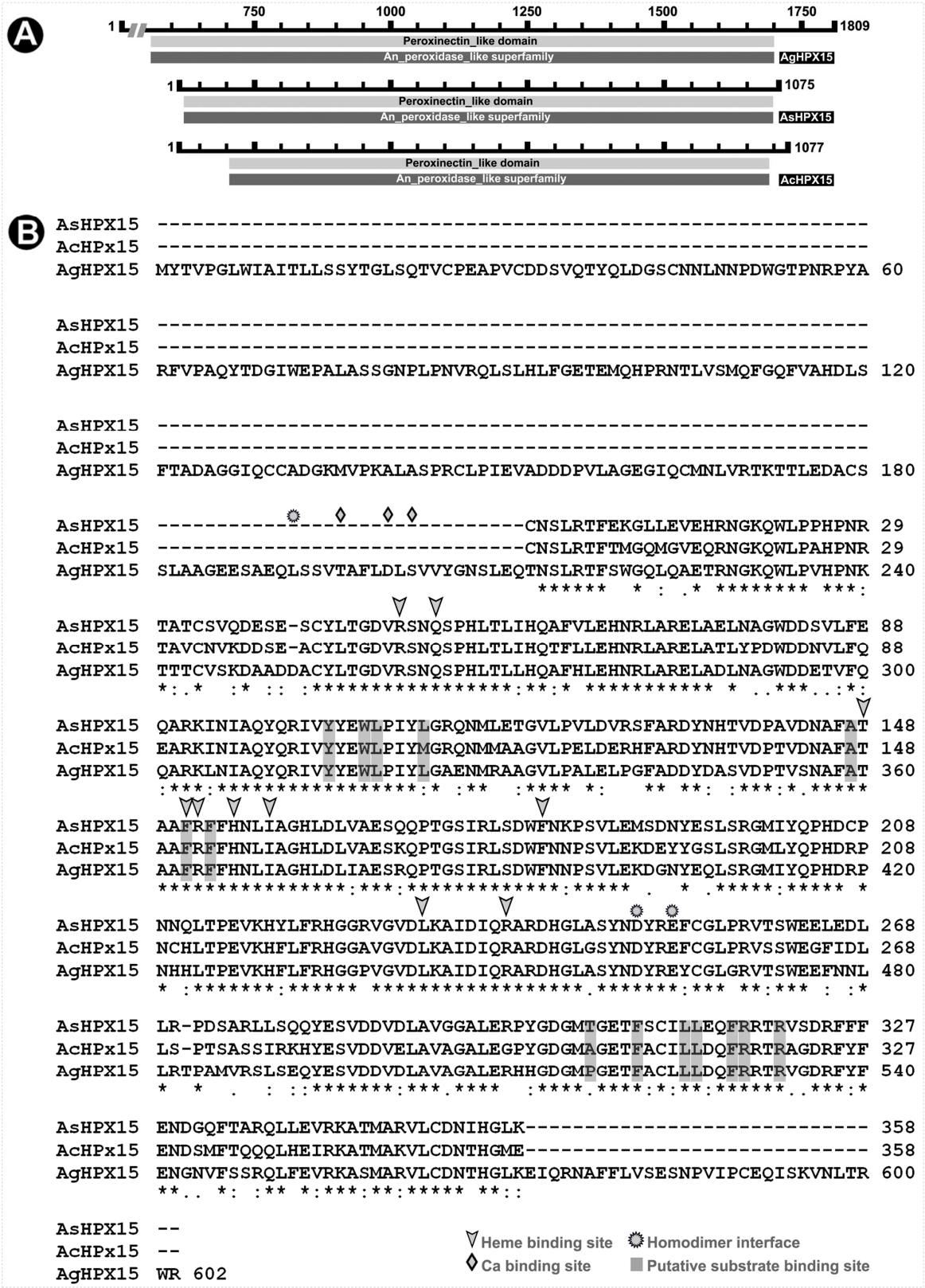

Figure 3.3: Analysis of conserve domains in AgHPX15, AsHPX15 and AcHPX15. A) Signature domains in protein sequences of three heme peroxidases were determined through the Conserved Domain Database (CDD) search tool available online at NCBI. The number scale indicates amino acids in corresponding peroxidase proteins. Thick gray and black bars depict the peroxinectin-like conserved domain and animal heme peroxidases superfamily, respectively. **B)** Numerous CDD predicted binding sites such as heme binding, calcium binding, putative substrate binding and homodimer interface sites are represented by the characteristic symbols in the aligned amino acids sequences of AgHPX15, AsHPX15 and AcHPX15.

3.3.3 HPX15 is a unique anopheline-specific heme peroxidase

The CDD analysis revealed that the domain structure of AgHPX15, AsHPX15 and AcHPX15 is identical and they all are designated heme peroxidases (**Figure 3.3**). In vertebrates and invertebrates heme peroxidases catalyze protein crosslinking, which is generally a crucial process to stabilize the extracellular matrix (Dunford, 1999; Kumar et al., 2010). The basic mechanism of peroxidase-mediated protein crosslinking is evident in *A. gambiae* (Kumar et al., 2010). Thus, we believe that AsHPX15 and AcHPX15 may also demonstrate a similar mechanism in Indian malaria vectors. Therefore, these heme peroxidases were further analyzed to understand their common features.

As we discussed before that the nucleotide and predicted protein general BLAST of AsHPX15 and AcHPX15 revealed *A. gambiae* AgHPX15 as closest match. However, they do not have a considerable match with any peroxidase from other organisms. Thus, we hypothesized that HPX15 is a unique type of heme peroxidase and its orthologs may be present only in the genus *Anopheles*. To understand the novelty of anopheline HPX15 peroxidases, we used WAG model to reconstruct their phylogenetic relationship with other peroxidases as explained in Chapter 2 Material and Methods. For this analysis, we selected heme peroxidases from numerous blood feeding and non blood feeding insects, human and plant (as mentioned in **Table 3.1**).

Results presented in **Figure 3.4** revealed that these peroxidases appear in two major clades. Each clade defines separate lineage for plants and animal heme peroxidases. The clade for animal heme peroxidases is further divided into 11 subclades that are designated based on *A. gambiae* peroxidase representative (this nomenclature was adopted from VectorBase database) in the cluster of that particular subclade. For example, AgHPX4, AgHPX3, AgDBLOX, AgHPX6, AgHPX5, AgHPX7, AgHPX8, AgHPX1, AgHPX16 and AgDUOX (**Figure 3.4**).

Among 16 *A. gambiae* heme peroxidases, AgHPX4 and AgDUOX reveal orthology to a wide range of animal heme peroxidases that include human EPO and MPO and peroxidases from *Caenorhabditis elegans*, mosquitoes and other insects. This shows the ubiquitous nature of these genes that have been conserved during the evolution through lower to higher organisms.

Interestingly, AgHPX3 orthologs are present only in arthropod as well as *C. elegans*. AgHPX1, AgHPX5, AgHPX6, AgHPX7 and AgDBLOX are arthropod-specific

Table 3.1: List of peroxidases from diverse organisms selected for phylogenetic analysis. The heme peroxidases protein sequences for various organisms were obtained from NCBI and Vectorbase databases as mentioned in the Materials and Methods. Each sequence is also represented by its abbreviation in parenthesis, which we used for the phylogenetic analysis. Asterisk (*) indicates the non heme peroxidases from *A. gambiae*.

Organisms name (Abbreviation)	Peroxidase nomenclature	Gene/sequence ID	Amino acids in full length protein	Amino acids in trimmed sequence
A. stephensi (As)	AsHPX15	KP223285	-	358
A. culicifacies (Ac)	AcHPX15	KP299257	-	353
A. gambiae (Ag)	DBLOX	gi/347972907	1381	482
	DUOX	gi/347973195	1000	329
	HPX1	gi/158289807	827	336
	HPX2	gi/158299743	812	353
	HPX3	gi/347970469	1470	335
	HPX4	gi/158286012	1654	328
	HPX5	gi/347963064	749	337
	HPX6	gi/347970011	866	347
	HPX7	gi/347971118	784	474
	HPX8	gi/57619500	767	335
	HPX10	gi/333466682	589	333
	HPX11	gi/347972511	593	332
	HPX12	gi/158289809	1226	335
	HPX14	gi/333469638	605	341
	HPX15	gi/347972481	602	335
	HPX16	gi/347972569	575	424
	* GPXH1	gi/118783685	167	167
	* GPXH2	gi/333467578	59	59
	* GPXH3	gi /58384280	171	171
	* TPX1	gi/119113794	234	234
	* TPX2	gi/58377838	196	196
	* TPX3	gi/158285485	250	250
	* TPX4	gi/116117223	221	221
	* TPX5	gi/58376628	223	223
Aedes aegypti (Ae)	Chorion Peroxidase	gi/166208492	790	333
	DBLOX	gi/403182607	1405	394
	DUOX	gi/403182881	1452	329
	HPX4	gi/403182346	910	328
	HPX5	gi/403183503	748	337
	HPX6	gi/403183282	730	353
	HPX7	gi/403182638	744	326
	HPX8A	gi/403182640	720	436
	HPX8B	gi/403182639	788	362
	HPX1	gi/108878203	683	357
	HPX2	gi/108870372	679	347
	Oxi-peroxidase	gi/108868308	719	357
	Oxi-peroxidase	gi/108878879	770	335
	Peroxinectin	gi/108880850	397	361
	Peroxidasin	gi/108884376	886	328
Culex quinquefaciatus (Cq)	Chorion Peroxidase	gi/170039127	843	343
	Chorion Peroxidase	gi/170043090	775	420
	Chorion Peroxidase	gi/170066961	753	342
	Chorion Peroxidase	gi/170031127	685	323

	DUOX	gi/170033274	1482	466
	Oxi-peroxidase	gi/170044848	1476	398
	Oxi-peroxidase	gi/170052031	1401	394
	Peroxinectin	gi/170043088	747	332
	Peroxidase	gi/170044240	685	358
	Peroxidase	gi/170065480	697	357
	Thyroid Peroxidase	gi/170063064	888	330
Drosophila melnogaster (Dm)	Peroxidase	gi/386765938	649	343
	Peroxidase	gi/24647689	753	336
	Peroxidase	gi/19921482	1394	390
	Peroxidase	gi/24649775	1439	361
	Chorion Peroxidase	gi/290457651	690	336
	DUOX	gi/380865378	1537	335
	Peroxidasin	gi/74871953	1527	329
	Peroxinectin	gi/229462993	809	400
Apis melifera (Ap)	DBLOX	gi/328776732	1448	357
	DUOX	gi/328779750	1483	361
	HPX6	gi/328780340	1401	345
	HPX1	gi/328776817	703	334
	Peroxidasin	gi/66499817	1293	334
	Peroxinectin	gi/328782858	1707	336
Pediculus humanus corporis (Ph)	Chorion Peroxidase	gi/242008911	924	354
	Chorion Peroxidase	gi/242023785	792	337
	DUOX	gi/212514898	1441	398
	Peroxidase	gi/242006324	599	425
	Thyroid Peroxidase	gi/242022412	1266	331
Tribolium castaneum (Tc)	DUOX	gi/89235882	1512	332
	Peroxidase	gi/189241488	902	336
	Oxi-peroxidase	gi/91076232	761	366
	Oxi-peroxidase	gi/189240397	1443	356
	Peroxidasin	gi/91094043	1388	334
	Peroxinectin	gi/91076750	747	334
Caenorhabditis elegans (Ce)	DUOX	gi/74959793	1400	338
	Peroxidase	gi/3879533	1490	333
	Peroxidase	gi/351065684	724	327
	Peroxinectin	gi/351063213	1285	334
Arabidopsis thaliana (At)	Peroxidase1	gi/384950711	325	325
	Peroxidase72	gi/26397792	336	336
Homo sapiens (Hs)	Duox1	gi/74719102	1551	345
	Eiosinophil peroxidase (EPO)	gi/1352738	715	332
	Myeloperoxidase (MPO)	gi/129825	745	358
	Thyroid peroxidase (TPO)	gi/160281455	933	337
	Vascular peroxidase (VPO)	gi/126643889	1479	331

heme peroxidases (**Figure 3.4**) and might have a conserved function across insect species irrespective of their blood feeding or non blood feeding behaviors as observed in the case of other genes (Shi et al., 2012). These peroxidases might have been selected by gene duplications that occurred prior to the most recent common ancestor (MRCA) of hemimetabolous (e.g. *Pediculus humanus,* Ph) and holometabolous (e.g. mosquitoes) insects. AgHPX16 has no ortholog in other mosquitoes such as, *Aedes* and *Culex* however, its ortholog is present in *Drosophila*. AgHPX2 and AgHPX8 are mosquito-specific heme peroxidases and their orthologs are present in *Aedes* and *Culex* mosquitoes (**Figure 3.4**).

The above phylogenetic analysis also indicated the presence of lineage-specific mosquito heme peroxidases. Our findings revealed that there is a cluster of unique *Anopheles* heme peroxidases, which includes AgHPX10, AgHPX11, AgHPX12, AgHPX14 and AgHPX15. These *A. gambiae*-specific peroxidases do not have any ortholog in other arthropods that we analyzed. Interestingly, AgHPX10 and AgHPX15 have their own paralogs named AgHPX11 and AgHPX14, respectively. However, the heme peroxidase AgHPX12 has no paralog even in *A. gambiae* (**Figure 3.4**). These unique peroxidases might have some crucial role in biology, physiology, geographical distribution or environmental adaptations of *Anopheles* mosquito as reported in the case of other genes (Shi et al., 2012). We emphasize that these peroxidases may be considered unique targets to synthesize blockers for regulating the biological activities of the malaria vector. However, the involvement of these peroxidases in the regulation of *Plasmodium* development needs further investigations and our group is actively engaged in that direction.

It is also evident from the phylogenetic analysis that AsHPX15, AcHPX15 and AgHPX15 are evolutionary closer orthologs (**Figure 3.4**). Thus, overall this data represents that HPX15 is a novel peroxidase that is present at least in three different anopheline mosquitoes (*A. gambiae, A. stephensi and A. culicifacies*) and does not have orthologs in any other dipterans.

Further, we analyzed the phylogenetic relationship of AsHPX15 and AcHPX15 with all heme peroxidase proteins of related mosquitoes (all belonging to family *Culicidae*). For that, we selected total 42 HPX proteins from the genome of *A. aegypti*, *C. quinquefasciatus* and *A. gambiae* (as mentioned in **Table 3.1**).

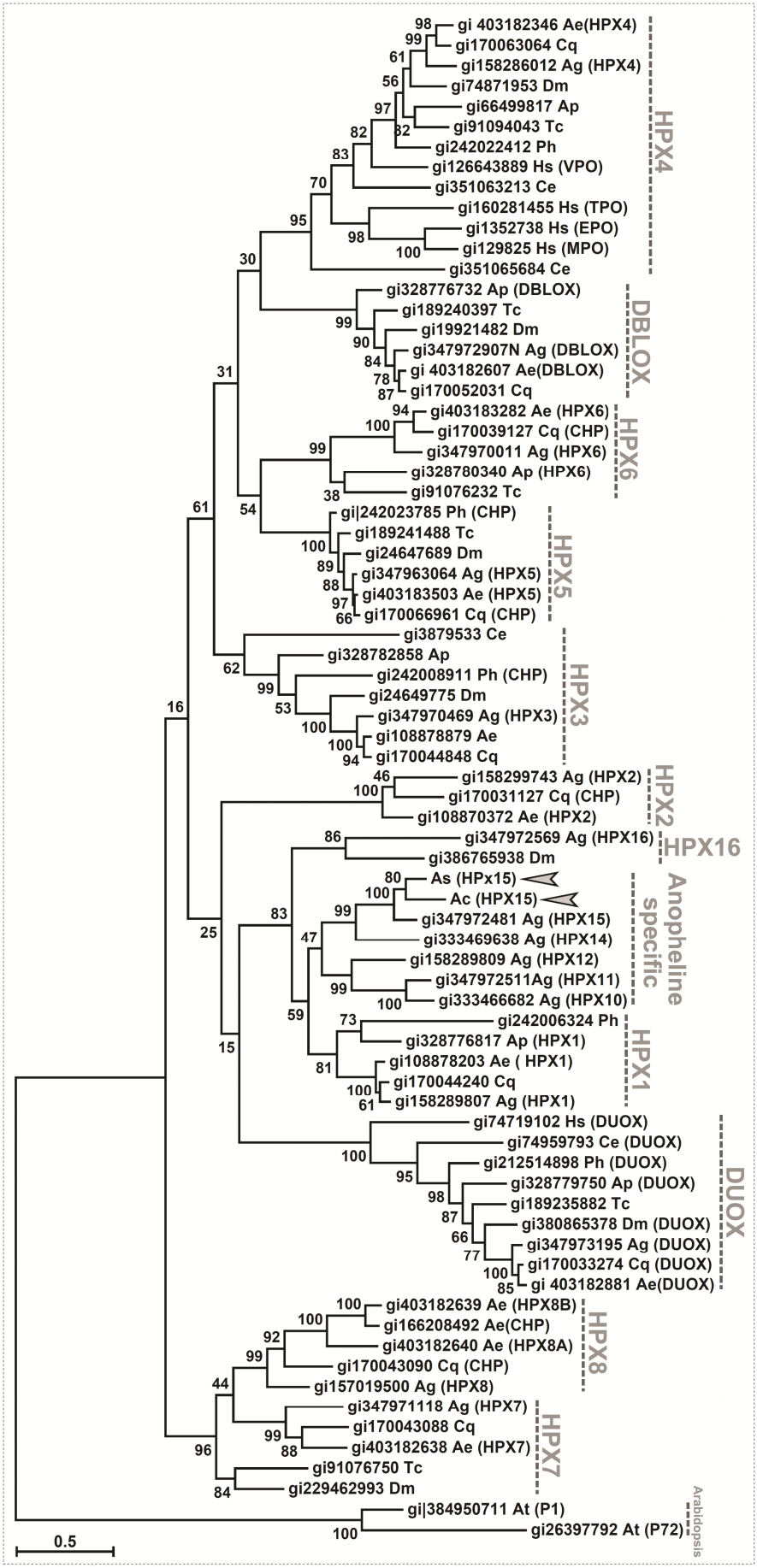

Figure 3.4: Phylogenetic analysis of selected heme peroxidases from various organisms. The Maximum likelihood (ML) method was used to construct the phylogenetic tree for 76 heme peroxidase (HPX) proteins selected from different organisms. The gene ID and abbreviations of organisms' scientific names have been mentioned in **Table 3.1**. Arrowheads indicate AsHPX15 and AcHPX15 clones. Vertical broken gray lines indicate specific clusters, which are named after the representative *A. gambiae* HPX. The scale bar represents base substitutions per site. The numbers on the branches represent the % of 1000 bootstrap.

These sequences were trimmed as mentioned before in the Materials and Methods and reconstructed a phylogenetic tree using the WAG model (**Figure 3.5**). Interestingly, the topology of this phylogenetic relationship is broadly similar to that of the corresponding subclade in the previously constructed phylogenetic tree (comparing **Figures 3.4** and **3.5**).

This phylogenetic analysis clearly demonstrated that out of 16 *A. gambiae* heme peroxidases 10 have their orthologs in *Aedes* and *Culex* mosquitoes. These heme peroxidases are AgHPX1, AgHPX2, AgHPX3, AgHPX4, AgHPX5, AgHPX6, AgHPX7, AgHPX8, AgDUOX and AgDBLOX. This topology supports that these orthologs are selected by gene

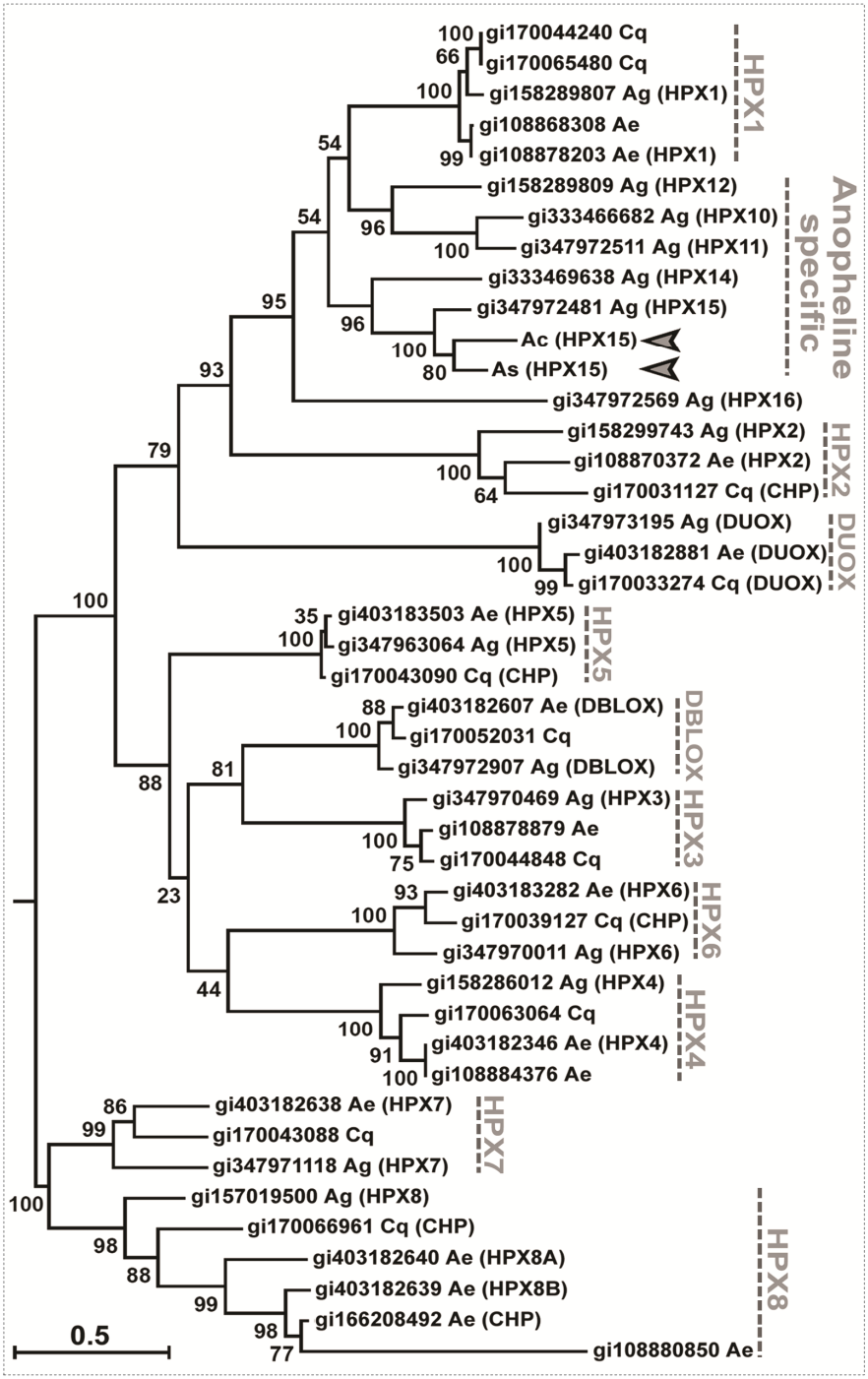

Figure 3.5: Phylogenetic analysis of mosquitoes heme peroxidases. The ML method was used to construct the phylogenetic tree of 44 heme peroxidases selected from *Aedes aegypti, Culex quinquefasciatus* and *Anopheles gambiae* as discussed in Materials and Methods. The gene ID and organisms details are mentioned in Table 3.1. Arrowheads indicate AsHPX15 and AcHPX15 clones. Vertical broken gray lines indicate specific clusters, which are named after the representative *A. gambiae* HPX. The scale bar represents base substitutions per site. The numbers on the branches represent the % of 1000 bootstrap.

duplications that occurred prior to the most recent common ancestor (MRCA) of family *Culicidae*. Importantly, 5 heme peroxidases that further exhibited anophelines lineage specificity are AgHPX10, AgHPX11, AgHPX12, AgHPX14 and AgHPX15 (**Figure 3.5**). AgHPX16 seems to be the most divergent *A. gambiae* heme peroxidase and does not have any known paralog however, we observed its ortholog in *Drosophila* (**Figure 3.4**). In addition, the anophelines heme peroxidases also experienced a lineage-specific expansion as reported in other insects (Shi et al., 2012). The phylogenetic relationship among 16 *A. gambiae* heme peroxidases and 8 non heme peroxidases revealed that both types of peroxidases appear in two different clades and have diverged from each other a long before (**Figure 3.6**). It is also noteworthy to mention that gene expansion and duplication is dominant in *A. gambiae* heme peroxidases. For example, AgHPX15 and HPX14 are in the same cluster (99% bootstarp value), HPX12 is forming

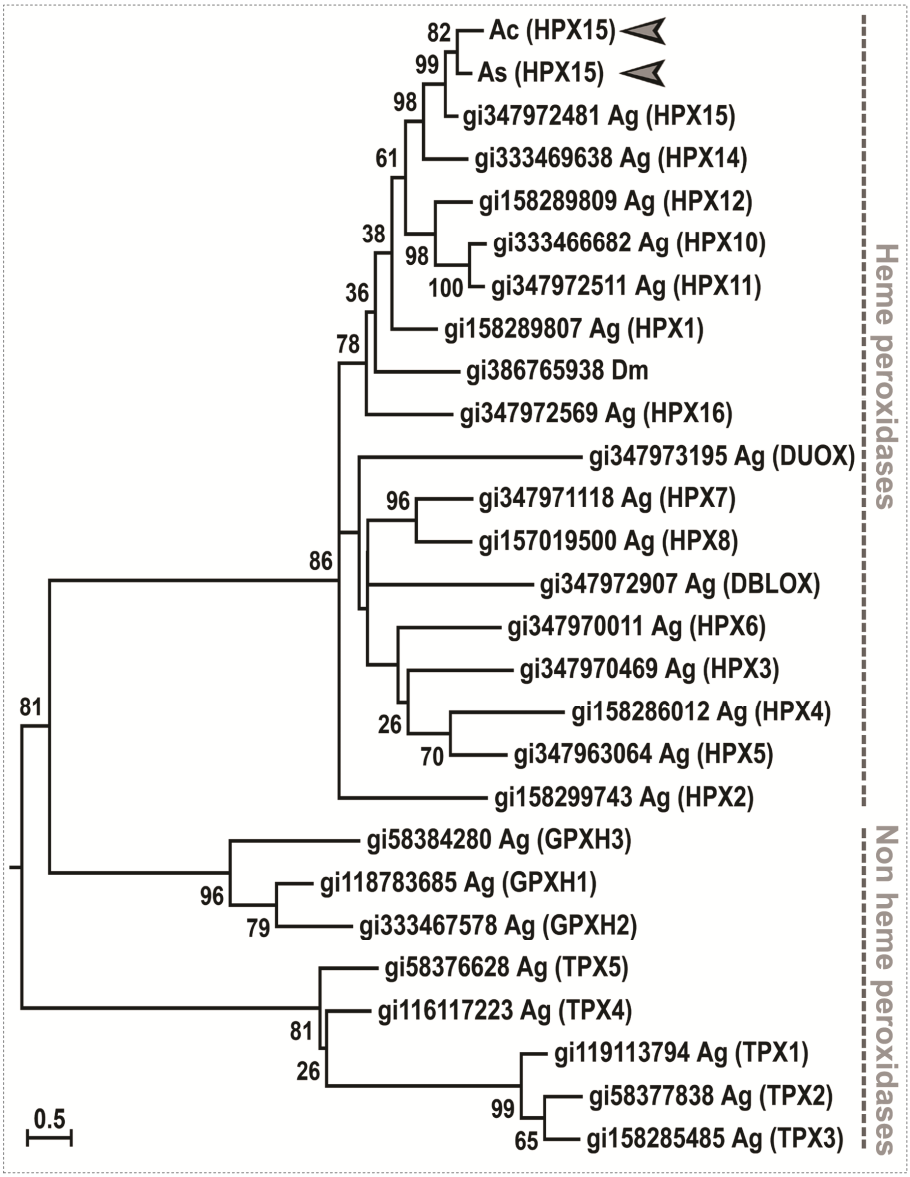

Figure 3.6: Phylogenetic analysis of *A. gambiae* heme and non heme peroxidases. ML tree was constructed for 16 heme and 8 non heme *A. gambiae* peroxidases. The sequenced of all these peroxidases were retrieved from NCBI and their details are provided in Table 3.1. The numbers on the branches represent the % of 1000 bootstrap. The scale bar represents base substitution per site. Arrowheads indicate AsHPX15 and AcHPX15.

cluster with HPX10-HPX11 (98% bootstarp value), HPX7-HPX8 and HPX4-HPX5 are also appearing in their own clusters, respectively (**Figure 3.6**). These clusters represent gene duplication (origin of paralogs) in heme peroxidases and explain the expansion of HPX family in *A. gambiae*. However, AgHPX1, AgHPX2, AgDUOX, AgHPX16 and AgDBLOX do not reveal any characteristic duplication pattern (**Figure 3.6**).

3.3.4 HPX15 orthologs are present in the malaria vector and non vector species of *Anopheles* mosquitoes

Our previous phylogenetic analyses revealed that HPX15 orthologs are present at least in three major malaria transmitting species of *Anopheles* mosquito such as, *A. gambiae*, *A. stephensi* and *A. culicifacies* (**Figures 3.4** and **3.5**). The recent availability of whole genome shotgun sequences of 16 additional species of anopheline mosquitoes drew our attention to understand the universality of HPX15 in these worldwide-distributed *Anopheles* mosquitoes. Nucleotide BLAST of AsHPX15 clone against these shotgun sequences provided the matching contigs (recently named as ensemble identifier as mentioned in **Table 3.2**).

We found that all of these 16 species of *Anopheles* mosquitoes also have the putative HPX15 gene in their genome. Interestingly, in this comprehensive analysis of 19 above-mentioned anophelines (see **Table 3.2**) there are 12 major, 5 minor and 2 non malaria vector species as defined by others (Neafsey et al., 2013). Thus, the presence of HPX15-like peroxidases in the genome of vectors and non vector species may not reveal its direct association with their vectorial capacity. We believe that HPX15 might have a general physiological role in these blood feeding vectors or non vector species of *Anopheles* mosquitoes and managing the phenomenon of 'immune balance in midgut' during food digestion as we reported before in case of *A. gambiae* (Kumar et al., 2010). This further warrants the detailed investigations of these mechanisms in other anophelines.

3.3.5 HPX15 proteins are highly conserved among anophelines

We compared the predicted protein sequences of all the sixteen HPX15 peroxidases to analyze their relative identity with AgHPX15, AsHPX15 and AcHPX15 proteins. The amino acids identity among these total 19 HPX15 peroxidases was found to be highly conserved (70-99%, **Table 3.3**).

Table 3.2: List of putative HPX15 peroxidases retrieved from different species of *Anopheles* mosquitoes. The putative HPX15 peroxidase contig (or Ensembl identifier) from the genome of different anophelines were retrieved using nucleotide sequences of AsHPX15 clone (GenBank: KP223285) as query. The overhanging sequences of the contigs were trimmed based on AsHPX15 sequences as mentioned in the Materials and Methods. The BLAST query coverage, identity of corresponding HPX15 contig with AsHPX15 clone and the nucleotides and total amino acids in trimmed sequences are presented in the table. The abbreviation for individual mosquito is also mentioned in parenthesis.

Vectorial capacity	*Anopheles* spp. (abbreviation)	Ensembl identifier or gene bank identity	Retrieved contig	% nucleotide query coverage with AsHPX15 (KP223285)	% nucleotide Identity with AsHPX15 (KP223285)	Nucleotides (Amino acids) in trimmed sequence
Major vectors	*A.arabiensis* (Aar)	AARA008901	1.3480	96	75	1011(337)
	A.atroparvus (Aat)	AATE013459	1.2435	90	70	934 (311)
	A. darling (Ada)	ADAC006384	7077	77	71	985(335)
	A. dirus (Adi)	ADIR011596	1.4912	83	72	909(303)
	A.farauti (Afa)	AFAF010327	2.1809	93	73	1015(337)
	A.funestus (Afu)	AFUN008618	1.6688	98	76	995(331)
	A.maculatus (Ama)	AMAM004556	1.2526	98	83	986 (328)
	A.sinensis (Asi)	Not known	012260	96	69	1009(336)
	A.nili (Ani)	Not known	19203	84	71	915 (304)
	A. gambiae (Ag)	AGAP013327	-	89	76	1005 (335)
	A. culicifacies (Ac)	KP299257	1.17233	84	79	1059 (353)
	A. stephensi (As)	KP223285	5285	100	100	1075 (358)
Minor vectors	*A.albimanus* (Aal)	AALB010446	1.835	78	71	1050 (323)
	A.epiroticus (Aep)	AEPI000890	1.174	93	73	980 (326)
	A. melas (Amel)	AMEC000291	2.2419	96	74	995 (331)
	A. merus (Amer)	AMEM005191	2.5072	96	74	994 (331)
	A.minimus (Ami)	AMIN007008	1.3585	98	83	1009 (336)
Non-vectors	*A.quadriannulatus* (Aq)	AQUA003275	1.8077	96	75	1011 (337)
	A.christyi (Ach)	ACHR005516	1.2278	97	75	986 (328)

Table 3.3: Percentage amino acids identity among HPX15 peroxidases from nineteen different anophelines. The percentage identity among 19 different HPX15 peroxidase proteins was analyzed through their ClustalW alignments. The total amino acids (AA) used for analysis and the name of individual peroxidases (1 to 19) are also mentioned in the table. The protein sequences, gene ID and abbreviations of anophelines' scientific names are same as mentioned in **Table 3.2**.

		AA	1	2	3	4	5	6	7	8	9	10	11	12	13	14	15	16	17	18	19
1	AarHPX15	337		98.81	99.10	97.58	97.28	84.76	72.46	69.97	74.28	72.54	74.67	77.89	76.05	72.24	79.04	77.34	78.96	76.88	75.46
2	AqHPX15	337	98.81		99.10	97.58	97.28	84.76	73.19	70.27	74.28	71.94	74.01	77.56	76.35	71.64	79.34	77.64	78.66	76.58	74.54
3	AgHPX15	335	99.10	99.10		97.89	97.58	85.37	73.55	70.87	74.92	72.37	74.01	77.56	77.11	72.97	80.18	78.25	79.57	77.48	74.85
4	AmerHPX15	331	97.58	97.58	97.89		96.68	84.36	72.46	69.91	73.63	71.73	73.36	77.56	76.83	72.95	79.64	77.51	78.96	77.20	74.54
5	AmelHPX15	331	97.28	97.28	97.58	96.68		85.89	72.83	70.21	73.95	72.04	74.01	77.23	77.13	73.25	80.55	78.72	79.27	78.12	74.85
6	AchHPX15	328	84.76	84.76	85.37	84.36	85.89		75.82	72.87	75.32	73.78	73.42	76.33	77.06	74.09	80.18	80.79	79.38	76.22	79.57
7	AalHPX15	323	72.46	73.19	73.55	72.46	72.83	75.82		91.34	74.28	74.28	70.65	71.64	74.64	71.01	72.83	72.83	71.38	69.20	67.03
8	AdaHPX15	335	69.97	70.27	70.87	69.91	70.21	72.87	91.34		73.95	72.97	70.72	72.28	72.59	65.77	70.57	71.00	69.51	67.87	66.26
9	AatHPX15	311	74.28	74.28	74.92	73.63	73.95	75.32	74.28	73.95		87.46	77.96	76.79	76.45	70.42	74.60	73.31	73.31	72.67	67.85
10	AsiHPX15	336	72.54	71.94	72.37	71.73	72.04	73.78	74.28	72.97	87.46		76.97	77.23	75.22	66.67	72.54	72.21	73.48	71.77	67.18
11	AniHPX15	304	74.67	74.01	74.01	73.36	74.01	73.42	70.65	70.72	77.96	76.97		77.85	76.32	71.71	72.37	73.03	72.70	72.37	70.07
12	AdiHPX15	303	77.89	77.56	77.56	77.56	77.23	76.33	71.64	72.28	76.79	77.23	77.85		85.15	76.24	77.89	76.90	77.56	73.60	71.62
13	AfaHPX15	337	76.05	76.35	77.11	76.83	77.13	77.06	74.64	72.59	76.45	75.22	76.32	85.15		69.94	76.42	76.36	75.54	74.40	71.08
14	AcHPX15	337	72.24	71.64	72.97	72.95	73.25	74.09	71.01	65.77	70.42	66.67	71.71	76.24	69.94		85.12	79.76	81.40	75.08	71.78
15	AmiHPX15	336	79.04	79.34	80.18	79.64	80.55	80.18	72.83	70.57	74.60	72.54	72.37	77.89	76.42	85.12		86.71	85.98	81.08	73.31
16	AfuHPX15	331	77.34	77.64	78.25	77.51	78.72	80.79	72.83	71.00	73.31	72.21	73.03	76.90	76.36	79.76	86.71		82.62	80.66	72.70
17	AmaHPX15	336	78.96	78.66	79.57	78.96	79.27	79.38	71.38	69.51	73.31	73.48	72.70	77.56	75.54	81.40	85.98	82.62		87.50	73.01
18	AsHPX15	333	76.88	76.58	77.48	77.20	78.12	76.22	69.20	67.87	72.67	71.77	72.37	73.60	74.40	75.08	81.08	80.66	87.50		70.25
19	AepHPX15	326	75.46	74.54	74.85	74.54	74.85	79.57	67.03	66.26	67.85	67.18	70.07	71.62	71.08	71.78	73.31	72.70	73.01	70.25	

This range of percentage identity, confirmed that all these peroxidases are orthologs as described in case of other proteins (Peterson et al., 2009). In addition, we also analyzed the evolutionary relationship among these 19 species-specific peroxidase proteins. Results presented in **Figure 3.7** revealed that the phylogenetic relationship of these nineteen HPX15 proteins follows a pattern similar to the evolutionary classification of these mosquito species as described by other researchers (figure 1 of (Neafsey et al., 2013). These findings explain that HPX15 is conserved among anopheline mosquitoes and might have evolved the same way as different species of *Anopheles* evolved.

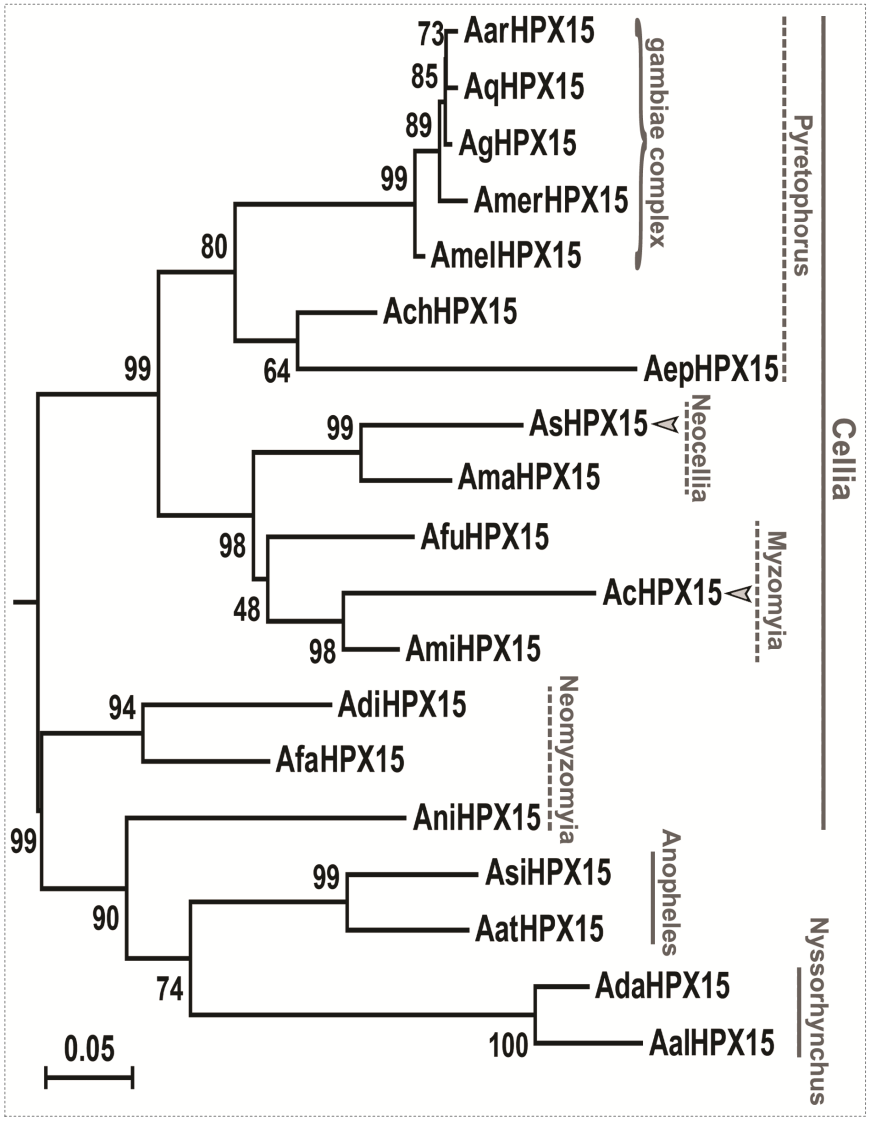

Figure 3.7: Phylogenetic analysis of putative HPX15 peroxidases from different species of *Anopheles* mosquitoes. ML tree was constructed using heme peroxidase protein sequences from 19 different species of *Anopheles* mosquitoes. Details regarding HPXs nomenclature and anopheline species are mentioned in Table 3.2. Arrowheads indicate AsHPX15 and AcHPX15. Gray color solid vertical lines represent three sub genera (*Cellia*, *Anopheles* and *Nyssorhynchus*) of the genus *Anopheles*. Broken vertical lines represent series (Neocellia, Myzomyia, Neomyzomyia and Pyretophorus) of sub genus *Cellia*. The gambiae complex is the part of series Pyretophorus. The scale bar represents base substitutions per site. The numbers on the branches represent the % of 1000 bootstrap.

In conclusion, HPX15 is a highly conserved anopheline lineage-specific peroxidase and present in the genome of globally distributed major/minor malaria vectors. These findings have great advantage to the society in terms of blocking the activity of this single molecule might interrupt the malaria cycle in those vectors.

3.4 Discussion

Heme peroxidases (HPXs) are found almost in all living organisms and generally catalyze the one- and two-electron oxidation of numerous organic and inorganic substrates. The redox cofactor is heme b or post translationally modified heme that is ligated to either histidine or cysteine residue. Four heme peroxidase super families (peroxidase-catalase, peroxidase-cyclooxygenase, peroxidase-chlorite dismutase and peroxidase-peroxygenase) have differences in their enzymatic activities and also evolved independently (Zámocký et al., 2015).

In general, heme peroxidases play an important role in development and immunity. In vertebrates and invertebrates, heme peroxidases catalyze protein crosslinking that is a crucial process to stabilize the extracellular matrix. This crosslinking is a fundamental feature of basal membranes and essential as an elemental mechanism of tissue biogenesis (Péterfi and Geiszt, 2014; Kumar and Barillas-Mury, 2005). Heme peroxidases are also extensively involved in the evolution and adaptations to the environment (Shi et al., 2012). Thus, HPXs super family is considered to be a group of highly diversified members. Our phylogenetic analysis of the heme peroxidases (HPXs) from different phyla revealed the existence of two separate lineages of highly diversified HPXs, namely animals and plants (**Figure 3.4**). These results are supported by the previous reports where heme peroxidases are classified into two major families, namely the animal and non-animal peroxidases that include fungal and protist heme peroxidases (Passardi et al., 2007).

Our phylogenetic analysis of 74 animal heme peroxidases (16 from *A. gambiae* and 58 from other animals) reveal that they appear in 11 different clades. Some of the *A. gambiae* heme peroxidases have their orthologs in other organisms, including human (**Figure 3.4**). For example, an extensively conserved HPX4 and DUOX clusters, which are originated by gene duplication events that occurred during the evolution of the kingdom Animalia. In addition, some of the *A. gambiae* heme peroxidases (e.g. HPX1, HPX3 and HPX5) are more close relatives of other arthropods and emerged by gene duplications that occurred prior to the most recent common ancestor (MRCA) of hemimetabola and

holometabola in the late carboniferous period, 318-300 million years ago (Wiegmann et al., 2009; Hughes, 2012). Thus, it is clearly evident that gene duplication event in heme peroxidase super family is crucial in the evolution of biological complexity and offers raw material that diverged under positive selection (Ohno, 1970). These events are critical during evolution, speciation and the birth of new life forms.

In *A. gambiae* there are 16 heme and 8 non heme peroxidases, which are evolutionary separated from each other (**Figure 3.6**). This indicates that in *A. gambiae* there is a large expansion of heme peroxidases and that may be associated with their geographical distribution or biological behaviors as reported in other organisms (Shi et al., 2012). It is also noticeable that some lineage-specific heme peroxidases are present only in anophelines and do not have any ortholog in other animals including *Aedes* and *Culex* mosquitoes. These unique *Anopheles* heme peroxidases are HPX10, HPX11, HPX12, HPX14 and HPX15 (**Figure 3.4**). In this group, HPX12 has no paralog in *A. gambiae*. However, HPX10-HPX11 and HPX14-HPX15 are paralogs.

As we have mentioned before that heme peroxidases are important to perform numerous biological functions in living organisms including insects. *Anopheles* mosquito is a known vector for human malaria therefore, we were interested to identify those novel heme peroxidases in this insect that regulate *Plasmodium* development. Among these above-mentioned unique *A. gambiae* peroxidases, AgHPX15 demonstrated a general physiological role in the blood fed mosquitoes, which indirectly supports the *Plasmodium* development (Kumar et al., 2010). Thus, we believe that AgHPX15 might be considered a potent target to block the malaria cycle in *A. gambiae*.

The advocacy of AgHPX15 as a potent candidate for blocking malaria parasite development in mosquito requires that two important issues should be addressed. Whether, HPX15 is also present in all the known species of *Anopheles,* which are considered to be major/minor malaria vectors. So this single molecule may be a central point of interest to target all these vector species. Secondly, how conserved this molecule is so that a common approach to block its activity will be enough to control *Plasmodium* development in all worldwide-distributed malaria vectors. To address the first issue, we provided evidences that AgHPX15 orthologs are present in major Indian malaria vectors, *A. stephensi* and *A. culicifacies* (**Figures 3.1, 3.4** and **3.5**). In addition, our phylogenetic analysis with the retrieved sequences from 16 additional vector as well as non-vector anophelines also proved that the putative HPX15 gene is present in all these species (**Figure 3.7**). It is

interesting to note that HPX15 is present in both vector and non vector anophelines. This may be due to the reason that all these mosquitoes are hematophagous in nature and thus, HPX15 may be required to crosslink the midgut barrier around the ingested blood in a way similar to *A. gambiae* (Kumar et al., 2010). However, it warrants further analysis and understanding the correlation between the HPX15 expression and blood feeding in these mosquito species individually.

For developing blocking strategies, the polymorphism in the target molecules is also a hurdle as reported in other systems (Mahajan et al., 2005). Thus, it is important to understand the genetic diversity in HPX15 orthologs as a general rule. The conserved domain (CD) analysis of AgHPX15, AsHPX15 and AcHPX15 provided the details about their identity and functional relationships (**Figure 3.3**). Moreover, we also found the same conserved domain architectures when we analyzed other 16 anopheline putative HPX15 protein sequences. A further comparison of amino acids among total 19 HPX15 peroxidases also revealed 70-99% identity (**Table 3.3**). These observations strengthen our hypothesis that HPX15 can be a central plausible target and a common strategy may be applied to block its functioning to regulate the vectorial capacity of worldwide-distributed malaria vectors. Our previous double stranded (ds) RNA-mediated gene silencing experiments add in proof to this concept. Here the dsAgHPX15 RNA, prepared from *A. gambiae* cDNA, could silence HPX15 gene in both *A. gambiae* and *A. stephensi*. Moreover, the silencing-mediated effects on *Plasmodium* development were same in these mosquitoes (figures 2 and S6 of (Kumar et al., 2010). These effects were probably due to the high (~75%) sequence identity between AgHPX15 and AsHPX15, which is evident now from the present study.

Recently a remarkable role of *A. gambiae* AgHPX15 gene is also reported in a study. Here this research group demonstrated that AgHPX15 induction in spermatheca is regulated by sexually transferred 20-hydroxyecdysone (20E), which is essential to preserve the functionality of stored sperm and long-term fertility (Shaw et al., 2014). Thus, targeting AgHPX15 will disrupt the reproductive cycle and numbers of mosquitoes in the field. These findings indicate that blocking the function of HPX15 will be beneficial in many ways and can be easily achieved as reported previously for other mosquito targets (Dinglasan et al., 2003; Shahabuddin et al., 1998). In these studies, a midgut-specific monoclonal antibody demonstrated a dose-dependent blocking effect against *P. yoelii* development in *A. stephensi*. Thus, we propose that the evolutionary conserved HPX15 protein in several

anopheline mosquitoes can also be targeted in a similar way and may certify this molecule as a unique candidate to block mosquito cycle of *Plasmodium* development.

3.5 Conclusion

A lineage-specific heme peroxidase HPX15 is present in several globally distributed species of *Anopheles* mosquito. The highly conserved nature of HPX15 reveals that this molecule can be a potent target for blocking *Plasmodium* development. These findings may be a great help to fight against malaria, one of the world's deadliest diseases.

Chapter 4

Characterization and expression analysis of gene encoding heme peroxidase HPX15 in major Indian malaria vector *Anopheles stephensi*

The entire work presented in this chapter has been published in the journal *Acta Tropica*

Acta Tropica 158 (2016) 107–116

Contents lists available at ScienceDirect

Acta Tropica

journal homepage: www.elsevier.com/locate/actatropica

Characterization and expression analysis of gene encoding heme peroxidase HPX15 in major Indian malaria vector *Anopheles stephensi* (Diptera: Culicidae)

Mithilesh Kajla[1], Parik Kakani[1], Tania Pal Choudhury, Kuldeep Gupta, Lalita Gupta, Sanjeev Kumar*

4.1 Abstract

The interaction of mosquito immune system with *Plasmodium* is critical in determining the vector competence. Thus, blocking the crucial mosquito molecules that regulate parasite development might be effective in controlling the disease transmission. In this study, we characterized a full-length AsHPX15 gene from the major Indian malaria vector *Anopheles stephensi*. This gene is a true ortholog of *Anopheles gambiae* heme peroxidase AgHPX15 (AGAP013327), which modulates midgut immunity and regulates *Plasmodium falciparum* development. We found that AsHPX15 is highly induced in mosquito developmental stages and blood fed midguts. In addition, this is a lineage-specific gene that has identical features and 65-99% amino acids identity with other HPX15 genes present in eighteen worldwide-distributed anophelines. We discuss that the conserved HPX15 gene might serve as a common target to manipulate mosquito immunity and arresting *Plasmodium* development inside the vector host.

4.2 Introduction

Malaria is the fatal human disease that is caused by *Plasmodium* and transmitted by various species of female anopheline mosquitoes. *Plasmodium* completes its sexual life cycle in mosquito and asexual cycle in the human host. One effective method of controlling malaria might be to impede parasite development inside the mosquito through transmission blocking strategies. For that exploring the molecular interaction of *Plasmodium* with mosquito key immune molecules is unequivocally required.

Major studies carried in *Anopheles gambiae* revealed that several mosquito innate molecules regulate antiplasmodial immunity (Dimopoulos et al., 2002; Fraiture et al., 2009; Gupta et al., 2009 and 2010; Luckhart et al., 2003; Vizioli et al., 2001). Interestingly, many of these immune molecules effectively regulate mouse malaria (*Plasmodium berghei*) development, however, they are ineffective against human malaria parasite *P. falciparum* (Fraiture et al., 2009).

Recent studies identified that *A. gambiae* heme peroxidases have regulatory effects against both mouse and human malaria parasites (Kumar et al., 2010; Oliveira et al., 2012). One important *A. gambiae* heme peroxidase AgHPX15 (AGAP013327) has a potent role in modulation of gut immunity against *Plasmodium.* Silencing of AgHPX15 gene in *A. gambiae* decreased *P. berghei* as well as *P. falciparum* oocyst numbers (Kumar et al., 2010) and its orthologs are present in 19 other *Anopheles* species, including Indian malaria vector *A. stephensi* (Kajla et al., 2015b). We studied a partial clone of this gene in *A. stephensi* and found that it has no ortholog in human and

arthropods (Chapter 3 and Kajla et al., 2015b). Furthermore, we analyzed the detailed genomic organization and expression profile of AsHPX15 gene to understand its unique features and regulation in *Anopheles* mosquitoes.

4.3 Results

4.3.1 Characterization of full-length *Anopheles stephensi* AsHPX15 gene

As mentioned in Chapter 3 that the partial AsHPX15 clone (1075 bp, GenBank: KP223285) does not have orthologs in other mosquitoes, insects or even humans.

Figure 4.1: Genomic organization of AsHPX15 gene. A) AsHPX15 gene predicted by GENSCAN software revealed the presence of three exons viz. E1 372 bp, E2 738 bp and E3 675 bp (total CDS 1785 bp). Two introns, I_1 79 bp and I_2 77 bp are represented by black dotted line. The gene promoter (P) was predicted 379 bp 5′ upstream to the protein initiation codon. 5′ UTR (343 bp) and 3′ UTR (90 bp) were also predicted in AsHPX15 gene **B)** AsHPX15 CDS sequencing revealed the presence of three exons viz. E1 369 bp, E2 743 bp and E3 682 bp (total CDS 1794 bp). Two introns, I_1 76 bp and I_2 71 bp are represented by black dotted line. Numbering indicates the nucleotide position of the gene. The positions of various forward (F) and reverse (R) primers are depicted here (as mentioned in **Table 2.1,** Chapter 2).

Therefore, we were interested to analyze full length AsHPX15 gene, protein structure and regulatory elements to reveal its importance in *Anopheles*-pathogen interactions. For that, we predicted 1941 bp full-length gene of AsHPX15 in *A. stephensi* genome with the help of GENSCAN software. The predicted AsHPX15 cDNA has three exons (372 bp, 738 bp and 675 bp) and two introns (79 bp and 77 bp) as depicted in **Figure 4.1A**. Full length AsHPX15 was cloned from *A. stephensi* midgut cDNA

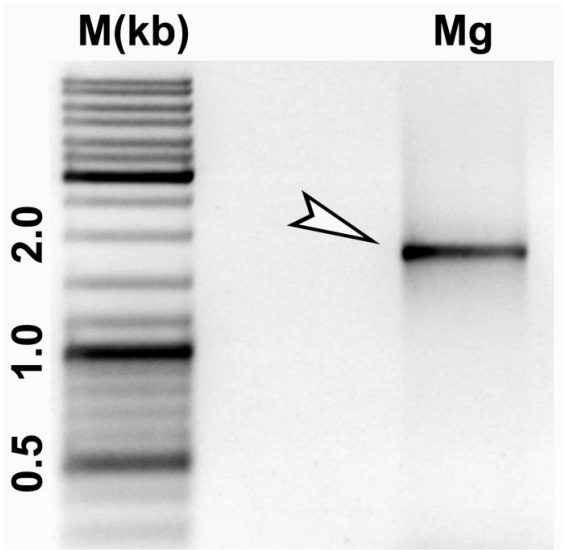

Figure 4.2: PCR amplification of full-length *A. stephensi* AsHPX15 gene. *A. stephensi* midguts (Mg) cDNA template was amplified using F5 and R5 primers and a single band of expected size ~1800 bp was observed in the gel as indicated by the arrow head. The left lane (M) represents the DNA ladder used as reference for identifying the product size.

templates. PCR amplification of midgut cDNA with the help of F5 and R5 primers (**Table 2.1**) amplified an expected fragment of ~1800 bp (**Figure 4.2**). The PCR product was cloned and sequenced using four different primers F2, F4, F5 and R5 (as shown in **Figure 4.1A** and **Table 2.1** of the Chapter Materials and Methods) and the sequence was submitted to NCBI (GenBank database accession number: KT825861). The sequence identity of 1794 bp full length AsHPX15 clone was confirmed by general nucleotide BLAST and it revealed closest match with *A. gambiae* AgHPX15 (e value 0, 75% identity). Interestingly, the clone does not have considerable match with any other organism, including *Aedes* and *Culex* mosquitoes. This data strengthen our previous findings that HPX15 is a unique gene that is present exclusively in anopheline mosquitoes (Kajla et al., 2015b).

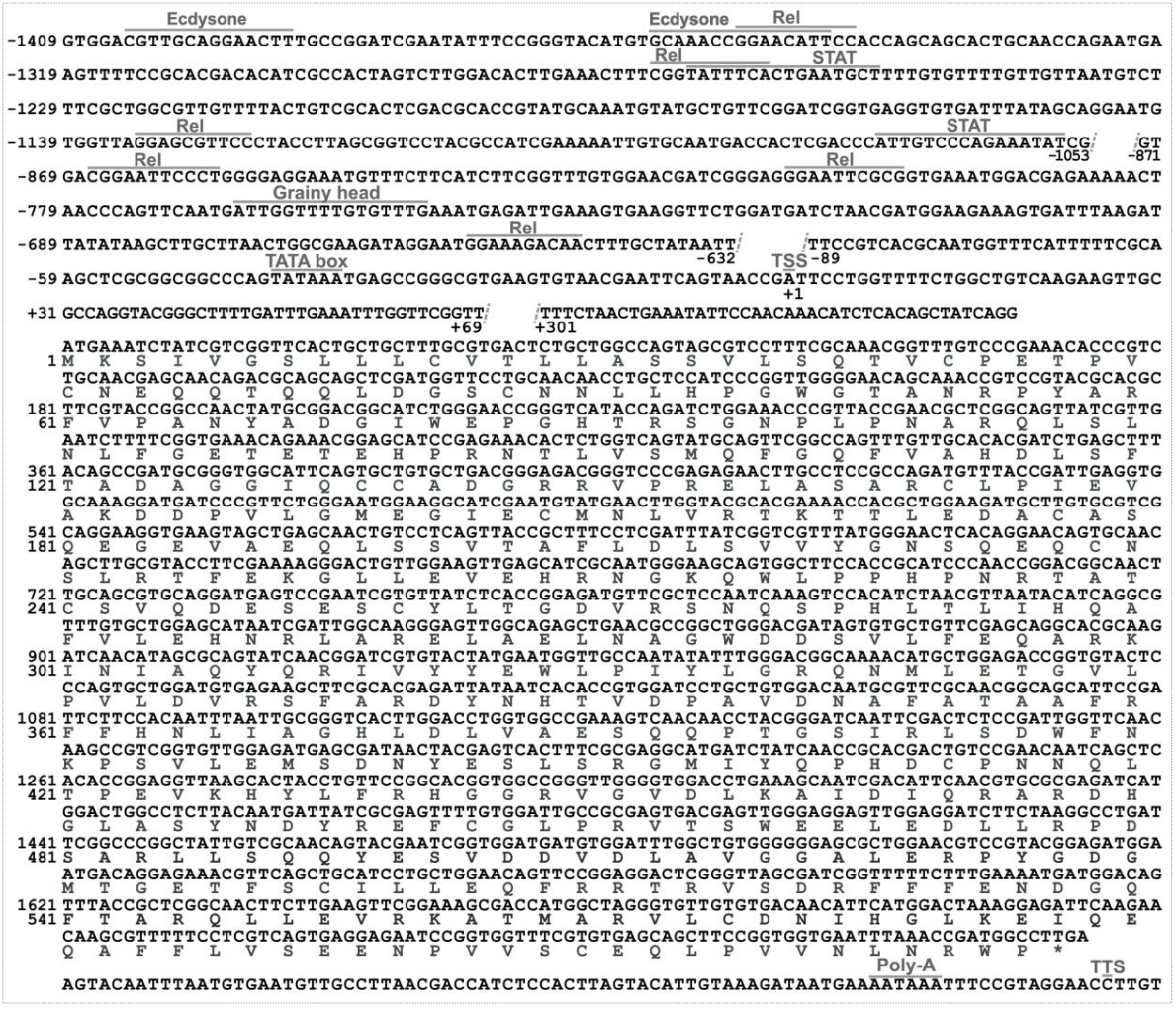

Figure 4.3: Analysis of regulatory elements in AsHPX15 gene. Binding sites for various transcription factors such as, Ecdysone, Rel, STAT and Grainy head are depicted in the regulatory region of AsHPX15 gene as predicted by MatInspector and JASPAR software. The TATA Box and transcription start site (TSS) are also shown in the regulatory region. The AsHPX15 gene (1794 bp) encodes for a 597 amino acids long protein. At the end, predicted Poly-A site and transcription termination site (TTS) are also mentioned in the figure.

Sequence analysis and comparison of the full-length AsHPX15 clone with *A. stephensi* genome database confirmed the presence of three exons (E1 369 bp, E2 743 bp and E3 682 bp) separated by two introns, 76 bp and 71 bp (**Figure 4.1B**). While predicted cDNA revealed three corresponding exons (E1 372 bp, E2 738 bp and E3 675 bp) and two introns (79 bp and 77 bp) as depicted in **Figure 4.1A**. Interestingly, the number and position of exons and introns are equivalent in predicted CDS (1785 bp) and the full length cDNA clone (1794 bp). Further analysis of AsHPX15 gene structure using GSDS (Gene Structure Drawing Server) software revealed that the open reading frame of 1794 bp codes for a 597 amino acids long protein with molecular weight of 67.13 kDa (**Figure 4.3**).

4.3.2 AsHPX15 conserve domains are identical to *A. gambiae* AgHPX15

To understand details regarding the sequence identity, structure and functional relationships, AsHPX15 and its true ortholog *A. gambiae* AgHPX15 proteins were subjected to conserved domain database (CDD) analysis. Results depicted in **Figure 4.4** revealed that these two peroxidases exhibit characteristics, identity similar to the peroxinectin-like conserved domain of animal heme peroxidases superfamily. Peroxinectins are generally secreted proteins and play an important role in invertebrate immunity, including arthropods. They are cell-adhesive and opsonic molecules and interact with transmembrane receptors of integrin family (Sritunyalucksana et al., 2001). We also observed that identical sites are present in the conserved domains of *A. stephensi* and *A. gambiae* HPX15 proteins. These sites are three calcium binding, ten heme binding, fourteen putative substrate binding and three homodimer interface sites (**Figure 4.4**). These results indicated that full-length HPX15 proteins are identical, at least in these two anophelines. Furthermore, we analyzed the relative identity of full-length AsHPX15 peroxidase protein with the putative HPX15 proteins of seventeen other anophelines as mentioned in **Table 4.1.**

The amino acids identity among these total 19 HPX15 peroxidases was found to be highly conserved (65-99%, **Table 4.2**). This conserved identity indicated that all these anopheline peroxidases are orthologs as discussed in case of other proteins (Peterson et al., 2009). In conclusion, full length HPX15 is also a conserved protein, at least in 19 globally distributed anopheline mosquitoes that we analyzed.

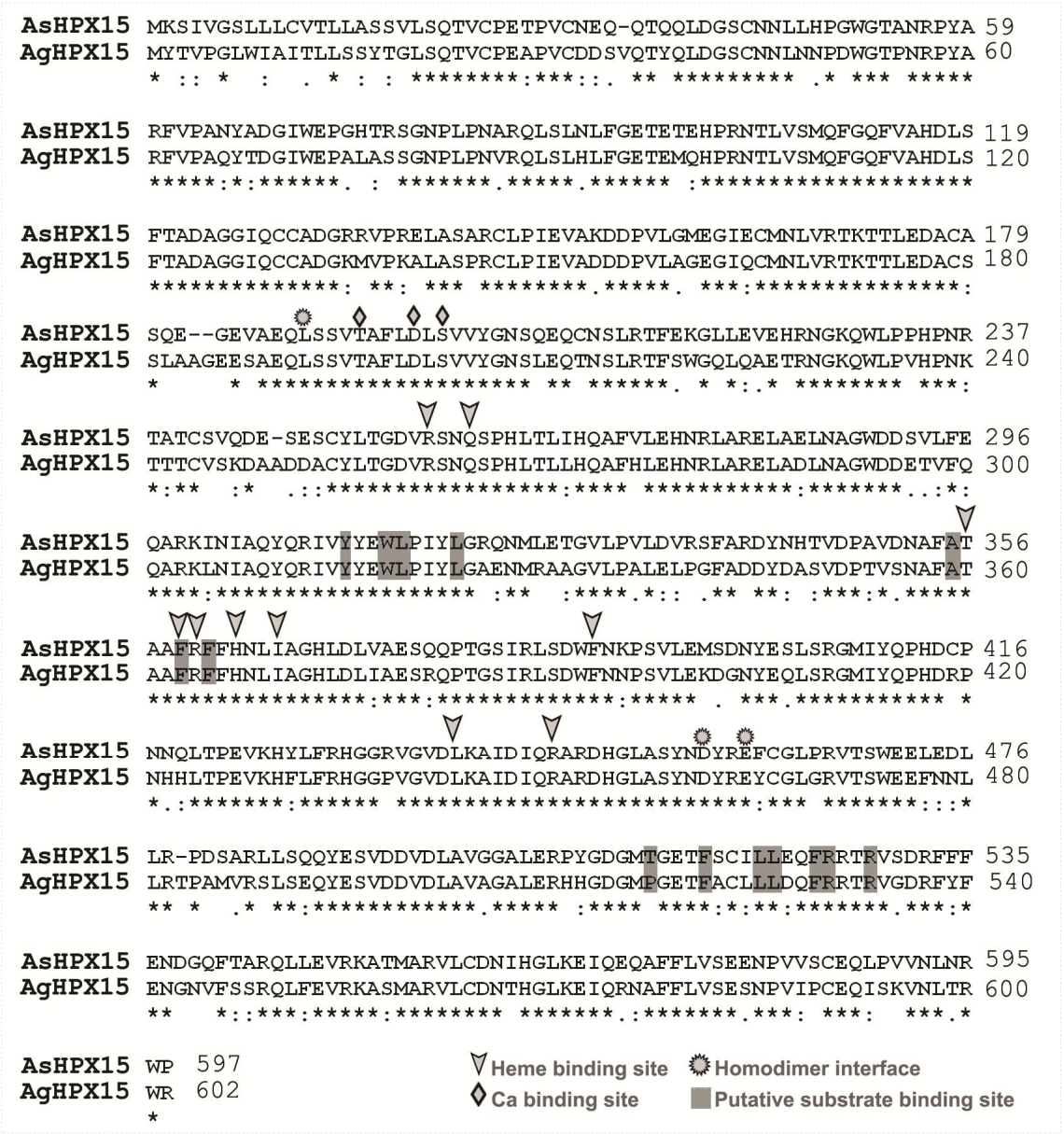

Figure 4.4: Conserve domains in AsHPX15 and AgHPX15 proteins. The conserved domain database (CDD) predicted numerous binding sites such as, heme binding, calcium binding, putative substrate binding and homodimer interface sites as represented by the characteristic symbols in the alignment of full-length AgHPX15 and AsHPX15 proteins.

4.3.3 Putative transcription factor binding sites in the regulatory region of AsHPX15 gene

To understand the regulation of AsHPX15 gene, we screened its regulatory region using NNPP2.2 software. The presence of promoter was analyzed in the randomly selected 1800 bp 5′ upstream region from the protein initiation codon of the predicted gene. This program predicted the transcription start site (TSS) 343 bp upstream to the first codon and it was assigned the position +1 (**Figure 4.3**). The presence of TATA box (TATAAA) was located at position -36 from the transcription start site. The software also predicted

343 bp 5' untranslated region (UTR) just before the protein start codon ATG. Furthermore, we analyzed the putative transcription factor binding sites in the same regulatory region of AsHPX15 gene with the help of MatInspector and JASPAR software. The search criteria for these transcription factors binding motifs were defined within the insect family. Importantly, two STATs, six Rel and two ecdysone putative transcription factors binding sites were predicted by these software. In addition, the presence of one transcription factor grainy head binding site was also predicted at -750 position in the regulatory region of AsHPX15 gene (**Figure 4.3**).

Table 4.1: The putative HPX15 peroxidases retrieved from different species of *Anopheles* mosquitoes. The putative HPX15 peroxidase contigs (or Ensembl identifiers) were retrieved from the genome of different anophelines using nucleotide sequence of full-length AsHPX15 clone as query. HPX15 contig and total amino acids in HPX15 protein are shown in the table. The abbreviation for individual mosquito is mentioned in parenthesis.

Vectorial capacity	*Anopheles* species (abbreviation)	Gene ID/ GenBank acc. No./Contig	HPX15 protein (amino acids)
Major vectors	*A. stephensi* (As)	KT825861	597
	A. gambiae (Ag)	AGAP013327	602
	A. arabiensis (Aarb)	cont1.3480	602
	A. atroparvus (Aatp)	cont1.2435	603
	A. culicifacies (Acul)	cont1.17233	594
	A. darlingi (Adar)	cont7077	611
	A. dirus (Adir)	cont1.4912	603
	A. farauti (Afar)	cont2.1809	602
	A. funestus (Afun)	cont1.6688	588
	A. maculatus (Amac)	cont1.2526	596
	A. sinensis (Asin)	cont012260	606
	A. nili (Anil)	cont19203	485
Minor vectors	*A. albimanus* (Aalb)	cont1.835	608
	A. epiroticus (Aepi)	cont1.174	596
	A. melas (Amel)	cont2.2419	602
	A. merus (Amer)	cont2.5072	602
	A. minimus (Amin)	cont1.3585	596
Non-vectors	*A. quadriannulatus* (Aqua)	cont1.8077	602
	A. christyi (Achr)	cont1.2278	598

Table 4.2: Percentage amino acids identity among full-length HPX15 peroxidases obtained from nineteen different anophelines. The identity among 19 different HPX15 peroxidase proteins was analyzed through their alignment in Clustal Omega. The total amino acids (AA) used for analysis and the nomenclature of individual peroxidase (1 to 19) are shown in the table. The HPX15 gene ID and abbreviations of *Anopheles* species are adopted from the **Table 4.1.**

		AA	1	2	3	4	5	6	7	8	9	10	11	12	13	14	15	16	17	18	19
1	AalbHPX15	608		89.97	69.12	68.05	65.04	66.84	67.06	66.05	67.51	65.43	68.86	65.27	66.95	67.11	67.45	67.11	67.15	66.94	68.90
2	AdarHPX15	611	89.97		68.50	67.77	65.27	66.72	66.27	65.77	67.39	64.48	68.24	65.16	66.67	67.00	67.34	67.00	66.32	66.17	67.95
3	AatpHPX15	603	69.12	68.50		83.08	68.17	69.46	67.01	67.68	69.30	65.55	68.23	67.00	67.50	67.50	68.17	68.00	72.29	70.78	70.90
4	AsinHPX15	606	68.05	67.77	83.08		69.85	71.14	67.86	67.85	69.30	64.54	68.90	67.00	67.17	67.50	68.17	68.33	70.33	69.72	70.83
5	AsHPX15	597	65.04	65.27	68.17	69.85		86.74	78.91	78.62	79.36	69.24	74.79	75.34	76.51	76.17	76.85	76.51	68.83	71.31	73.28
6	AmacHPX15	596	66.84	66.72	69.46	71.14	86.74		78.88	81.11	82.18	71.55	75.76	75.29	76.64	76.13	76.81	76.81	69.46	73.45	73.91
7	AfunHPX15	588	67.06	66.27	67.01	67.86	78.91	78.88		82.42	84.01	71.55	76.32	74.49	75.00	75.00	75.51	75.34	69.57	72.40	73.21
8	AculHPX15	594	66.05	65.77	67.68	67.85	78.62	81.11	82.42		88.72	72.51	74.03	72.56	73.74	73.06	73.57	73.74	68.49	71.16	71.79
9	AminHPX15	596	67.51	67.39	69.30	69.30	79.36	82.18	84.01	88.72		73.45	76.81	76.17	77.52	76.85	77.35	77.18	69.04	72.61	73.74
10	AepiHPX15	596	65.04	64.48	65.55	64.54	69.24	71.55	71.55	72.51	73.45		78.28	72.82	74.33	73.99	74.16	73.99	67.71	69.19	69.81
11	AchrHPX15	598	68.86	68.24	68.23	68.90	74.79	75.76	76.32	74.03	76.81	78.28		82.27	83.11	83.44	83.11	82.44	70.35	71.14	72.61
12	AmelHPX15	602	65.27	65.16	67.00	67.00	75.34	75.29	74.49	72.56	76.17	72.82	82.27		94.85	95.35	95.18	94.68	69.52	70.35	71.98
13	AmerHPX15	602	66.95	66.67	67.50	67.17	76.51	76.64	75.00	73.74	77.52	74.33	83.11	94.85		97.51	97.51	97.01	70.56	72.03	73.32
14	AquaHPX15	602	67.11	67.00	67.50	67.50	76.17	76.13	75.00	73.06	76.85	73.99	83.44	95.35	97.51		98.50	98.01	70.56	72.03	73.49
15	AgHPX15	602	67.45	67.34	68.17	68.17	76.85	76.81	75.51	73.57	77.35	74.16	83.11	95.18	97.51	98.50		99.17	70.77	72.36	73.66
16	AarbHPX15	602	67.11	67.00	68.00	68.33	76.51	76.81	75.34	73.74	77.18	73.99	82.44	94.68	97.01	98.01	99.17		70.98	72.19	73.49
17	AnilHPX15	485	67.15	66.32	72.29	70.33	68.83	69.46	69.57	68.49	69.04	67.71	70.35	69.52	70.56	70.56	70.77	70.98		71.90	73.50
18	AdirHPX15	603	66.94	66.17	70.78	69.72	71.31	73.45	72.40	71.16	72.61	69.19	71.14	70.35	72.03	72.03	72.36	72.19	71.90		82.72
19	AfarHPX15	602	68.90	67.95	70.90	70.83	73.28	73.91	73.21	71.79	73.74	69.81	72.61	71.98	73.32	73.49	73.66	73.49	73.50	82.72	

Among these transcription binding factors, ecdysone is reported as a crucial regulator of many genes that are involved in insect development especially, during molting and metamorphosis (Akagi and Ueda, 2011; Swevers and Iatrou, 2003). The other two transcription factor binding sites, STAT and Rel, regulate the expression of those genes that are involved in development as well as in immunity (Gupta et al., 2009; Han and Ip, 1999). Grainy head (*grh*) transcription factor binding sites are conserved in vertebrates and invertebrates and regulate those genes that contribute to manage the impermeable apical layer in epithelia (Narasimha et al., 2008). With these facts, we assume that AsHPX15 gene might be participating in the mosquito development, tissue biogenesis and immunity.

4.3.4 AsHPX15 gene is induced in various stages of mosquito development

The expression pattern of AsHPX15 gene was determined in different developmental stages of the mosquito. For that, relative mRNA levels of AsHPX15 gene were analyzed by semi quantitative real-time PCR in eggs, all four instars larvae, pupae, adult males and females. Results presented in **Figure 4.5** revealed that AsHPX15 gene is expressed in all stages of the mosquito development, with the minimum expression in the eggs. The relative levels of AsHPX15 mRNA gradually increase to 9 folds and 19 folds in first and fourth instar larvae, respectively in comparison to the eggs. Interestingly, AsHPX15 expression levels are largely induced in the pupal stage of the development. Our analysis revealed that AsHPX15 mRNA levels increased 2126 folds in

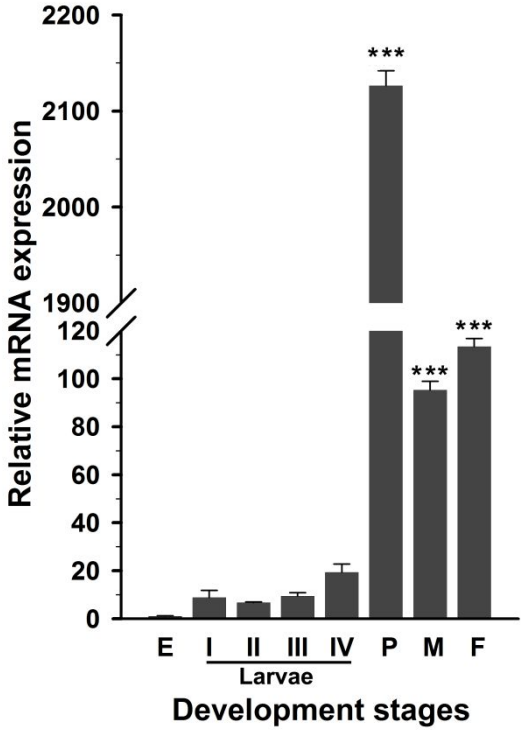

Figure 4.5: Relative AsHPX15 mRNA levels in different developmental stages. Results are representing the mean ± SD of relative mRNA levels in different developmental stages of *A. stephensi*. The mRNA expression levels of eggs were considered as controls. Significant differences ($P < 0.0001$) in the relative mRNA levels of different stages against controls are indicated by three asterisks.

pupae, 95 folds in adult males and 113 folds in adult females in comparison to the eggs. Our comparative statistical analysis revealed that the relative levels of AsHPX15 mRNA in pupae, males and females are highly significant in comparison to other stages of development (**Figure 4.5**). We believe that the induction of AsHPX15 in larvae and pupae might be due to the ecdysone hormone, which regulates larval molting and metamorphosis in mosquitoes in a way similar to other insects (Akagi and Ueda, 2011; Telang et al., 2007).

4.3.5 AsHPX15 is an early blood feeding induced midgut gene

The effect of blood feeding on the expression of AsHPX15 gene in different body compartments was analyzed by semi quantitative real time PCR. For that, we compared the relative levels of AsHPX15 mRNA in sugar or 24h post blood fed females midgut and carcass. In sugar fed mosquitoes, the relative levels of AsHPX15 mRNA are 45

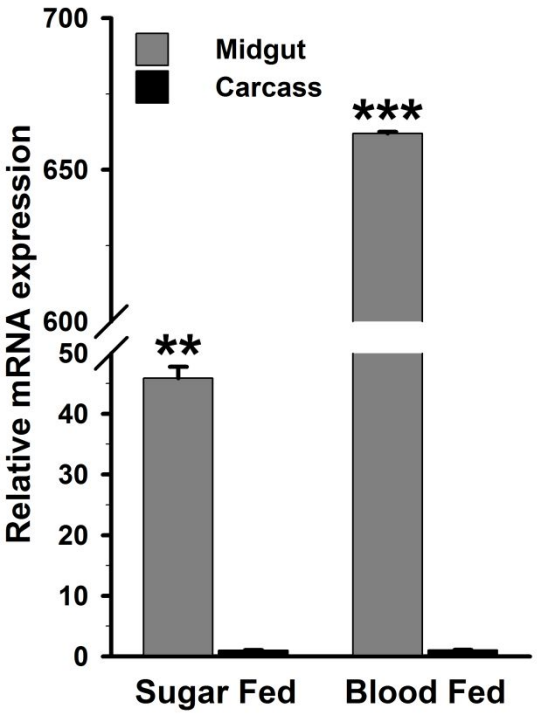

Figure 4.6: Relative mRNA levels of AsHPX15 in different mosquito body compartments. Relative mRNA expression levels were analyzed in midgut and carcass of sugar fed and 24h post blood fed female mosquitoes. The mRNA expression levels of sugar fed carcass were considered as controls. Significant differences where *P<0.001* and *P<0.0001* are indicated by two and three asterisks, respectively.

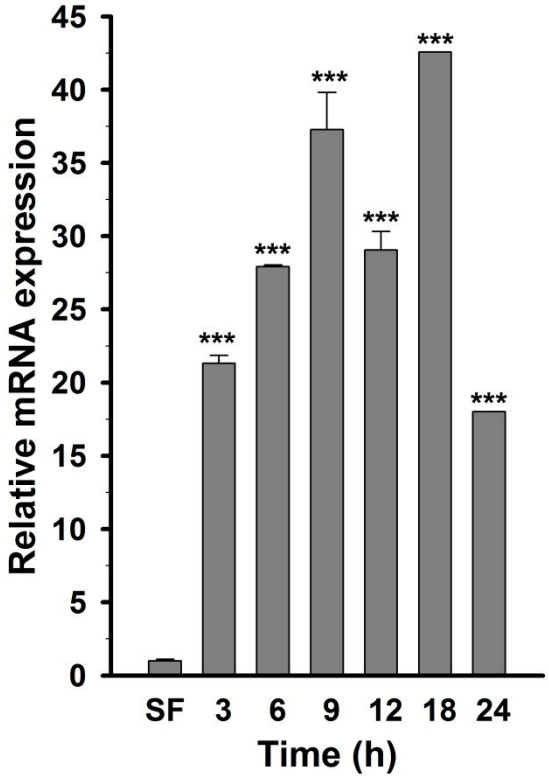

Figure 4.7: Expression kinetics of AsHPX15 gene in blood fed midguts. Relative levels of AsHPX15 mRNA were analyzed in sugar fed (SF) and blood fed midguts collected at various time points after blood feeding. The mRNA expression levels of sugar fed were considered as controls. Significant differences *(P<0.0001)* between each time point and controls are indicated by three asterisks.

folds higher in midgut in comparison to the carcass. After blood feeding the mRNA levels further increased to 670 times in midgut (**Figure 4.6**). However, there is no significant induction of AsHPX15 mRNA in the body wall of 24h blood fed females. In other words, the AsHPX15 mRNA levels are indifferent in the body wall before and after the blood feeding (**Figure 4.6**). Thus, AsHPX15 is exclusively expressed in midgut and induced by blood feeding.

To understand the expression kinetics of AsHPX15 gene, we analyzed its relative mRNA levels in the midgut at different time intervals after blood feeding. The results presented in **Figure 4.7** indicated that AsHPX15 is induced 20 times at 3h post blood feeding against the sugar fed controls. The mRNA expression of AsHPX15 gene in blood fed midguts is further induced with time and a maximum induction of 42 folds is observed at 18h. Afterwards, the relative mRNA levels of AsHPX15 are reduced at 24h. These results indicated that AsHPX15 is an early blood feeding-induced gene (**Figure 4.7**). These data are in agreement with the findings in *A. gambiae* where AgHPX15, an ortholog of AsHPX15, is an early blood feeding induced midgut gene (Kumar et al., 2010).

4.3.6 AsHPX15 is a secreted globular protein

Our sequence analysis revealed that AsHPX15 gene contains 1794 bp open reading frame (ORF) that encodes a 597 amino acids long protein. The SignalP analysis of AsHPX15 protein revealed the presence of a signal peptide (1-21 amino acids) at the N-terminal (**Figure 4.8**). The cleavage site for signal peptidase (SPase) is present between the amino acids 21 and 22 (VLS_{21}-$Q_{22}T$, the D=0.838. D cutoff=0.450). This indicated that AsHPX15 is a secreted protein. These findings are similar to the *A. gambiae* AgHPX15, which is also reported to be a secreted protein (Kumar et al., 2010). We also predicted the secondary structure of AsHPX15 protein with the help of Phyre^2 software. The resultant output revealed that AsHPX15 contains 44% alpha helix and 1% beta sheets (**Figure 4.8**). This indicated that AsHPX15 is a globular protein, as this category of proteins contains more alpha helices than beta sheets (Pace and Scholtz, 1998).

The deduced AsHPX15 polypeptide was also subjected to three-dimensional structural prediction by Phyre^2 software. Interestingly, 93% amino acid residues (554 amino acids) of the full-length protein (total 597 amino acids) were modeled with buffalo lactoperoxidase available in protein data bank (PDB ID:2GJM) with 100% level of

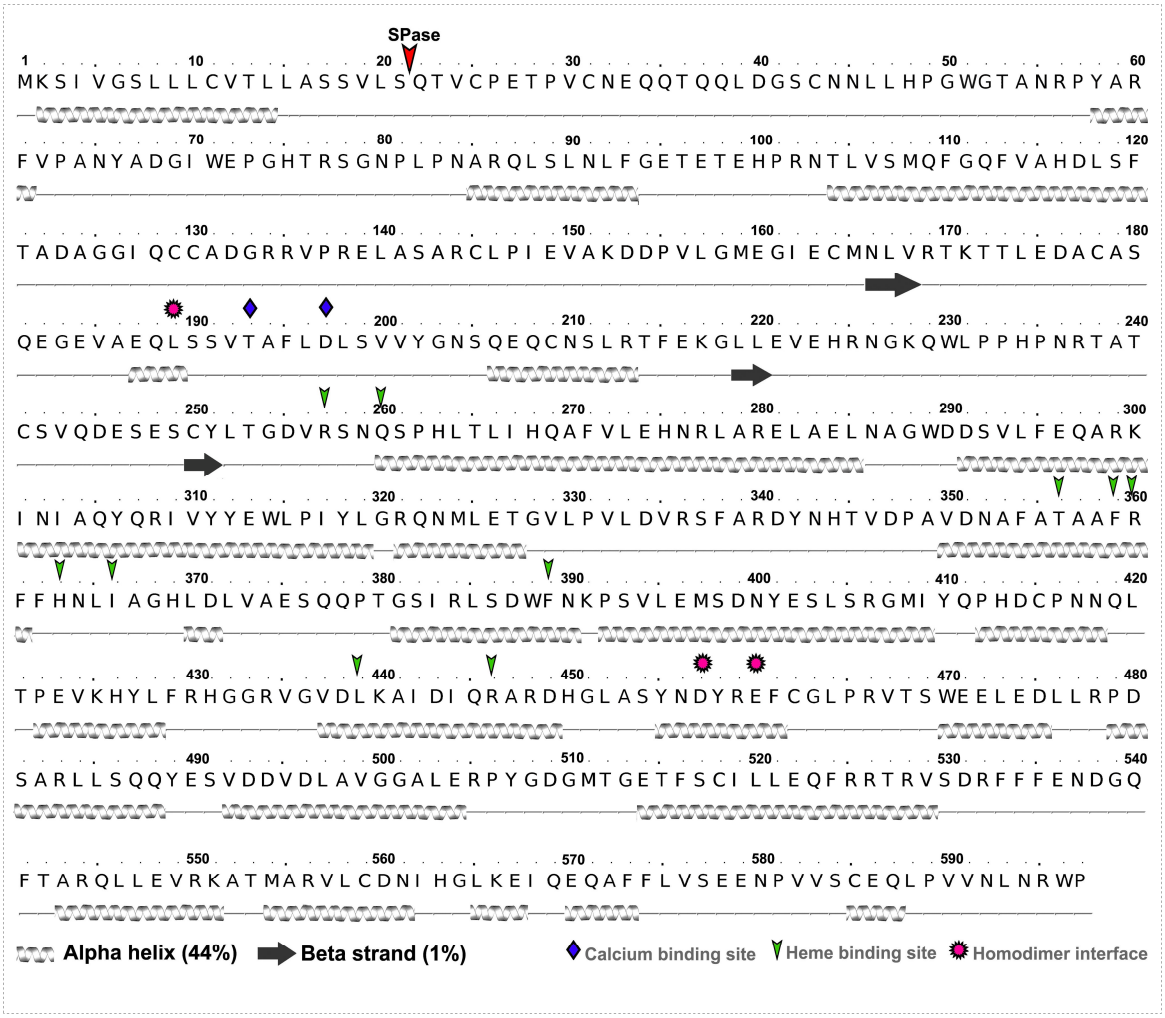

Figure 4.8: Deduced secondary structure of AsHPX15 protein. AsHPX15 protein contains 44% alpha helix (represented by spirals) and 1% beta sheets (shown by arrows) as predicted by Phyre[2] software. The red arrowhead indicates the cleavage site for signal peptidase (SPase) as predicted by the SignalP software. Various conserved binding sites in the protein are represented by characteristic symbols.

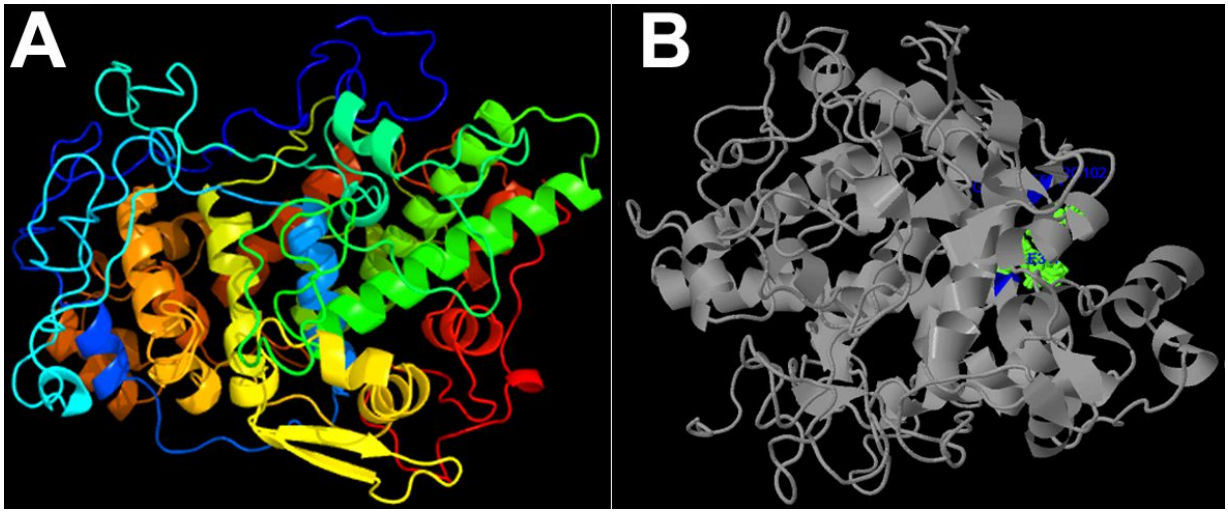

Figure 4.9: 3D structure analysis of AsHPX15 protein. A) 3D structure of AsHPX15 protein was predicted by Phyre[2] software using lactoperoxidase as template. **B)** Ligand binding site in AsHPX15 protein was predicted by 3DLigandSite server. The residues shown in blue color are the part of active site. The green color represents the ligand bound to the active site.

confidence (**Figure 4.9A**). The active site of AsHPX15 peroxidase enzyme consists of ARG_{102}, ILE_{317}, GLN_{571} and PHE_{574} as predicted by 3DLigandSite software using NAG (N-acetyl D-glucosamine) as heterogen (**Figure 4.9B**).

4.4 Discussion

In general, heme peroxidases play an important role in insect development and immunity (Shi et al., 2012). They catalyze tyrosine crosslinking, which is a fundamental feature of basal membranes and essential as an elemental mechanism of tissue biogenesis (Péterfi and Geiszt, 2014). In case of malaria vector similar mechanism of peroxidase-mediated crosslinking is also reported in different organs at various stages of development for example, sclerotization of the cuticle and crosslinking during chorion hardening (Andersen, 2010; Kajla et al., 2015a; Kumar et al., 2010; Li and Li, 2006).

In *A. gambiae* midgut, a heme peroxidase AgHPX15 (AGAP013327) catalyzes tyrosine crosslinking of the mucin layer to form a physical barrier that creates a 'low immunity' zone in the midgut lumen area to support the growth of endogenous bacteria and the progression of food digestion without the activation of mosquito immunity (Kajla et al., 2015a). The malaria parasite *Plasmodium* takes advantage of this low immunity zone to support its own development.

To understand the specific features of HPX15 gene in the Indian major malaria vector we cloned the full-length AsHPX15 gene (KT825861) and its general BLAST provided the closest match to *A. gambiae* AgHPX15 (AGAP013327) gene (e value 0 and 77% identity). Our results also revealed that full length HPX15 gene is also conserved among worldwide-distributed 19 anophelines and these HPX15 orthologs share 65-99% amino acids identity (**Table 4.2**). The full-length AsHPX15 protein has several identical features that are common to *A. gambiae* AgHPX15 protein. For example, both these orthologs have characteristic identity to the peroxinectin-like conserved domain of animal heme peroxidases superfamily. In addition, the calcium binding, heme binding, putative substrate binding and homodimer interface sites are also identical between AsHPX15 and AgHPX15 (**Figure 4.4**). These properties revealed that HPX15 is a unique and evolutionary conserved anopheline-specific molecule that may serve as a common target to arrest malaria parasite development inside the insect host.

AsHPX15 gene is induced in different developmental stages of mosquito such as, larvae and pupae (**Figure 4.5**). This might indicate that AsHPX15 is playing an important role in the mosquito development. It is of note that in case of larvae each

instar stage is completed with molting that includes formation of a new cuticle and its sclerotization. This process is governed by ecdysone, a steroidal hormone, which is secreted by the prothoracic glands. In addition, pupa is the transient stage of mosquito development where metamorphosis takes place and the role of ecdysone hormone in regulation of this process is also reported in mosquitoes as well as other insects (Akagi and Ueda, 2011; Telang et al., 2007). Thus, we believe that increased ecdysone activity in larvae and pupae might be one of the factors regulating AsHPX15 gene expression. Our *in silico* analysis of AsHPX15 gene regulatory region revealed the transcription binding sites for ecdysone (**Figure 4.3**) that explain the expression profile of this gene in different developmental stages (**Figure 4.5**).

Interestingly, the ecdysone levels increase soon after the blood feeding in the insect body (Swevers and Iatrou, 2003). Thus, we speculated that this hormone might be initiating the early expression of AsHPX15 gene in blood fed mosquito midguts (**Figures 4.6** and **4.7**). The exclusive induction of AsHPX15 gene in midgut might be regulated by the presence of Grainy head (*grh*) transcription factor binding site in its regulatory region (**Figure 4.3**). In general, the transcription factors of Grainy head family are required to generate the impermeable apical layer in epithelia that protects the epithelium against the external environment (Narasimha et al., 2008)**.** In other words, the Grainy head regulated genes contribute the barrier properties to the epithelia. It is evident in *Drosophila* that the absence of *grh* causes altered morphology of epithelia with suppressed expression of enzymes that cross-link the apical extracellular matrix (Bray and Kafatos, 1991; Mace et al., 2005). Our analysis also revealed the presence of N-terminal signal peptide in AsHPX15 protein (**Figure 4.8**). Thus, we believe that it is secreted into the midgut lumen and might be playing a crucial role in tyrosine crosslinking of the mucin layer at the surface of the midgut epithelium in a way similar to AgHPX15 protein (Kumar et al., 2010).

It is interesting to note that the increased levels of ecdysone also stimulate the expression of immune molecules in mosquito hemolymph. For example, an immune protein LRIM9 is upregulated by blood feeding or by the inoculation of ecdysone into the hemolymph of *Anopheles* mosquito (Upton et al., 2015). Thus, the orchestrated action of ecdysone prepares the mosquito body to opt for the physiological changes induced after the blood feeding. In one way, the HPX15-mediated crosslinking of mucin layer strengthen the epithelial layer and finely tune the system to balance the process of digestion and immunity in parallel. On the other hand, the induction of immune molecules in hemolymph might be related to the pre-preparedness against the blood-

borne pathogens, if they breach the midgut barrier and reach this site. In addition, the HPX15-mediated midgut barrier also inhibits the interaction of proliferating natural gut flora with the immunoreactive gut epithelium therefore, the induction of HPX15 gene in the blood fed midgut is univocally a favorable phenomenon for the mosquito physiology.

A recent report also indicated an interesting finding that *A. gambiae* AgHPX15 crosslinks proteins in other compartments such as, spermatheca of the inseminated females under the regulation of sexually transferred 20-hydroxy-ecdysone (20E) hormone. This phenomenon is essential to manage the functionality of stored sperms and their long-term fertility (Shaw et al., 2014). Based on these observations, we believe that the inhibition of HPX15 function will be beneficial in many ways and can be easily achieved through gene knockout or antibody-mediated inhibition as reported for other mosquito targets (Dinglasan et al., 2003; Shahabuddin et al., 1998).

4.5 Conclusion

In conclusion, HPX15 is a unique gene that is exclusively present in the genome of nineteen species of *Anopheles* mosquitoes. AsHPX15 is 1941 bp long gene, which has different binding sites in its 5' UTR region and codes for a 597 amino acids long globular secretory protein. It has a crucial role in the mosquito development and general immunity. The highly conserved nature of HPX15 protein might designate it as a common target to arrest the malaria parasite development inside anopheline vectors.

Chapter 5

Silencing of *Anopheles stephensi* Heme Peroxidase HPX15 Activates Diverse Immune Pathways to Regulate the Growth of Midgut Bacteria

5.1 Abstract

Anopheles mosquito midgut harbors a diverse group of endogenous bacteria that proliferate extensively after the blood feeding and help in food digestion and nutrition in many ways. Although, the growth of endogenous bacteria is regulated by various factors, however, the robust antibacterial immune reactions are generally suppressed in this body compartment by a heme peroxidase HPX15 crosslinked mucins barrier. This barrier is formed on the luminal side of the midgut and blocks the direct interactions and recognition of bacteria or their elicitors by the immune reactive midgut epithelium. We hypothesized that in the absence of HPX15, an increased load of exogenous bacteria will enormously induce the mosquito midgut immunity and this situation in turn, can easily regulate mosquito-pathogen interactions. In this study, we found that the blood feeding induced HPX15 gene in *Anopheles stephensi* midgut and promoted the proliferation of endogenous as well as exogenous fed bacteria. In addition, the mosquito midgut also efficiently regulated the growth of these bacteria through the induction of classical Toll and Imd immune pathways. In case of AsHPX15 silenced midguts, the proliferation of midgut bacteria was largely reduced through the induction of nitric oxide synthase (NOS) gene, a downstream effector molecule of the JAK/STAT pathway. Interestingly, no significant induction of the classical immune pathways was observed in these midguts. Importantly, the NOS is a well known negative regulator of *Plasmodium* development, thus, we proposed that the induction of diverged immune pathways in the absence of HPX15 mediated midgut barrier might be one of the strategies to manipulate the vectorial capacity of *Anopheles* mosquito.

5.2 Introduction

Mosquito midgut is the first organ where mosquito-parasite interactions are initiated. In the midgut, *Plasmodium* undergoes a series of complex developmental transitions and majority of parasites are killed during this process (Sinden and Billingsley, 2001; Ghosh et al., 2000; Pradel, 2007). It is of note that the number of *Plasmodium* is regulated by the ingested blood factors as well as mosquito innate immunity (Lensen et al., 1998; Ramiro et al., 2011; Simon et al., 2013; Michel and Kafatos, 2005; Vlachou et al., 2005). Several studies revealed that wild type or laboratory reared mosquito midgut is housed by a variety of bacteria (Kajla et al., 2015a; Minard et al., 2013) and their interaction with different development stages of *Plasmodium* also determines the mosquito cycle of the parasite (Cirimotich et al., 2011a; Touré et al., 2000; Wang et al., 2011; Boissière et al.,

2012; Dong et al., 2009). In addition, the type and number of bacteria also vary during different development stages and habitat of the mosquito (Kajla et al., 2015a; Minard et al., 2013; Wang et al., 2011). Researchers exploited these findings to identify the mosquito gut-specific symbionts that can regulate *Plasmodium* development (Boissière et al., 2012). Gram-negative bacteria (for example, *Serratia marcescens, Entobacter* species such as *E. amnigenus, E. cloacae, E. sakazaki*) have been identified in anophelines midgut that inhibit *Plasmodium falciparum or P. vivax* sporogonic development. Mosquitoes treatment with antibiotics reduced the number of midgut bacteria that, in turn, reversed their effect on *Plasmodium* development (Pumpuni et al., 1993 and 1996; Beier et al., 1994; Gonzalez-Ceron et al., 2003; Cirimotich et al., 2011b). Interestingly, in an artificial feeding, the co-infection of bacteria with *Plasmodium* in field collected or lab-reared mosquitoes also reduced the number of developing parasites (Dong et al., 2009; Cirimotich et al., 2011b). Thus, understanding the mechanisms behind these regulations will provide an excellent tool to develop *Plasmodium* control strategies. Earlier reports indicated that the bacteria suppressed *Plasmodium* infection through numerous mechanisms. For example, various enzymes and toxins produced by bacteria or the mosquito immunity or reactive oxygen species (ROS) induced against bacteria might kill the parasite (Dong et al., 2009; Pumpuni et al., 1993; Cirimotich et al., 2011b; Azambuja et al., 2005).

It is noteworthy to mention that the endogenous bacteria proliferate extensively after the blood feeding. In addition, the feeding of exogenous bacteria supplemented blood also increases bacterial burden in the mosquito midgut. However, the midgut has a remarkable capacity to manage the midgut environment in a way to minimize the deleterious effects of the increased bacterial load (Kajla et al., 2015a; Dong et al., 2009; Gupta et al., 2009; Meister et al., 2009; Warr et al., 2008). Recent studies in *A. gambiae* mosquito identified a mechanism that modulates the innate immunity against bolus bacteria (Kajla et al., 2015a; Kumar et al., 2010). In these mosquitoes, a heme peroxidase AgHPX15 catalyzes the crosslinking of a mucin layer at the luminal surface of the midgut epithelium. This crosslinked mucin acts like a barrier to block the interaction of bolus bacteria or bacterial elicitors with the immune reactive midgut epithelium. This mechanism also provides a protected environment for the development of *Plasmodium* inside the midgut. Interestingly, AgHPX15 silencing resulted in induction of key antibacterial immune genes and decreased bacterial load in the midgut (Kajla et al., 2015a; Kumar et al., 2010). In addition, the reduction of *Plasmodium* development was also evident in these silenced midguts. It is also noteworthy to mention that HPX15

is a unique anopheline-lineage specific gene and its orthologs are absent in insects and human however, they are present in the genome of nineteen worldwide distributed species of *Anopheles* mosquito and share 65-99% amino acids identity (Kajla et al., 2015b and 2016).

These facts prompted us to develop a hypothesis that an increased load of exogenous bacteria in HPX15 silenced midguts will markedly induce the mosquito immunity due to the uninterrupted interactions of bacterial elicitors with the immune reactive midgut epithelium. Exploitation of this mechanism will be helpful to manipulate the vectorial capacity of the insect host. Thus, in the present study, we analyzed the mechanism of immunomodulation in the HPX15 silenced *Anopheles stephensi* midguts to understand the overview of microbial interactions with the mosquito defense system in this body compartment.

5.3 Results

5.3.1 Exogenously fed bacteria proliferate in mosquito midgut

Mosquito midgut is housed by a diverged group of naturally acquired (endogenous) bacteria. The majority of these bacteria are Gram-negative and their proliferation is induced after blood feeding (Wang et al., 2011; Boissière et al., 2012; Rani et al., 2009; Chavshin et al., 2012). In parallel, the blood feeding also induces the formation of peritrophic matrix, an acellular barrier that separates blood bolus from the midgut epithelium (Kumar et al., 2010; Injera et al., 2013). Additionally, a heme peroxidase HPX15 crosslinked mucin barrier on the luminal surface of the epithelium also help to maintain a low immunity zone in the blood fed midgut to support the growth of endogenous bacteria (Kajla et al., 2015a; Kumar et al., 2010). We were interested to understand the relationship between the growth of exogenous fed bacterial and midgut immune responses in the presence of HPX15 crosslinked mucin barrier. For that, the adult females were fed on blood supplemented without or with a mixture of $Gram^+$ (*Micrococcus luteus*) and $Gram^-$ (*Escherichia coli*) bacteria and the proliferation kinetics of midguts bacteria was analyzed. Results presented in **Figure 5.1** revealed that the relative levels of 16S rRNA for endogenous bacteria increased 25 folds after 3 h of blood feeding when compared to the sugar fed midguts (p=0.010). Afterwards, the endogenous bacteria proliferated 1900, 133 and 270 times after 6 h, 12 h and 18 h of blood feeding, respectively against the sugar fed controls (**Figure 5.1**). This showed significant reduction in the levels of endogenous bacteria at 12 h (p=0.0008) and 18 h (p=0.0011) when compared to the 6h blood fed midguts. Furthermore, the endogenous

bacteria levels increased 7000 times in 24 h blood fed midguts in comparison to the sugar fed midguts (**Figure 5.1**). These results are in agreement with previous findings where an increase in endogenous bacteria was observed after 6 h of blood feeding and that further followed the similar growth pattern (Kumar et al., 2010; Luckhart et al., 1998).

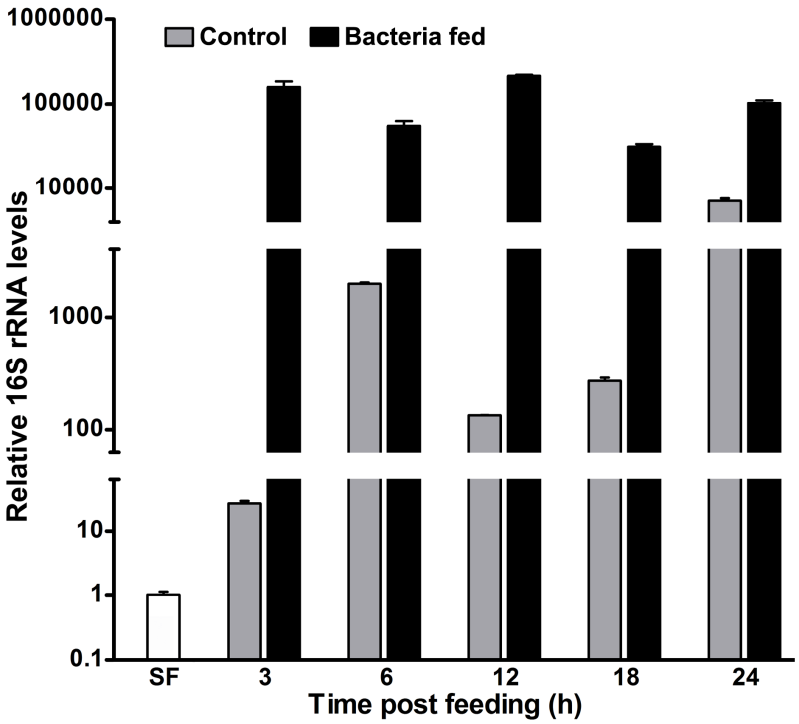

Figure 5.1: The kinetics of 16S rRNA levels in blood fed mosquito midguts. Mosquitoes were fed either on blood alone (controls) or supplemented with a mixture of *M. luteus* and *E. coli* bacteria (10^9 cells/ml blood). The relative levels of 16S rRNA were analyzed in the pool of mosquito midguts collected at different time interval after the feeding and represented here in $\log_{10}$ scale

Parallelly, in case of exogenous bacteria fed midguts, the relative levels of 16S rRNA were hundred fifty thousand folds at 3 h in comparison to the sugar fed midguts (**Figure 5.1**). Interestingly, the relative 16S rRNA levels were indifferent at 6 h (p=0.0645) and 12 h (p=0.1696), respectively when compared to 3 h post bacteria fed midguts. However, the expression levels of 16S rRNA gene at 18h were reduced 5 folds (p= 0.0041) against 3 h post fed midguts (**Figure 5.1**). Thus, these altered levels of 16S rRNA at different time points indicated that the growth of bacteria is regulated rhythmically, most probably by the midgut immunity.

It is noteworthy to mention that in our study, we fed a large amount of bacteria (10^9 bacterial cells/ml blood) to the mosquitoes. The comparative levels of 16S rRNA revealed that the exogenously bacteria fed midguts have 28 folds and 15 folds higher bacteria load at 6 h and 24 h, respectively when compared to the just blood fed midguts (**Figure 5.1**). The reduction in the fold ratio at 24 h seems to be due to the decreased levels of 16S rRNA in exogenous bacteria fed midguts and increased levels of endogenous bacteria in the corresponding blood fed controls. This might indicate that the midgut environment is particularly favorable for the growth of endogenous bacteria in comparison to the exogenous fed microbes.

5.3.2 HPX15 gene is induced in bacteria fed midguts

Previously we found that the heme peroxidase HPX15 gene is highly induced in *Anopheles gambiae* or *A. stephensi* blood fed midguts (Kajla et al., 2016a; Kumar et al., 2004). This molecule is important to suppress the immune activation and facilitating the growth of endogenous bacteria in the blood fed midguts (Kajla et al., 2015a; Kumar et al., 2010). We also analyzed the expression kinetics of AsHPX15 gene in the midguts that are mentioned in **Figure 5.1**. We found that AsHPX15 gene was induced 23 folds and 27 folds at 6 h and 12 h post blood feeding, respectively when compared to the sugar fed midguts (**Figure 5.2**). The induction of AsHPX15 gene in 6 h post bacteria supplemented blood fed midguts was similar to the blood fed controls (p=0.6485). However, its expression levels were reduced drastically at 12 h and 18 h in bacteria fed midguts against blood

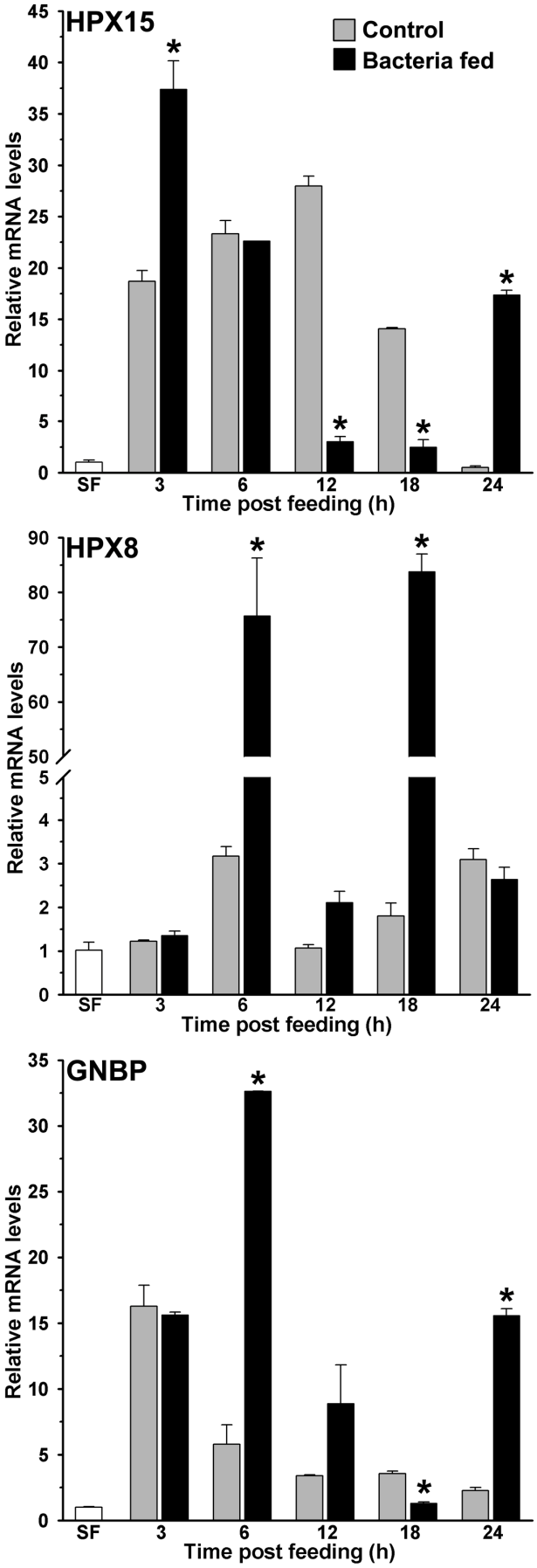

Figure 5.2: Expression kinetics of heme peroxidases and pattern recognition receptor (PRR) in bacteria fed midguts. The kinetics of relative mRNA levels of AsHPX15, HPX8 or GNBP gene were analyzed in the blood alone (controls) or supplemented with a mixture of *M. luteus* and *E. coli* bacteria fed midguts. Significant differences in the gene expressions between control and bacteria fed midguts are denoted by asterisks.

fed controls (p=0.0018 for 12 h and p=0.0038 for 18 h**)**. Interestingly, HPX15 mRNA levels were relatively higher at 3 h and 24 h post bacteria fed midguts against the blood fed controls. Thus, the heavy load of exogenous bacteria in the midgut had no effect on the early phase of AsHPX15 gene expression (**Figure 5.2**). This may be simply due to the regulation of this gene by ecdysone hormone, which is induced in blood fed mosquitoes as reported before (Kajla et al., 2016). We also believed that HPX15 catalyzed mucin barrier might be completed or its formation started within first 12 h of post blood feeding because the presence of mucin and HPX15 protein is detected at the luminal surface of *A. gambiae* midgut epithelium by this time (Kumar et al., 2010; Injera et al., 2013). On the other hand, if the mucin barrier formation is completed and it suppresses the midgut antibacterial immunity, then the over proliferation of exogenous bacteria might be lethal for the mosquito. However, we found that the mortality in blood fed controls and exogenous bacteria fed mosquitoes were indifferent. This indicated that mosquito gut immunity is capable of counteracting the increased load of bacteria without compromising its survival.

5.3.3 The antibacterial heme peroxidase HPX8 is induced in exogenous bacteria fed midguts

Our results revealed that the exogenously fed bacteria not only proliferate in the mosquito midgut, their number is also regulated at different time points (**Figure 5.1**). Thus, we hypothesized that some of the immune genes might be controlling the overgrowth of bacteria in these midguts. To test this concept, we analyzed the expression of a heme peroxidase HPX8, which has been reported to be an antibacterial gene in *A. gambiae* (Kumar et al., 2010). Results presented in **Figure 5.2** revealed that HPX8 mRNA is induced 25 folds and 42 folds at 6 h and 18 h, respectively in bacteria fed midguts against the blood fed controls (p=0.0206 for 6h and p=0.0015 for 18h) however, at other time points, HPX8 mRNA levels in test and controls were indifferent. This induction pattern of HPX8 gene (**Figure 5.2**) corroborated with the bacterial 16S rRNA levels in these midguts (**Figure 5.1**). These findings indicated that HPX8 is one of the candidate genes that participate in the midgut antibacterial immunity.

5.3.4 Classical immune pathways are induced in exogenous bacteria fed midguts

In insects Gram-negative binding protein (GNBP) acts like the pattern recognition receptor (PRR) and triggers classical innate immunity through Toll or Imd pathway

against Gram-positive or Gram-negative bacteria, respectively (Lemaitre et al., 1995; Michel et al., 2001; Waterhouse et al., 2007; Osta et al., 2004). In anopheline mosquitoes, several isoforms of GNBP have been identified (Warr et al., 2008; Osta et al., 2004; Dimopoulos et al., 1998; Christophides et al., 2002) thus, we designed a set of common primers to detect the expression of any given isoform of GNBP in our study (primer sequences are provided in **Table 2.1**). Our analyses revealed that mRNA levels of GNBP were induced ~17 folds after 3 h of blood feeding when compared to the sugar fed midguts and that remained unaffected by the presence of bacteria in the blood (**Figure 5.2**). However, at 6 h and 12 h post bacteria feeding, the relative mRNA levels of GNBP were 6 folds and 2 folds higher, respectively against the normal blood fed controls (**Figure 5.2**). Furthermore, the relative mRNA levels of GNBP were 7 folds higher in 24 h post bacteria fed midguts in comparison to the blood fed controls (**Figure 5.2**, p=0.0019). These findings indicated that GNBP induction represents two episodes, an early event around 6 h and a late phase expression around 24 h post bacteria feeding. Thus, to further explore the immune regulatory mechanism that balances the mosquito midgut immunity against exogenous bacteria, these two time points were further analyzed in detail.

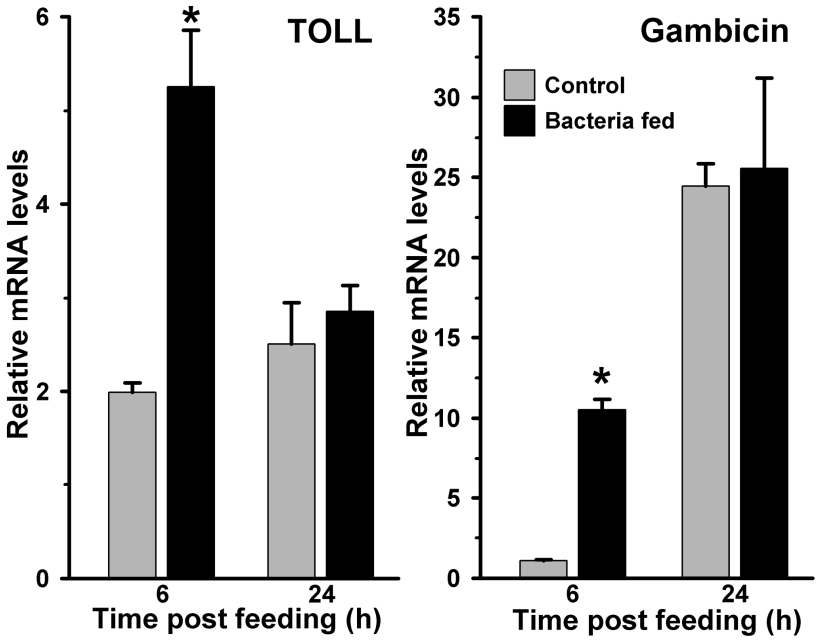

Figure 5.3. Expression of Toll and gambicin immune genes in bacteria fed *Anopheles stephensi* midguts. mRNA levels of midgut Toll or gambicin gene were analyzed at 6 h and 24 h after feeding the blood alone (controls) or supplemented with a mixture of *E. coli* and *M. luteus*. Relative levels of mRNA are presented against the sugar fed midguts. Significant differences in the gene expression levels are shown by asterisk.

We studied the induction of Toll and Imd pathways in the above-mentioned samples those were collected at early 6 h and late 24 h post feeding. The gene expression analyses revealed that the Toll mRNA levels were ~3 folds higher in the 6 h post bacteria fed midguts in comparison to the blood fed controls (**Figure 5.3**, p=0.036). However, the induction of this gene was indifferent at 24 h in those samples (p=0.563). In addition, we also analyzed the

expression of gambicin in these samples. Gambicin is an effector antimicrobial peptide, which is regulated by both Toll and Imd pathways (Vizioli et al., 2001). The results presented in **Figure 5.3** revealed that gambicin was induced 10 folds higher in 6 h post bacteria fed midguts when compared to the blood fed controls (p= 0.004). Although, gambicin expression is further induced in 24 h post bacteria fed midguts however, these levels were similar to the blood fed controls (p=0.294). Because gambicin is effective against both $Gram^+$ and $Gram^-$ bacteria thus, its expression at early and late time points corroborate with the increased number of midgut bacteria (compare **Figures 5.1** and **5.3**). In conclusion, the induction of classical Toll and Imd immune pathways regulate the proliferation of bacteria in blood fed midguts.

5.3.5 JAK/STAT pathway is not induced in exogenous bacteria fed midguts

Another mosquito immune pathway, known as JAK/STAT, is also reported to involve in gut immunity against a variety of pathogens (Gupta et al., 2009; Kumar et al., 2010). In this pathway, the receptor mediated activation of tyrosine kinases (JAKs) initiates the phosphorylation of cytosolic STAT (Signal transducer and activator of transcription) proteins. The phosphorylated STATs make dimer and upon translocation into the nucleus, they regulate the expression of numerous immune genes. One of such STAT-mediated effector gene nitric oxide synthase (NOS) is reported to play a crucial role in controlling the pathogenic development in *Anopheles* mosquito (Gupta et al., 2009; Kumar et al., 2010; Bahia et al., 2011). We were also interested to understand the activation of STAT pathway in exogenous bacteria

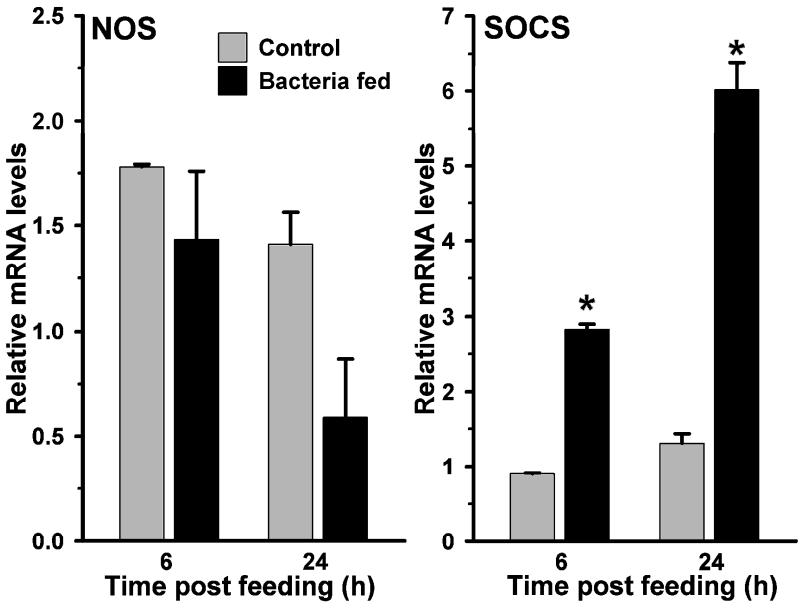

Figure 5.4: Expression of NOS and SOCS immune genes in bacteria fed *Anopheles stephensi* midguts. Midgut mRNA levels of NOS or SOCS gene were analyzed at 6 h and 24 h after feeding the blood alone (controls) or supplemented with a mixture of *E. coli* and *M. luteus*. Relative levels of mRNA are presented against the sugar fed midguts. Significant differences in the gene expression levels are shown by an asterisk.

fed midguts. Results presented in **Figure 5.4** revealed that the NOS mRNA levels in 6 h and 24 h post bacteria fed midguts were indifferent from the blood fed midguts (p=0.399 at 6 h and p=0.123 at 24 h). Collectively, these results suggested that NOS is not induced in the midgut against exogenous fed bacteria. Thus, we believed that STAT pathway does not participate in the midgut antibacterial immunity and confirms the previous findings as reported in other mosquitoes (Gupta et al., 2009; Kumar et al., 2010; Agaisse and Perrimon, 2004).

We hypothesized that either the STAT pathway in above-mentioned midguts remain uninduced or it is suppressed by the bacteria through some specific mechanism. For that, we analyzed the expression of the suppressor of cytokine signaling (SOCS) gene, which is a downstream feedback repressor of the STAT pathway (Gupta et al., 2009; Wormald and Hilton, 2004; Dhawan et al., 2015). Interestingly, the SOCS is induced ~4 folds and ~5 folds at 6 h and 24 h, respectively in the bacteria fed midguts against blood fed controls (**Figure 5.4**, p=0.001 for 6 h and p=0.006 for 24 h). These results revealed that the induction of SOCS gene in bacteria fed midguts might be responsible for inhibiting the activation of STAT pathway and NOS expression in a way similar to other systems (Demirel et al., 2013; Zhang et al., 2011; Maehr et al., 2014).

5.3.6 HPX15 silencing suppressed the proliferation of exogenous bacteria in the midgut

We were interested to understand the mosquito midgut immune regulation against high load of the exogenous bacteria when HPX15 crosslinked mucin barrier formation is suppressed. For that, we silenced AsHPX15 gene through dsRNA-mediated interference as discussed in Materials and Methods.

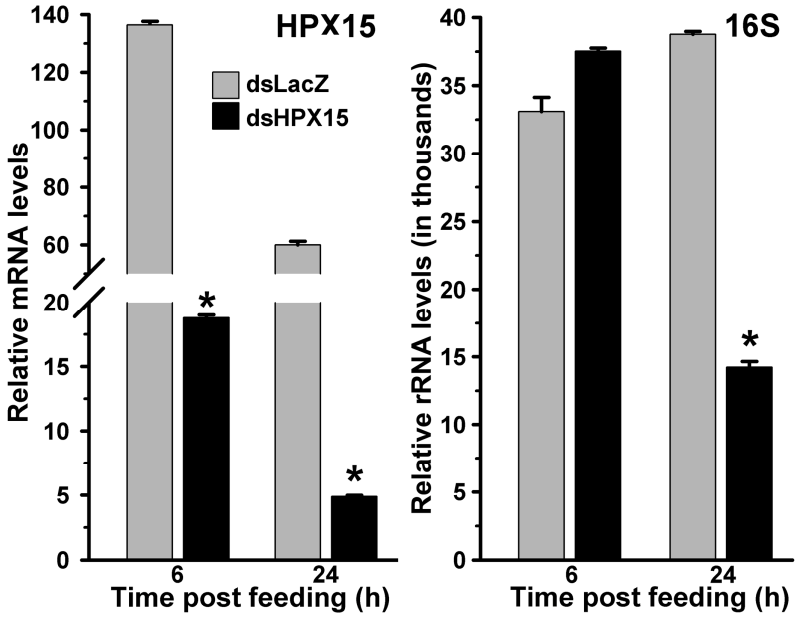

Figure 5.5: Relative levels of AsHPX15 mRNA and 16S rRNA in bacteria fed HPX15 silenced midguts. Mosquitoes injected with dsLacZ (controls) or dsHPX15 (silenced) were fed on bacteria supplemented blood and relative levels of AsHPX15 mRNA and 16S rRNA were analyzed in their midguts at different time points after feeding. Relative levels are presented against the sugar fed midguts. Significant differences are shown by an asterisk.

Silenced mosquitoes were fed on blood supplemented with bacteria (a mixture of *M. luteus* and *E. coli*). The midguts were collected at early 6 h and late 24 h post feeding to analyze the expression profiling of the immune genes as mentioned above. Our analysis of HPX15 mRNA levels in controls and silenced midguts revealed that this gene was silenced in the range of 80-90% (**Figure 5.5**). The relative 16S rRNA levels in controls and silenced midguts were similar at 6 h post feeding (p=0.053). However, at 24 h post feeding there was a 63% reduction in the 16S rRNA levels in the silenced midguts against the unsilenced controls (**Figure 5.5**, p=0.0004). Thus, AsHPX15 silencing reduces the overall proliferation of bacteria in the midgut bolus that might include the endogenous as well as exogenous bacteria. These findings are in partial agreement with previous reports where silencing of *A. stephensi* HPX15 ortholog drastically reduced the proliferation of endogenous bacteria in *A. gambiae* midguts (Kajla et al., 2015a; Kumar et al., 2010).

5.3.7 Classical antibacterial immune genes are suppressed in AsHPX15 silenced midguts

To understand the immune regulation of bacteria in the AsHPX15 silenced midguts, we analyzed the expression profile of important classical immune pathways. Results presented in **Figure 5.6** revealed that the mRNA levels of the pattern recognition

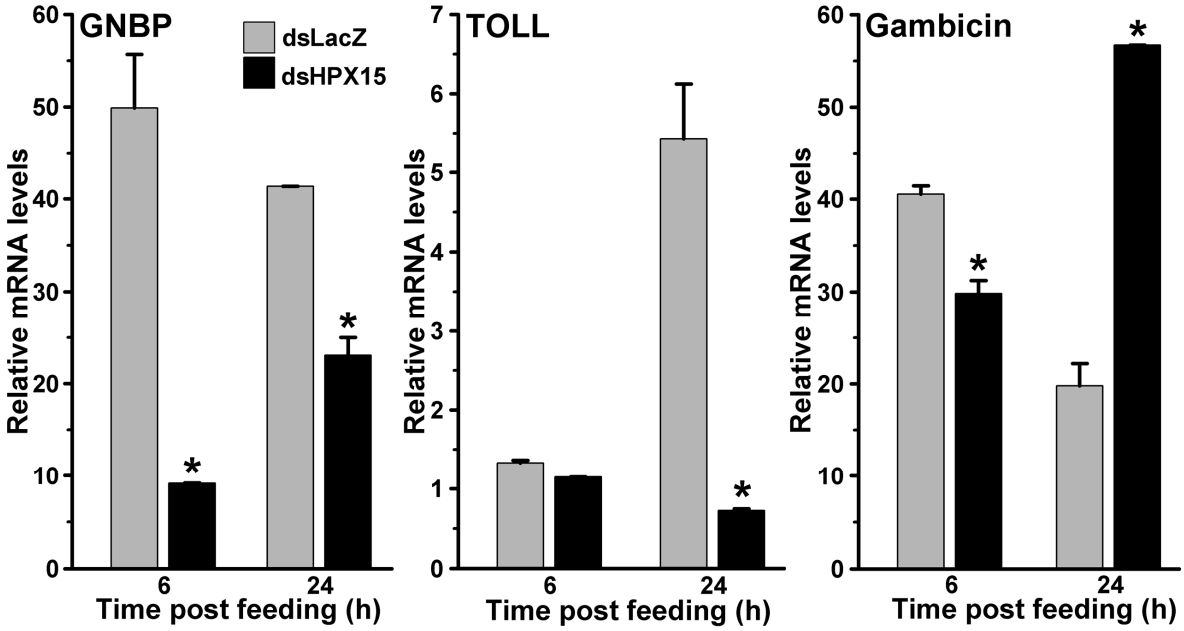

Figure 5.6: Expression of classical immune pathway genes in AsHPX15 silenced and bacteria fed midguts. Mosquitoes injected with dsLacZ (controls) or dsHPX15 (silenced) were fed on bacteria supplemented blood and relative mRNA levels of GNBP, Toll or gambicin gene were analyzed in their midguts after 6 h and 24 h post feeding. Relative levels of mRNA are presented against the sugar fed midguts. Significant differences between dsLacZ and dsAsHPX15 samples are shown by an asterisk.

receptor GNBP were reduced significantly in silenced midguts at 6 h (p=0.005) and 24 h (p=0.0111) post bacteria feeding, when compared to their respective unsilenced controls. Thus, the reduced levels of GNBP expression in silenced midguts might reflect the compromised situation for the recognition and induction of classical immune pathways. This fact was further confirmed after analyzing the gene expression of Toll and Imd pathways in these samples. We found that the levels of Toll mRNA were indifferent in silenced and control midguts after 6 h of bacteria feeding (**Figure 5.6**, p=0.123). However, Toll mRNA levels were suppressed seven folds in the silenced midguts than controls at 24 h post bacteria feeding (p=0.0209). These results revealed that Toll pathway is not induced in HPX15 silenced midguts neither at early nor at late stage of post bacteria feeding. Furthermore, we analyzed the expression of gambicin in these HPX15 silenced samples. We observed that the expression of gambicin gene was significantly downregulated in the silenced midguts after 6 h post feeding against controls (**Figure 5.6**, p=0.023). Interestingly, at 24 h post feeding the expression of gambicin gene was induced ~3 folds in silenced midguts in comparison to the controls (p=0.004). These findings suggested that the induction of gambicin in 24 h silenced midguts might be regulated by some other mechanism(s) that is different from classical Toll and Imd pathways.

5.3.8 JAK/ STAT pathway is induced in AsHPX15 silenced midguts against exogenous bacteria

We further examined the JAK/STAT pathway genes in controls and AsHPX15 silenced midguts to understand the involvement of this pathway in antibacterial immunity. For that, we compared the expression of STAT pathway genes in silenced or sham treated mosquito midguts after bacteria supplemented blood feeding. Results presented in **Figure 5.7** revealed that NOS and SOCS genes were induced 15 folds and 3 folds, respectively in the silenced midguts after 6 h of bacteria feeding when compared to the controls (p=0.0002 for NOS and p<0.0001 for SOCS expression). However, the expressions of both these genes in the silenced midguts were reduced 4 folds and 1.3 folds, respectively after 24 h post feeding against unsilenced controls (p<0.0001 for NOS and p=0.068 for SOCS expression). This pattern of NOS and SOCS expression indicated the activation of STAT pathway in silenced midguts. Interestingly, the profile of NOS expression also corroborated with the levels of bacteria in the silenced midguts (Comparing **Figures 5.5** and **5.7**). We believed that the induced NOS during early hours (6 h, **Figure 5.7**) might be responsible for reducing the levels of bacteria at later time

points (24 h, **Figure 5.5**) as this gene is reported to play an antibacterial role in mosquitoes as well as other insects (Hillyer and Este´vez-Lao, 2010). These results collectively revealed that STAT pathway is actively engaged in antibacterial immunity in the AsHPX15 silenced *A. stephensi* midguts. This effect might be due to the reduction of HPX15 catalyzed mucin barrier crosslinking and that, in turn, allows direct interaction of bacteria or bacterial elicitors with immune reactive midgut epithelium. These findings are in agreement with the previous reports where NOS played an antibacterial role in HPX15 silenced *A. gambiae* mosquito (Kajla et al., 2015a; Kumar et al., 2010).

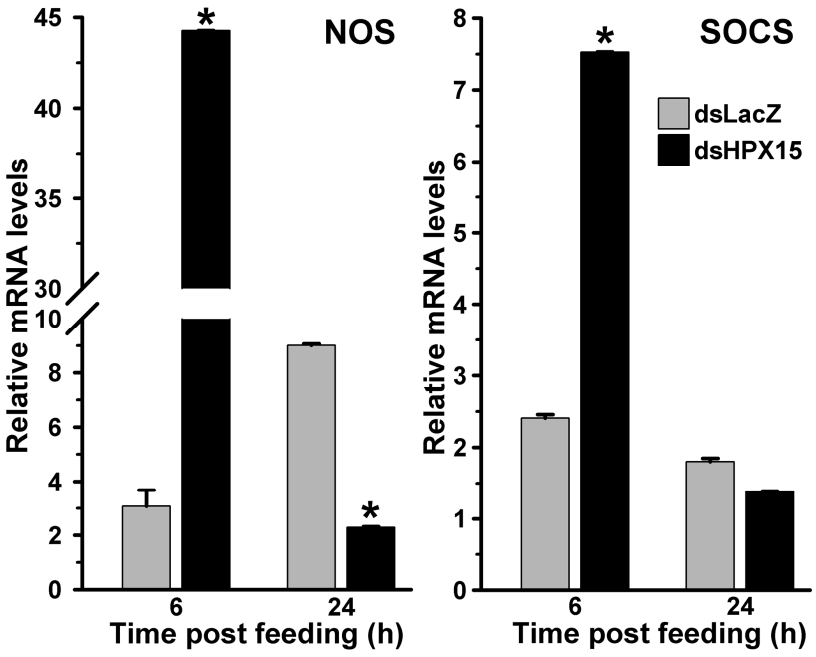

Figure 5.7: Relative levels of NOS and SOCS mRNA in bacteria fed AsHPX15 silenced midguts. Mosquitoes injected with dsLacZ (controls) or dsHPX15 (silenced) were fed on bacteria supplemented blood and relative levels of NOS or SOCS mRNA were analyzed in their midguts at different time points after feeding. Relative levels of mRNA are presented against the sugar fed midguts. Significance differences are denoted by an asterisk.

5.3.9 The antibacterial peroxidase HPX8 is suppressed in AsHPX15 silenced midguts

As we found before that HPX8, an antibacterial peroxidase, is induced after the exogenous bacteria feeding (**Figure 5.2**). We analyzed the expression of this gene in AsHPX15 silenced midguts to understand its role in regulating the bacterial load when HPX15 mediated physical barrier formation is interrupted. Results presented in **Figure 5.8** revealed that in dsLacZ injected control midguts, HPX8 gene was induced 650 folds after 24 h of exogenous bacteria feeding. However, its expression was reduced ~40 times in AsHPX15 silenced midguts against the unsilenced controls (**Figure 5.8**). Moreover, the expression levels of HPX8 gene in controls and silenced midguts at 6 h post feeding were indifferent (p=0.078).

These results collectively indicated that the classical antibacterial pathways are least effective in controlling the heavy load of exogenous bacteria in AsHPX15 silenced midguts. However, the induced NOS (an effector gene of the JAK/STAT pathway) and gambicin seem to be the major determinants of the antibacterial immunity in these midguts.

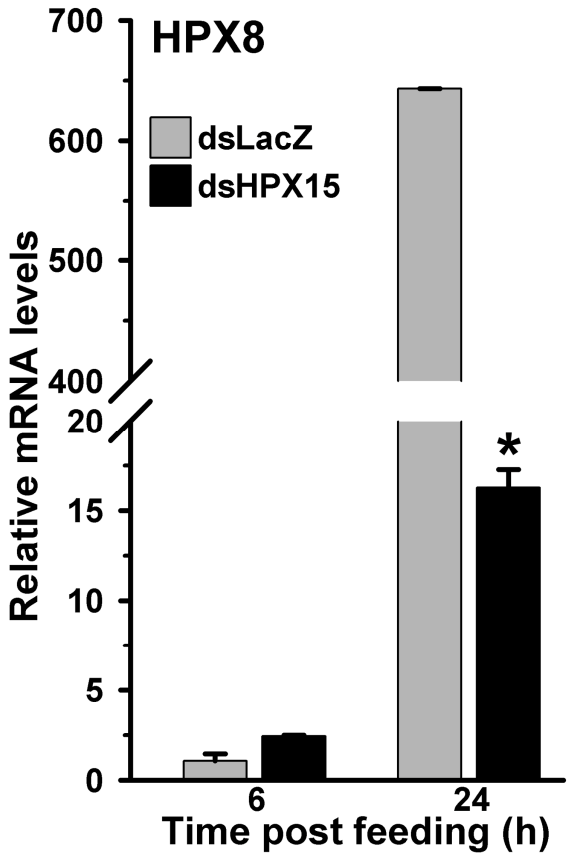

Figure 5.8: Expression of HPX8 gene in bacteria fed AsHPX15 silenced midguts. Mosquitoes injected with dsLacZ (controls) or dsHPX15 (silenced) were fed on bacteria supplemented blood and relative levels of HPX8 mRNA in their midguts were analyzed at different time points after feeding. Relative levels of mRNA are presented against the sugar fed midguts. Significant differences are shown by an asterisk.

5.4 Discussion

The mosquito midgut is an organ for food digestion and immunity. It is an excellent system to understand the interaction of innate immunity, exogenous food and endogenous natural microbial habitats. It is noteworthy to mention that a fine balance between the innate immunity and digestion process is required to drive the physiological functions of the midgut over the immune reactivity against bolus antigens. For that, mosquito midgut is equipped with a number of mechanisms (Kajla et al., 2015a). Among these mechanisms, the formation of a heme peroxidase HPX15 crosslinked mucin barrier is extremely important (Kumar et al., 2010). This mucin barrier does not allow the interaction of bolus bacteria with the immune reactive midgut epithelium and thus, protects them from the immune attack. As the result of that food digestion or other important physiological processes are driven forward without the induction of midgut immunity (Kajla et al., 2015a). Our data also supported this concept that the endogenous as well as exogenous fed bacteria easily proliferate in the midgut lumen and HPX15 gene is induced after feeding the normal or bacteria supplemented blood (**Figures 5.1** and **5.2**). Interestingly, we observed the reduction of AsHPX15 gene expression in 12 h post bacteria fed midguts (**Figure 5.2**). This effect might be due to

the SOCS mediated suppression of STAT pathway (**Figure 5.4**). The presence of STAT binding site in the regulatory region of AsHPX15 gene supported this assumption (Kajla et al., 2016). We also believed that the suppression of AsHPX15 gene expression in bacteria fed midguts might be least effective on the mucin barrier formation because the luminal secretion of mucins and localization of HPX15 protein occur by this time, which is well evident in case of *A. gambiae* midguts (Kumar et al., 2010; Injera et al., 2013).

Importantly, the proliferation of midgut bacteria does not increase continuously; however, there is variability in their growth pattern (**Figure 5.1**). It may be due to the selection and proliferation of specific types of midgut bacteria at certain time points or all types of bacteria have variable growth patterns at different time of post blood feeding. Moreover, these assumptions warrant further investigations. On the other hand, the midgut immunity might also play an important role in regulating the growth of bacteria at certain moments therefore, some of the classical immune genes such as, HPX8, GNBP, Toll and gambicin are induced at 6 h after bacteria supplemented blood feeding (**Figures 5.2** and **5.3**). However, in case of bacteria-free blood fed control midguts, the induction of these genes is comparatively minimal to facilitate the proliferation of endogenous bacteria. Thus, the mosquito midgut system might determine the degree and strength of immune activation on the basis of bacterial or antigenic load in blood bolus. These findings may also explain the previous observations by other researchers where feeding the exogenous bacteria with *Plasmodium* infected blood reduced the parasite development (Dong et al., 2009; Pumpuni et al., 1993 and 1996; Gonzalez-Ceron et al., 2003). We believed that the negative regulation of *Plasmodium* development in the presence of exogenous bacteria might be due to an early induction of midgut immunity as we observed in **Figure 5.7** because some of these immune pathways are also known to participate in antiplasmodial immunity (Cirimotich et al., 2011b; Bahia et al., 2014).

Our previous findings revealed that the anopheline heme peroxidase HPX15 is a unique lineage-specific gene and its role in the modulation of mosquito midgut immunity can be targeted to control *Plasmodium* development (Kajla et al., 2014, 2015b and 2016). Thus, we thought to combine our present knowledge of exogenous bacteria induced immunity with AsHPX15 gene silencing to understand the additive effect of these two events on mosquito midgut immunity. We found that AsHPX15 silencing induced innate immunity to suppress the bacterial load in the silencing midguts and capable of regulating the high load of exogenous fed bacteria (**Figure 5.5**). These findings are in agreement with the previous study where silencing of HPX15 ortholog in

A. gambiae suppressed the growth of endogenous bacteria through the induction of bacteria-specific classical immunity (Kumar et al., 2010). These effects are simply due to the disruption of mucin barrier in HPX15 silenced midguts and that leads to the recognition of the bolus bacteria by the immune reactive midgut epithelial cells (Kumar et al., 2010).

We observed that the regulation of exogenous fed bacteria in the mosquito midgut is due to the activation of classical Toll and Imd immune pathways when HPX15 mediated mucin barrier is present (**Figures 5.2** and **5.3**). The silencing of AsHPX15 gene and thus, reducing the formation of mucin barrier, might alter the number of bacteria in the midgut. In AsHPX15 silenced midguts the classical immune pathways are mostly ineffective (**Figure 5.6**) and the bacteria levels are regulated by another stronger immune mechanism. Thus, NOS is activated at early hours in AsHPX15 silenced midguts to control the heavy load of bacteria (that includes exogenous as well as endogenous bacteria) (**Figure 5.7**). In addition, the induction of SOCS gene in parallel to the NOS might again indicate the activation as well as balanced regulation of JAK/STAT pathway in HPX15 silenced midguts (**Figure 5.7**). Our findings also revealed that the levels of endogenous bacteria are very less in comparison to the exogenously fed bacteria (**Figure 5.1**) thus, NOS is induced in AsHPX15 silenced midguts to control the outsized load of these bacteria (**Figure 5.7**). In addition, the induction of gambicin, a classical immune pathway gene, in HPX15 silenced midguts might indicate its regulation through JAK/STAT pathway as suggested by other researchers (Buchon et al., 2009; Cheng et al., 2016).

Immune regulation of a huge exogenous bacterial load in the AsHPX15 gene silenced midgut revealed that there is a circumstantial activation of antibacterial immunity. In other words, classical immune pathways are most active against increasing load of bacteria when AsHPX15 gene is expressed (**Figures 5.2** and **5.3**) however, STAT pathway predominates as antibacterial in the absence of HPX15 gene expression (**Figure 5.7**). This might indicate that the bacterial load and its direct interaction with the midgut epithelium boosts more effective immune molecule to manage the microbial homeostasis. Thus, we proposed a model as shown in **Figure 5.9** that HPX15 helps in the formation of mucin barrier in *A. stephensi* midgut. This mucin barrier blocks the direct interactions of proliferating bolus bacteria with the immune reactive gut epithelial cells. However, the proliferating bacteria or their elicitors activate the classical Toll and Imd pathways that maintain gut bacterial homeostasis. On the other hand, in AsHPX15 silenced midguts the formation of mucin barrier is compromised and bacterial elicitors

activate the midgut epithelial immunity. As a result, midgut epithelial cells mount a strong immune response through the activation of STAT pathway to regulate the proliferation of midgut bacteria and protecting the mosquito against its deleterious effects (**Figure 5.9**).

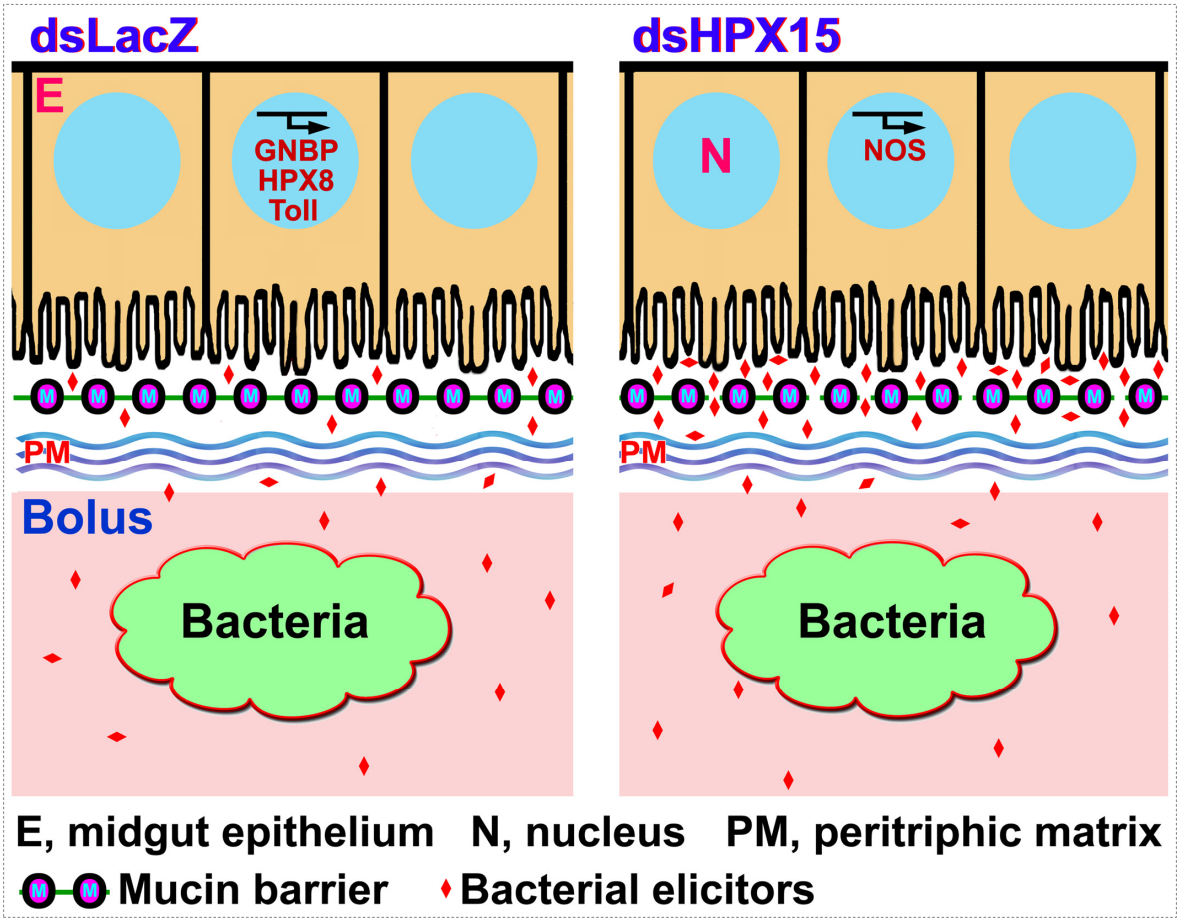

Figure 9: Model of *A. stephensi* midgut immunity in the presence or absence of HPX15 gene. HPX15 catalyzes the formation of mucin layer that blocks the direct interaction of proliferating lumen bacteria or bacterial elicitors with midgut epithelium. The increased load of bacteria induces classical immune pathways such as, GNBP, Toll and an antibacterial heme peroxidase HPX8 to regulate bacterial numbers. HPX15 silencing reduces the formation of mucin barrier that allows direct interaction of lumen bacteria or their elicitors with midgut epithelium. In this condition, STAT pathway effector molecule NOS is induced to regulate the numbers of midgut bacteria.

Based on our findings, we emphasized that manipulation of HPX15 gene in *A. stephensi* modulates the immune system and co-infection of *Plasmodium* with exogenous bacteria will result in the negative regulation of the parasite development through induction of specific immune pathways. Because HPX15 is highly conserved gene, exclusively among anophelines (Kajla et al., 2015b and 2016) then the proposed idea might be applicable for other worldwide distributed malaria vectors as a common strategy.

5.5 Conclusion

In conclusion, bacterial load in mosquito gut is regulated through induction of NOS after disruption of gut barrier via HPX15 silencing. On the basis of above results we proposed a hypothesis that HPX15 silencing in *A. stephensi* may modulate immune system in such a way that co-infection of *Plasmodium* along with exogenous bacteria, result in *Plasmodium* regulation through specific immune pathways. Because HPX15 is highly conserved gene exclusively among anophelines, then it can be a potent target to control *Plasmodium* development inside the vector host.

Chapter 6

Anopheles stephensi heme peroxidase HPX15 modulates midgut epithelial immunity against *Plasmodium*

6.1 Abstract

Heme peroxidase HPX15 is an anopheline lineage-specific gene. Although it is present in nineteen worldwide distributed species of *Anopheles* mosquito however, its orthologs are absent in other mosquitoes, insects or human. Interestingly, the 65-99% amino acids identity among nineteen orthologs of HPX15 revealed the uniqueness and evolutionary conserved nature of this gene. In this study, we found that *Anopheles stephensi* AsHPX15 gene is exclusively expressed in the midgut and largely induced after uninfected or infected blood feeding. RNA interference (RNAi)-mediated silencing of AsHPX15 induced an immune gene nitric oxide synthase (NOS) and drastically reduced the number of developing *Plasmodium* oocysts. These AsHPX15 silencing mediated regulation of mosquito immunity and *Plasmodium* development are identical with the findings in another anopheline, *A. gambiae,* where AgHPX15 forms a dityrosine network at luminal side of the midgut to prevent the activation of mosquito immunity against the malaria parasites. These indistinguishable functional behaviors and conserved homology of HPX15 among anophelines might designate this midgut peroxidase as a 'common target' to manipulate the mosquito immunity and controlling malaria parasite development inside the mosquito host. These findings will open new frontiers in the field of malaria transmission and disease control and might be applicable for numerous *Anopheles* vector species globally.

6.2 Introduction

Malaria parasite *Plasmodium* requires the mosquito host to complete its sexual development. *Plasmodium* undergoes various stages of the complex life cycle in different compartments of the host. Mosquito midgut is the first organ to interact with *Plasmodium.* To interrupt the cycle of malaria transmission, it is important to block the parasite development inside the mosquito host. For such transmission blocking strategies, the understanding of molecular interactions between *Plasmodium* and mosquito immunity is highly demanded.

In our previous work (Chapter 3 and 4), we have studied the *A. stephensi* heme peroxidase AsHPX15. This molecule modulates the midgut immunity to provide a 'low immunity' zone in the midgut region for the growth of bacteria (Kumar et al., 2010; Kajla et al., 2015a). It is noteworthy to mention that HPX15 is a unique anopheline-lineage specific gene and share 70-99% amino acid identity with its orthologs in 19 other Anopheles species (Kajla et al., 2015b). Thus, we have proposed HPX15 as a general target to modulate the midgut immunity and subsequently blocking the *Plasmodium*

development, at least in these above-mentioned 19 species of *Anopheles* mosquito (Kajla et al., 2015b and 2016). However, this hypothesis demands further investigations to establish the aforesaid regulatory role of HPX15 gene, in terms of *Plasmodium* development, in other anophelines. Thus, in the present study, we used the gene silencing approach to determined the functional role of AsHPX15 gene in the Indian malaria vector *A. stephensi* to support the belief that this unique heme peroxidase might be a designated 'common target' to manipulate mosquito midgut immunity and controlling *Plasmodium* development.

6.3 Results

6.3.1 Tissue specific expression analysis of AsHPX15 in *Plasmodium* infected mosquitoes

To understand the organ-specific expression of AsHPX15 gene, we compared its relative mRNA levels in different body compartments. For that, we collected 24 h post uninfected or *Plasmodium berghei* infected blood fed midguts and carcasses separately from a pool of mosquitoes and analyzed the mRNA levels of AsHPX15 gene. We selected the 24 h post fed samples because it corresponds to the time when ookinetes invade the midgut epithelium (Smith et al., 2014). Results shown in **Figure 6.1** revealed that in sugar fed midguts the basal levels of AsHPX15 mRNA were ~40 folds higher than carcasses. Furthermore, its expression in 24 h blood fed midguts was induced ~17 folds against sugar fed midguts (**Figure 6.1**). However, the expression of AsHPX15 gene was down regulated ~2 folds in *P. berghei* infected midguts when

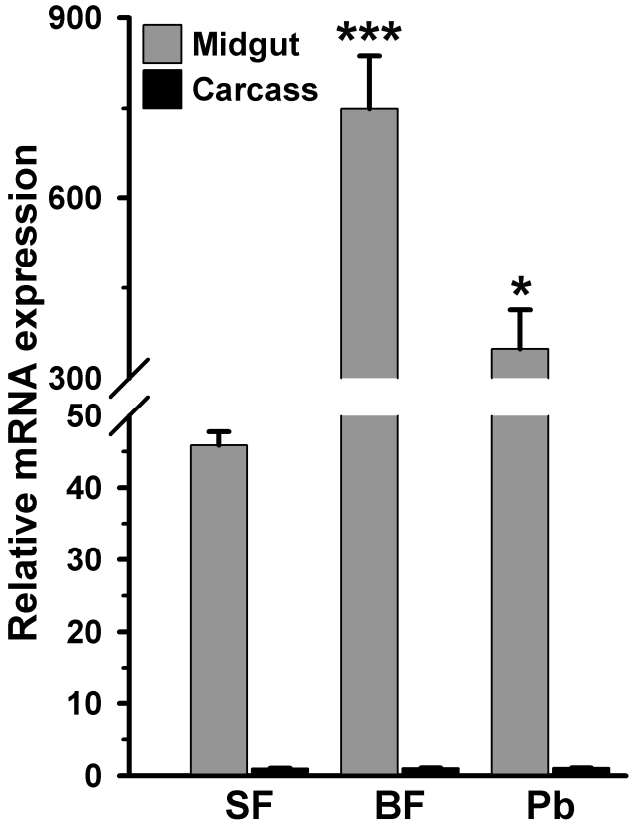

Figure 6.1: Body compartment specific expression of AsHPX15. Relative mRNA expression levels of AsHPX15 were analyzed in midgut and carcass of sugar fed (SF), 24h post normal blood fed (BF) and *P. berghei* (Pb)-infected female mosquitoes. Significant differences $p < 0.0001$ or $p < 0.01$ in relative mRNA levels of AsHPX15 are indicated by three or single asterisks (*) respectively.

compared to the uninfected blood fed controls (p= 0.008, **Figure 6.1**). Interestingly, the relative mRNA levels of AsHPX15 gene were indifferent in the carcasses of sugar fed and uninfected blood fed mosquitoes and also remained unchanged after *Plasmodium* infection (**Figure 6.1**). These results concluded that AsHPX15 is a blood induced midgut-specific gene and suppressed during the *Plasmodium* ookinete invasion of the midgut epithelium. These findings are in agreement with the previous reports where *A. gambiae* AgHPX15 gene, an ortholog of AsHPX15, is induced in blood fed midguts and negatively regulated after malaria infection (Kumar et al., 2004 and 2010).

In parallel, we also analyzed the kinetics of AsHPX15 expression in normal or *P. berghei* infected blood fed midguts to understand the regulation of this gene during malaria parasite development. For that, the controls or *P. berghei* infected blood fed midguts were collected at different time points after the feeding and expression levels of AsHPX15 gene were analyzed through qPCR. Results presented in **Figure 6.2** revealed that the relative mRNA levels of AsHPX15 gene were similar in controls and infected midguts for first 12 h after feeding (p=0.328, p=0.101 and p=0.945 at 3, 6 and 12 h post feeding, respectively). However, there was a significant reduction of AsHPX15 mRNA in *P. berghei* infected midguts against the blood fed controls at 18 h (p<0.0001) post feeding

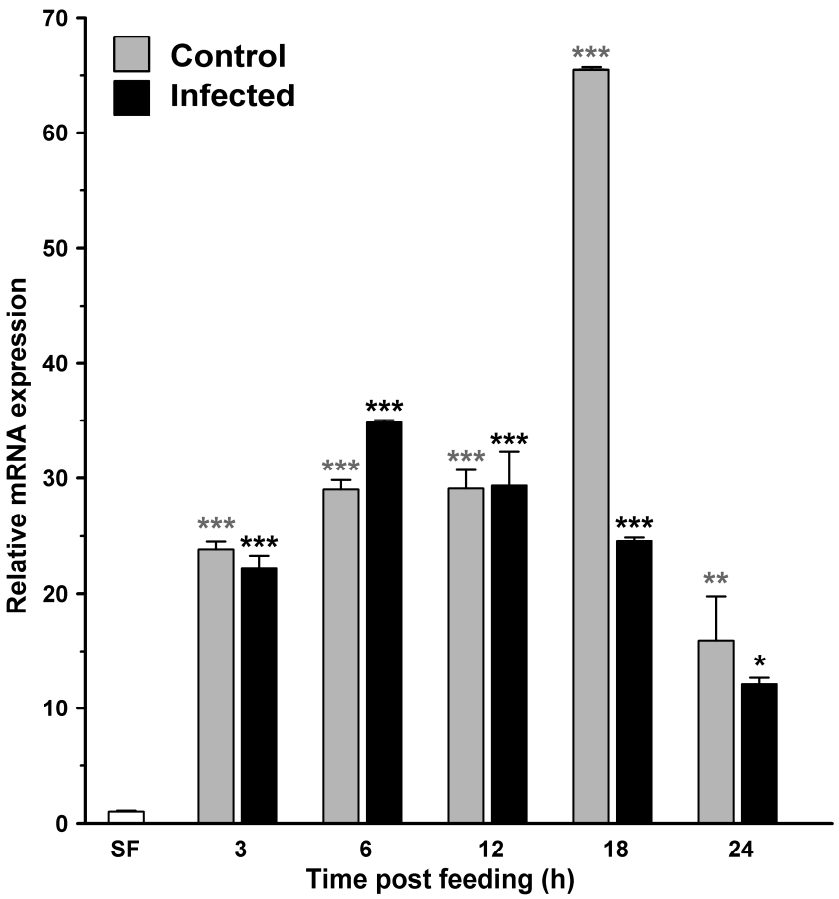

Figure 6.2: Kinetics of AsHPX15 expression in mosquito midguts. Relative mRNA expression levels of AsHPX15 were analyzed at different time points after normal (Control) or *P. berghei*-infected blood feeding in *A. stephensi* midguts. Relative fold induction was calculated against sugar fed midguts. Significant differences $p < 0.0001$ or $p < 0.001$ or $p < 0.01$ between each time point and controls are indicated by three or two or one asterisks (*) respectively.

(**Figure 6.2**). These results indicated that the expression of AsHPX15 gene is unaffected during the initial hours (up to 12 h) in infected midguts when the pre-ookinete stages of *Plasmodium* development predominate in the bolus (Smith et al., 2014). However, at later time points, the expression of this gene is suppressed when the mature ookinetes start invading the midgut epithelium. These observations are similar to the other mosquito *A. gambiae* where AgHPX15 gene is down regulated in *P. berghei* infected midguts after 24 h post blood meal (Kumar et al., 2004).

6.3.2 AsHPX15 silencing has a negative effect on *Plasmodium* development

Our previous findings revealed that the heme peroxidase AgHPX15 crosslinked mucin barrier at the luminal side of the midgut and does not allow the bolus antigens, especially the naturally acquired microbes, to interact with the immune-reactive midgut epithelium (Kumar et al., 2010). Thus, we hypothesized that the reduction of HPX15 mRNA levels through gene silencing approaches might initiate the recognition and killing of *Plasmodium* by the mosquito innate immunity. To test this assumption, we compared the number of *Plasmodium* oocysts in control and AsHPX15 silenced midguts as discussed in Chapter 2 Materials and Methods. Our analysis of the relative AsHPX15 mRNA levels in dsLacZ injected controls and AsHPX15 silenced midguts revealed that we could achieve 98% silencing of this gene (**Figure 6.3A**).

Further, we compared the number of developing oocysts in control and silenced midguts after 7 days of blood feeding. Results presented in **Figure 6.3B** revealed that the variable number of oocysts were observed in controls (oocysts range 0-1600) and silenced (oocysts range 0-600) midguts. However, the median value for the oocysts numbers in controls and AsHPX15 silenced midguts was 329 and 89, respectively. These results revealed that the oocysts numbers are reduced significantly in the silenced midguts when compared to the controls (**Figure 6.3B**, p=0.027). Representative *P. berghei* oocysts infected dsLacZ injected and AsHPX15 silenced midgut is shown in **Figure 6.3C**. Based on these data, we concluded that AsHPX15 is a natural agonist that positively regulates *Plasmodium* development inside the mosquito midgut. These results are in agreement with the previous findings where silencing of the AgHPX15 gene in *A. gambiae* also reduced *Plasmodium* survival (Kumar et al., 2010).

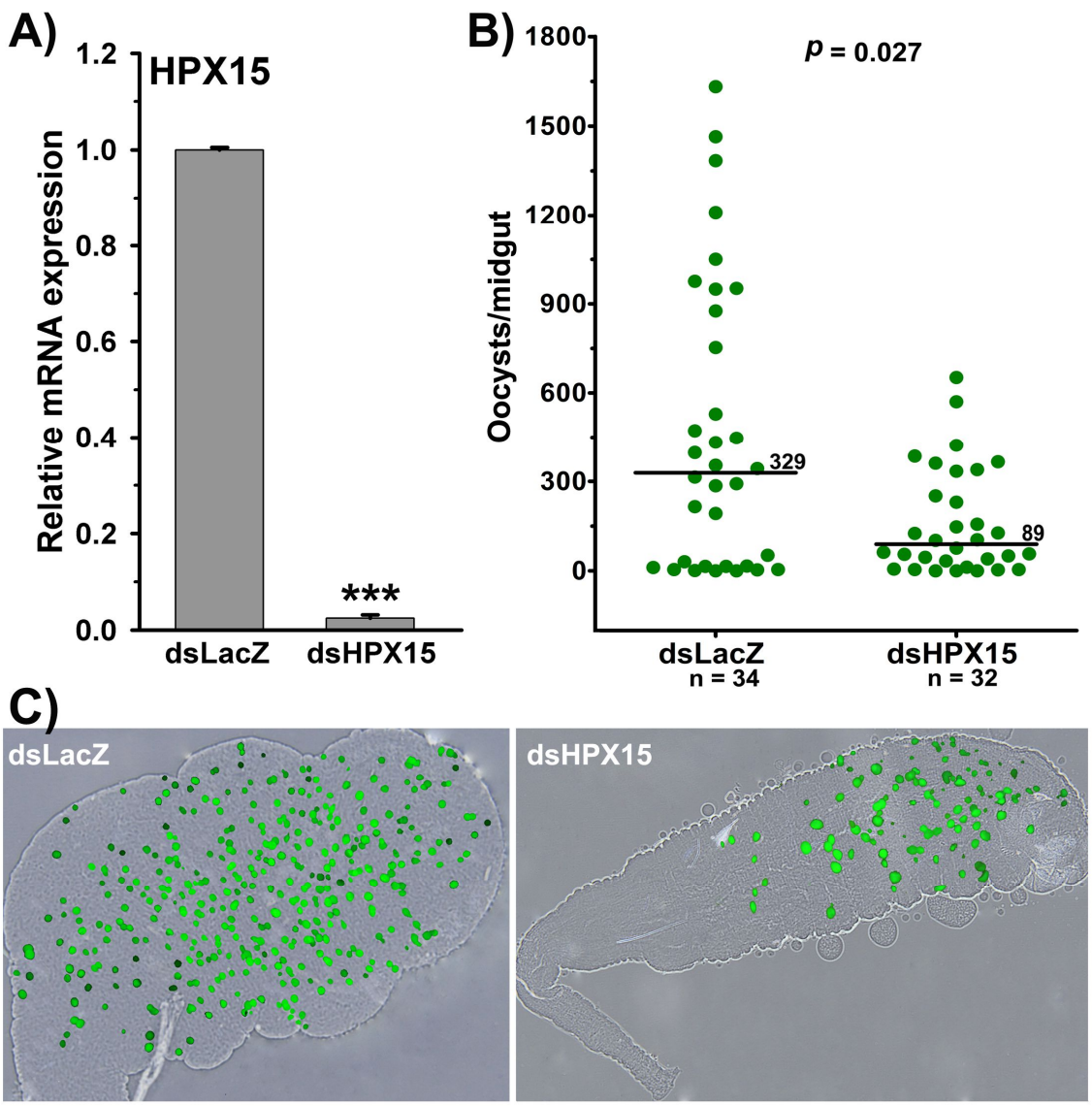

Figure 6.3: Effect of AsHPX15 silencing on *Plasmodium berghei* development in *Anopheles stephensi*. A) Relative mRNA abundance of AsHPX15 in 24h post *P. berghei* infected blood fed *A. stephensi* mosquitoes injected with dsLacZ or dsAsHPX15. Three asterisks shows significant difference ($p < 0.0001$). **B)** Effect of AsHPX15 silencing on the number of live oocysts (green dots) in midguts analyzed seven days post infection. Dots represent the number of parasites present on individual midguts, and the median number of parasites is indicated by the horizontal line. Distributions are compared using the Kolmogorov-Smirnov test (p=0.027); n = number of mosquitoes**. C)** Representative *A. stephensi* midgut showing *Plasmodium berghei* oocysts in dsLacZ or dsHPX15 injected mosquitoes.

6.3.3 Antiplasmodial immune responses are induced in AsHPX15 silenced midguts

The development of *Plasmodium* was suppressed in AsHPX15 silenced midguts (**Figure 6.3**). Thus, we hypothesized that the silencing of AsHPX15 gene might be inducing the antiplasmodial immunity due to the reduced crosslinking of the mucin barrier and recognition of the parasites by the midgut innate immune system. These assumptions were confirmed through analyzing the expression of various known

antiplasmodial genes (Blandin et al., 2004; Kumar et al., 2010) in the silenced and *P. berghei* infected blood fed midguts. Results presented in **Figure 6.4** revealed that the relative mRNA levels of an antiplasmodial immune gene thioester containing protein 1 (TEP1) were similar in dsLacZ (controls) and dsHPX15 injected (silenced) mosquito midguts at 24 h post *P. berghei* infected blood feeding (p=0.0959). Furthermore, the comparison of another antiplasmodial immune gene Nitric Oxide Synthase (NOS) in above samples revealed that this gene was induced ~13 folds in the silenced midguts against the controls (**Figure 6.4**, p=0.005). These findings suggested that the induced NOS might play an antiplasmodial role, as reported before (Gupta et al., 2009; Luckhart et al., 1998, Kumar et al., 2010).

In mosquitoes, the induction of NOS gene is regulated by the Janus kinase/signal transducers and activators of transcription (JAK/STAT) pathway. NOS catalyzed the formation of nitric oxide (NO), a highly diffusible and reactive immune molecule that modifies and inactivates the macromolecules (Bahia et al., 2011; Gupta et al., 2009; Luckhart et al., 1998). Previous studies revealed that the suppressor of cytokine signaling (SOCS) is also induced in parallel to the NOS and regulates the over activation of JAK/STAT pathway (Bahia et al., 2011; Dhawan et al., 2015; Gupta et al., 2009; Kumar et al., 2010). Thus, we also analyzed the activation of SOCS gene in the above mentioned AsHPX15 silenced midguts to understand the activation of NOS through JAK/STAT pathway. Results presented in **Figure 6.4** revealed that the SOCS

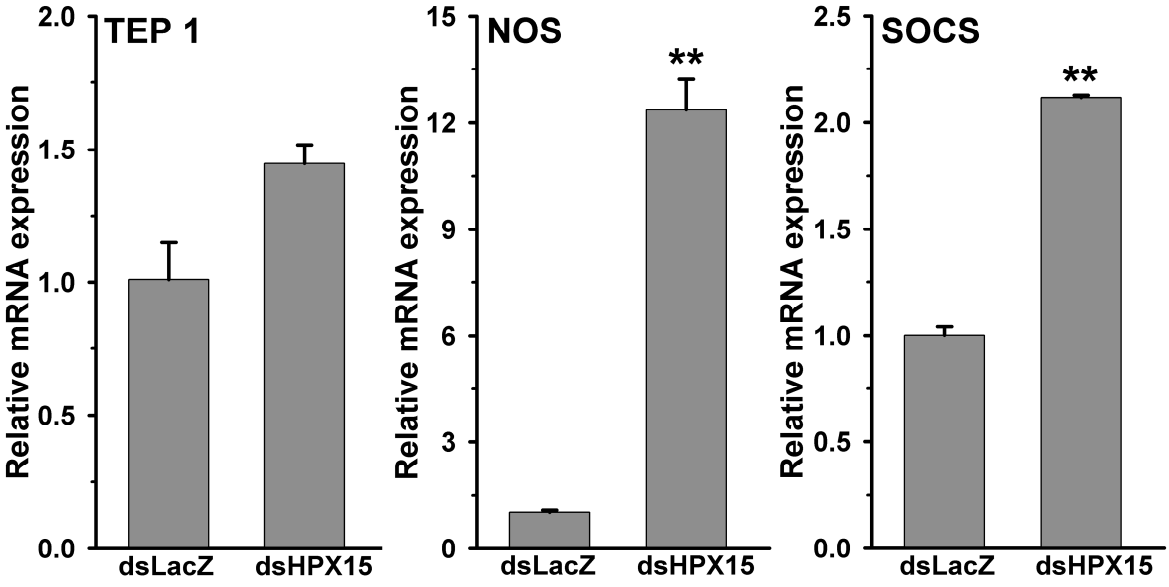

Figure 6.4: Expression of immune genes in *Plasmodium berghei* infected AsHPX15 silenced *Anopheles stephensi* midguts. Relative mRNA expression levels of various immune genes Thioester containing Protein 1 (TEP1), Nitric Oxide Synthase (NOS) and Suppressor of Cytokine Signaling (SOCS) in 24h post *P. berghei* infected blood fed *A. stephensi* mosquitoes injected with dsLacZ or dsAsHPX15 midguts. Significance of induction ($p < 0.001$) between dsLacZ and dsAsHPX15 is shown by two asterisks (*).

gene was induced ~ 2 folds in the silenced midguts against controls (**Figure 6.4**, *p*=0.001). Thus, the induction of NOS, an effector gene, and SOCS, a suppressor gene, indicated that the activation of JAK/STAT pathway regulates antiplasmodial immunity in AsHPX15 silenced midguts.

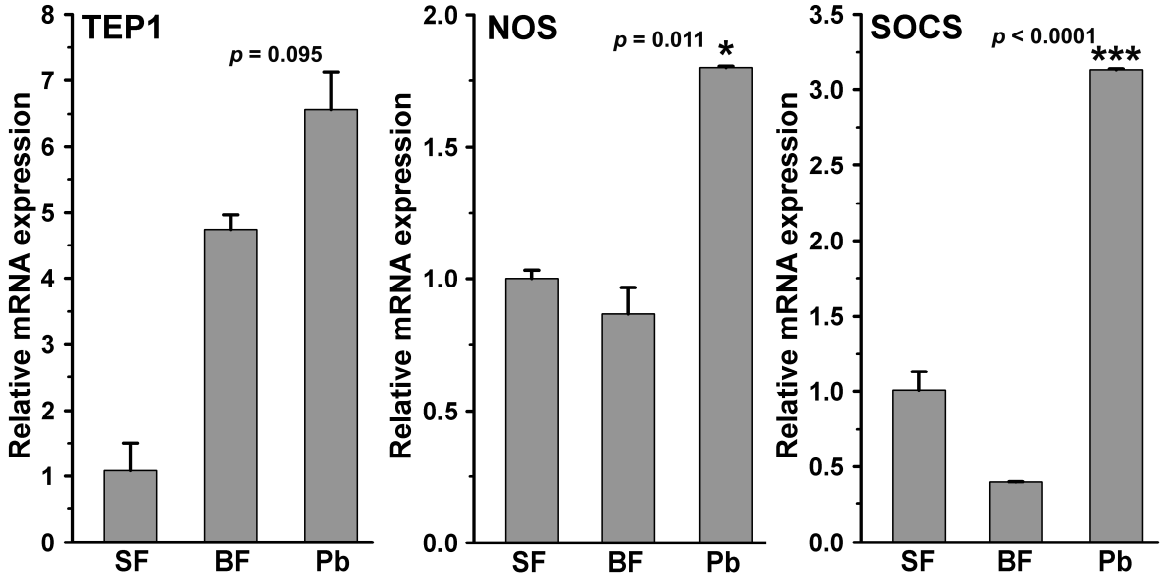

Figure 6.5: Expression of immune genes in *Plasmodium berghei* infected *Anopheles stephensi* midguts. Relative mRNA expression levels of various immune genes Thioester containing protein 1 (TEP1), Nitric Oxide Synthase (NOS) and Suppressor of Cytokine Signaling (SOCS) in sugar fed (SF), 24h post normal blood fed (BF) or *P. berghei* (Pb)-infected midguts of female mosquitoes. Significance of induction between BF and Pb is shown by asterisks (*). *p* value for the same is also shown in figure.

In addition, our analysis of these above-mentioned immune genes expression revealed that the relative levels of TEP1 mRNA were indifferent between uninfected or *P. berghei* infected blood fed midguts (**Figure 6.5**, *p*=0.095). However, both NOS and SOCS genes were significantly induced in *Plasmodium* infected midguts (**Figure 6.5**, *p*=0.011 for NOS and *p*<0.0001 for SOCS between infected and control midguts). These results collectively indicated that the activation of JAK/STAT pathway is the major regulator of the *Plasmodium* development and it is further induced in the HPX15 silenced midguts. In other words, the absence of HPX15 catalyzed mucin barrier in infected midgut provide a better opportunity for the innate immune system to recognize the malaria parasite that in turn, activates JAK/STAT pathway to regulate *Plasmodium* development.

6.4 Discussion

Mosquito midgut is the organ that plays a crucial role in food digestion. In addition, it is also an important immune organ that encounters the blood-borne pathogens. This might

be a critical condition for the mosquito system to take a wise decision for driving the process of food digestion over the immune activation. In addition, the presence of naturally acquired microbes are also the integrated part of the midgut compartment, which generally proliferate after the blood feeding and help in the digestion process (Kumar et al., 2010; Kajla et al., 2015a; Minard et al., 2013). Thus, the protection of these microbes is also a major responsibility of the midgut immune system. The mechanism that balances these events has been recently explored in the mosquito (Kajla et al, 2015a). Studies carried in African mosquitoes *A. gambiae* identified that a heme peroxidase HPX15 is induced in the midgut after the blood feeding and modulates the midgut immunity to protect the growth of gut bacteria.

We explored the HPX15 gene in Indian malaria vectors and found that this gene is present in *A. stephensi* midgut and induced after blood feeding (Kajla et al., 2014 and 2016 and Chapter 4, **Figure 4.6** and **4.7**). The functional aspects of HPX15 gene, in terms of regulating the *Plasmodium* development, were studied extensively in *A. gambiae* as discussed above (Kumar et al., 2010). We hypothesized that the highly conserved ortholog of HPX15 in other mosquitoes might be performing the similar function. Thus, we extended our studies to explore the role of HPX15 gene in regulation of *Plasmodium* development in Indian malaria vector *A. stephensi*. The present study clearly demonstrated that the functional properties of HPX15 gene are similar in two mosquitoes, *A. stephensi* and *A. gambiae*. For example, in both these anophelines, HPX15 gene is a) exclusively expressed in the midgut (**Figure 6.1**), b) an early blood feeding induced gene (**Figure 6.1** and **Figure 6.2**), c) induced in a pattern which is similar in uninfected or *Plasmodium* infected blood fed midguts for first 12 h (**Figure 6.2**), d) drastically suppressed in 24 h post *Plasmodium* infected blood fed midguts against uninfected blood fed controls (**Figure 6.2**), e) significantly suppressing the development of malaria parasite after silencing (**Figure 6.3**), f) this suppression in *Plasmodium* development is mediated through NOS (**Figure 6.4**).

The presence of ecdysone binding site in the regulatory region of AsHPX15 gene was reported in our previous study (Kajla et al., 2016). Because ecdysone levels increase after the blood feeding therefore, we believe that this hormone might be responsible for the induction of AsHPX15 gene in uninfected or *Plasmodium* infected blood fed midguts (**Figure 6.1** and **Figure 6.2**). Interestingly, the similar pattern of AsHPX15 mRNA induction in uninfected or *Plasmodium* infected blood feeding for first 12 h might indicate that in either condition the major role of this enzyme in crosslinking of the mucin barrier is fulfilled. These conclusions are supported by other published

reports where the formation of mucin layer and peritrophic matrix takes place by 12h after blood feeding in mosquito gut (Injera et al., 2013; Rayms-Keller et al., 2000).

The reduction of midgut AsHPX15 mRNA at 18 and 24 h post *Plasmodium* infection (**Figure 6.2**) might indicate the suppression of this gene by the mechanism regulated by the invading ookinetes. This is the time window where generally the mature ookinetes create molecular pores in the peritrophic matrix and start invading the midgut epithelium (Smith et al., 2014). Mosquito immune system is expected to induce during the ookinete invasion. Our results indicated that NOS is induced in *Plasmodium* infected midguts against blood fed controls (**Figure 6.5**), which is an antiplasmodial gene (Kumar et al., 2010; Luckhart et al., 1998). Interestingly the induction of SOCS gene also in these samples indicates the activation of STAT pathway as reported before (Gupta et al., 2009).

As we discussed before that the formation of HPX15-mediated mucin barrier is important for suppressing the midgut immunity against the bolus bacteria and this might be also true for the *Plasmodium* development. This was evident from our gene silencing experiments (**Figure 6.3**). *Plasmodium* development was drastically reduced in HPX15 silenced midguts. We believe that the absence of HPX15 protein would have resulted in the formation of a defective mucin barrier and that might be responsible for the induction of antiplasmodial immunity in silenced midguts. Interestingly, we found that NOS is highly induced in these samples and might be one of the important negative regulator of *Plasmodium* development (**Figure 6.4**) in the similar way as reported in *A. gambiae* (Kumar et al., 2010). These results collectively indicate that the silencing of HPX15 gene has negative effect on *Plasmodium* development at least in two anophelines, *A. stephensi* and *A. gambiae*.

6.5 Conclusion

HPX15 is a unique highly conserved protein among total 19 anophelines. Its functional properties in terms of regulating the malaria parasite development are also similar in two anophelines. Thus, we propose that anopheline HPX15 might serve as a 'potent candidate' that can be targeted to manipulate mosquito vectorial capacity and blocking the transmission of malaria infection.

Chapter 7

Biocontrol of human disease vectors: Identification of the temperature induced larvicidal efficacy of *Agave angustifolia*

The entire work presented in this chapter has been published in the journal *Frontiers in Public Health*

frontiers in Public Health

ORIGINAL RESEARCH
published: 12 January 2016
doi: 10.3389/fpubh.2015.00286

Identification of the Temperature Induced Larvicidal Efficacy of *Agave angustifolia* against *Aedes, Culex,* and *Anopheles* Larvae

Mithilesh Kajla[1†], Kurchi Bhattacharya[1,2†], Kuldeep Gupta[1], Ujjwal Banerjee[1,3], Parik Kakani[1], Lalita Gupta[1] and Sanjeev Kumar[1]*

7.1 Abstract

Synthetic insecticides are generally employed to control the mosquito population. However, their injudicious over usage and non-biodegradability are associated with many adverse effects on the environment and mosquitoes. The application of environment-friendly mosquitocidals might be an alternate to overcome these issues. In this study, we found that organic or aqueous extracts of *Agave angustifolia* leaves exhibited a strong larvicidal activity (LD_{50} 28.27 µg/ml) against *Aedes aegypti*, *Culex quinquefasciatus* and *Anopheles stephensi* larvae within a short exposure of 12h. The larvicidal activity of *Agave angustifolia* is inherited and independent of the plants vegetative growth. Interestingly, the plant larvicidal activity was observed exclusively during the summer season (April-August, when outside temperature is between 30°C to 50°C) and it was significantly reduced during winter season (December-February, when the outside temperature falls to ~4°C or lower). Thus, we hypothesized that the larvicidal components of *Agave angustifolia* might be induced by the manipulation of environmental temperature and should be resistant to the hot conditions. We found that the larvicidal activity of *Agave angustifolia* was induced when plants were maintained at 37°C in a semi-natural environment against the controls that were growing outside in cold weather. Pre-incubation of *Agave angustifolia* extract at 100°C for 1h killed 60% larvae in 12h, which gradually increased to 100% mortality after 24h. In addition, the dry powder formulation of *Agave angustifolia,* also displayed a strong larvicidal activity after a long shelf life. Together, these findings revealed that *Agave angustifolia* is an excellent source of temperature induced bioactive metabolites that may assist the preparedness for vector control programs competently.

7.2 Introduction

Mosquitoes are infamous vectors for numerous life-threatening diseases. Synthetic chemicals (insecticides) are mostly employed to control the vector population. However, the disadvantages associated with their applications warrant the discovery of environment-friendly approaches to control mosquitoes at various stages of their development. Secondary metabolites from the botanical world (called natural phyto-larvicides) may also be employed for controlling the mosquito population. These metabolites are easily obtained at reasonable cost and their intrinsic biodegradable nature makes them the best suitable for this purpose (Ghosh et al., 2012).

We screened several randomly selected plants to study their larvicidal properties. Interestingly, one of the plants *Agave angustifolia* 'Marginata' also known as

Caribbean *Agave* revealed a potent mosquito larvicidal activity. *Agave angustifolia* (family *Agavaceae*) is a medium-sized monocotyledonous plant with a dense round rosette atop a very short trunk. This xerophytic plant is a robust survivor and tolerant to hot and dry environments (Gilman, 1999). The genus *Agave* has more than 275 species that are globally distributed and *Agave angustifolia* is a common weed or sometime used as ornamental plant in our region. This plant mostly propagates through vegetative reproduction, either by rhizomes or by bulbils, and forms aggregations of individual plants. However, the sexual reproduction is also reported in this plant (Singh et al., 2014; Vargas-Ponce et al., 2009). In fact, *Agaves* are of economic importance as sources of fiber, steroids, spirits and other useful products (Piven et al., 2001).

The aim of this study was to evaluate the larvicidal nature of *Agave angustifolia* leaf extracts against three major human disease vectors, namely *Aedes aegypti, Culex quinquefasciatus* and *Anopheles stephensi* and understanding the novel features of this plant to establish its applicability for controlling mosquito population at grass root level.

7.3 Results

7.3.1 *Agave* leaf extracts proficiently kill *Aedes, Culex* and *Anopheles* larvae

The larvicidal properties of *Agave angustifolia* (**Figure 7.1A and B**) were analyzed against *A. aegypti*, *C. quinquefaciatus* and *A. stephensi* larvae. For that the crude

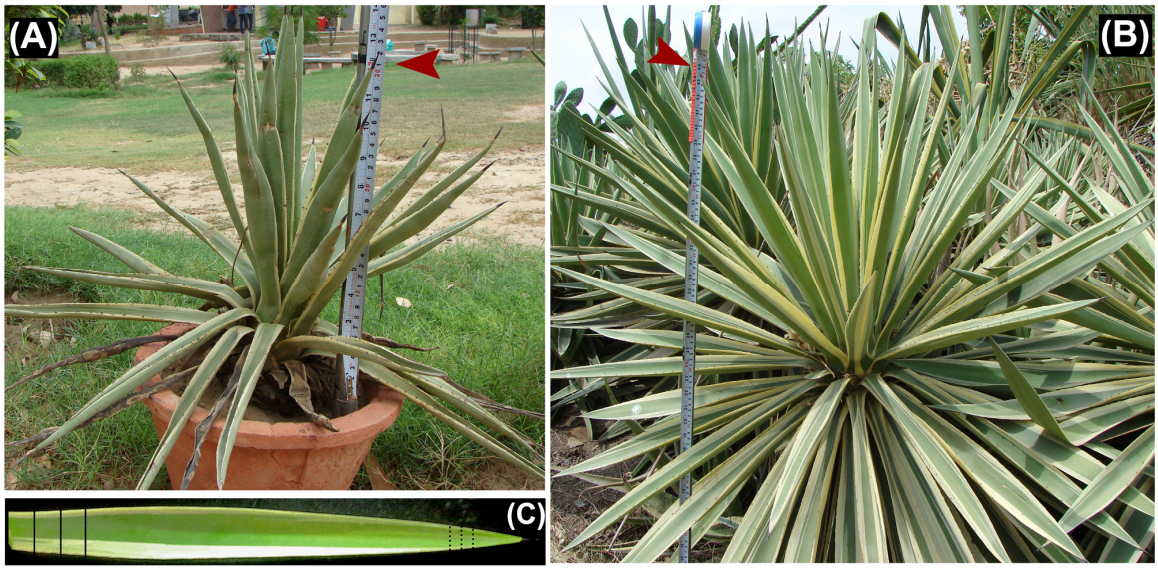

Figure 7.1: Representative *Agave angustifolia* plants selected for larvicidal activity. *Agave angustifolia* plants with different heights, which denote their vegetative growth, were selected for analyzing the larvicidal activity in their leaf extracts. (**A**) Smaller size plants (12 inches in height) growing in a pot or (**B**) a larger size plants (44 inches in height) growing in an open field are shown here. (**C**) *Agave angustifolia* leaf depicting the pattern of slicing for crude extract preparation. Solid and dotted vertical lines indicate leaf areas proximal or distal to the stem, respectively. Black arrowheads indicate the height of each plant on an inch scale.

extracts from the fleshy leaf (**Figure 7.1C**) were prepared in different organic solvents. The larvicidal properties of *Agave angustifolia* (**Figure 7.1A and B**) were analyzed against *A. aegypti*, *C. quinquefaciatus* and *A. stephensi* larvae. For that the crude extracts from the fleshy leaf (**Figure 7.1C**) were prepared in different organic solvents as described for other plants (Bansal et al., 2012; Edeoga et al., 2005; Govindarajan, 2009; Jayanthi et al., 2012; Kovendan et al., 2012; Panneerselvam et al., 2012; Rawani et al., 2010). Since, the polarity of organic solvent is important for the extraction of plant metabolites, we used three different organic solvents such as, hexane, acetone and ethanol for this purpose as discussed in Materials and Methods. We adopted the simplest method of crude extract preparation so that a common user can effortlessly prepare it.

We analyzed the larvicidal activity of the organic crude extracts against *A. aegypti* larvae under standard lab-rearing conditions. The larval mortality in controls or those exposed to 100 ppm crude extract are presented in **Figure 7.2A**.

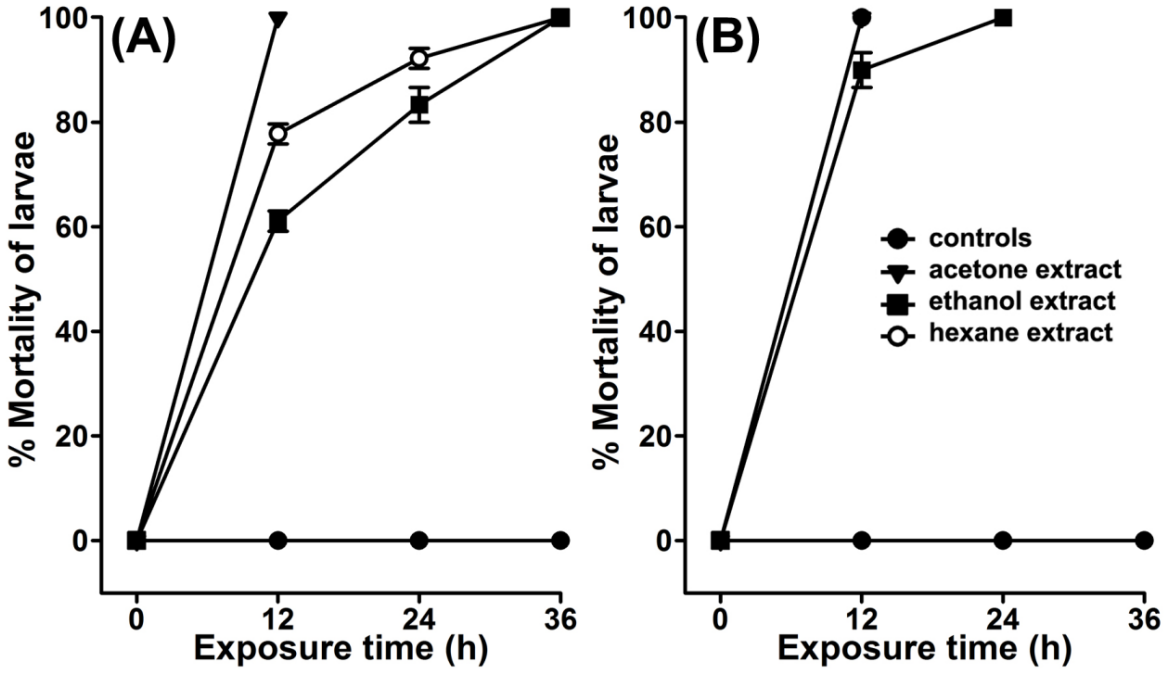

Figure 7.2: Larvicidal activity in the organic extracts of *Agave*. The extracts of *Agave angustifolia* leaves were prepared in different organic solvents such as acetone, ethanol or hexane. (**A**) *A. aegypti* or (**B**) *C. quinquefasciatus* larvae were treated with 100 ppm dose of these organic extracts separately. The percentage of larval mortality in each extract exposure was calculated against the sham treated controls and represented as the mean ± SD of triplicates.

These results revealed that *Agave angustifolia* crude extract in either of the organic solvents is effective to kill *A. aegypti* larvae in a time-dependent manner. The acetone

extract is most effective and killed all the larvae within 12h of exposure. Ethanol extract of *Agave angustifolia* demonstrated the same effect at 36h (100% mortality), however, it killed 61 ± 2% larvae in 12h. Moreover, the hexane extracts revealed intermediate larvicidal activity and likewise the mortality increased consistently (77 ± 2% to 100%) with time (12 to 36h) (**Figure 7.2A**). Several studies reported that organic extracts prepared from other plants exhibit larvicidal activity only against one genus of mosquito (Bansal et al., 2012; Govindarajan, 2009; Jayanthi et al., 2012; Kovendan et al., 2012; Panneerselvam et al., 2012; Rawani et al., 2010; Shahi et al., 2010). Thus, to understand the broad larvicidal spectrum of *Agave angustifolia* organic extracts we analyzed their effects against the larvae of other mosquitoes. We found that *Agave angustifolia* extract in hexane or acetone also killed 100% *C. quinquefasciatus* larvae within 12h (**Figure 7.2B**). However, the ethanol extract killed 90 ± 3% *C. quinquefasciatus* larvae in the same duration. Interestingly, the larvicidal efficacy of *Agave angustifolia* extract in the organic solvents is more pronounced against *C. quinquefasciatus* than *A. aegypti* larvae (**Figure 7.2**). In addition, we found that the above-mentioned *Agave angustifolia* organic extracts also have uniform lethality against *A. stephensi* larvae (**Figure 7.3**). The use of organic solvents in extract preparations may invite some issues such as, their incompatibility and toxicity to the natural environment, cost of preparation and availability for a common user. Thus, we prepared aqueous extract from *Agave angustifolia* leaves and estimated its dose-dependent larvicidal efficacy against *A. aegypti* larvae. Results presented in **Figure 7.4A** revealed that 50 µg/ml of *Agave angustifolia* aqueous extract is strong enough to kill all the *A. aegypti* larvae within 12h.

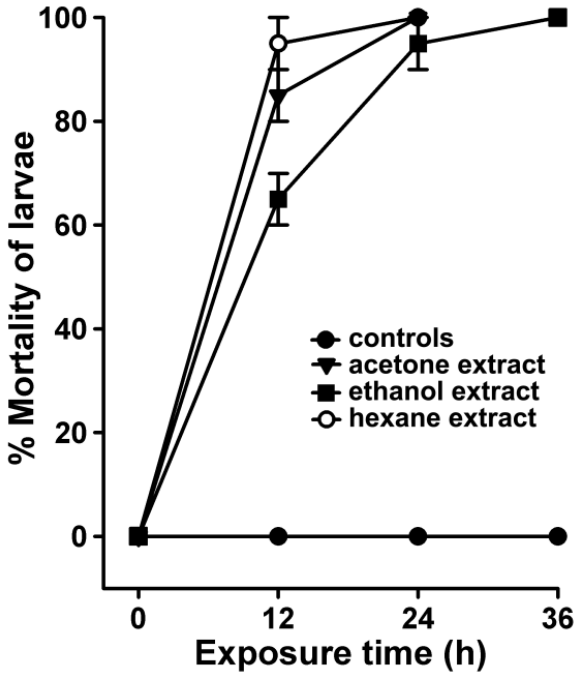

Figure 7.3: Larvicidal activity in the organic extracts of *Agave* against *A. stephensi* larvae. The extracts of *Agave angustifolia* leaves were prepared in different organic solvents such as acetone, ethanol and hexane. *A. stephensi* larvae were treated with 100 ppm dose of these organic extracts separately. The percentage of larval mortality in each exposure was calculated against the sham treated controls and represented as the mean ± SD of triplicates.

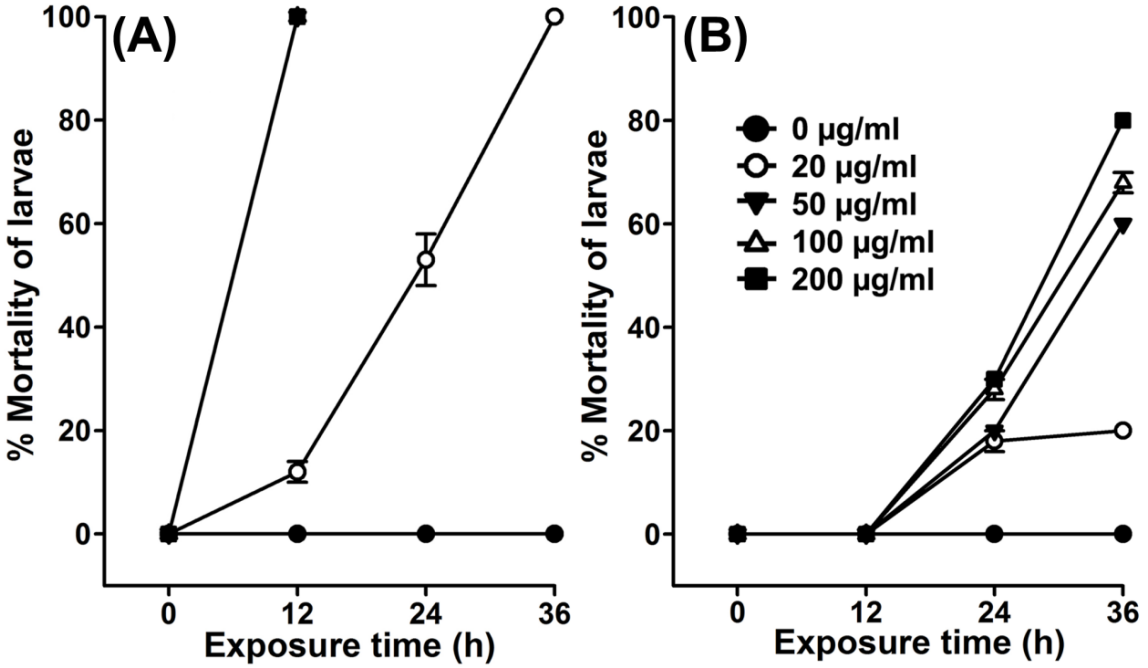

Figure 7.4: Effects of seasonal variations on *Agave*-mediated larvicidal activity. *A. aegypti* larvae were exposed to various doses (0 to 200 µg/ml) of aqueous extracts prepared from the plant leaves that were growing outside in an open area during (**A**) summer or (**B**) winter season. The percentage mortality of larvae at each time point was calculated against the sham treated controls (0 µg/ml) and represented as the mean ± SD of triplicates.

Table 7.1. Probit analysis of *Agave angustifolia* larvicidal activity against *Aedes aegypti* larvae.

Time (h)	N	LD 50 (µg/ml)	Slope ± SE	CL (95%)	Chi-square	*p*-value
12	30	28.270	5.560 ± 0.668	24.183 - 32.460	0.886	0.642
24	30	19.157	5.016 ± 1.012	14.243 - 23.001	0.995	0.996

The LD_{50} value at 12h was estimated to be 28.270 µg/ml by the probit analysis method (**Table 7.1**). Furthermore, 100 µg/ml *Agave angustifolia* aqueous extract also exhibited 100% killing efficiency against *A. aegypti*, *C. quinquefasciatus or A. stephensi* larvae within 12h (**Figure 7.5**). These findings are noteworthy in comparison to other reports where aqueous extract of many plants demonstrated the larvicidal activity, mostly between 24 to 72h and even later (Chansang et al., 2005; Farias et al., 2010; Singha and Chandra, 2011).

This least effectual time for *Agave angustifolia*-mediated larval mortality is a unique feature and to the best of our knowledge, it is never reported before.

7.3.2 *Agave* larvicidal activity is highly thermostable, inherited and independent of plant vegetative growth

In our region or other parts of the world, the environmental temperature reaches up to 50°C during summer. Because *Agave angustifolia* is a drought deciduous plant thus, we postulated that its larvicidal activity must be mediated by heat- resistant secondary metabolites. To demonstrate, we pre-incubated the aqueous extract for 1h at different temperatures before performing the larvicidal assays. Prior incubation of aqueous extract at RT or 50°C killed 86 ± 6% and 80 ± 0% *A. aegypti* larvae, respectively in 12h (**Figure 7.6**, p=0.2). However, the extracts pre-incubated at 75°C or 100°C killed 58 ± 8% and 60 ± 0% larvae, respectively in 12h (p=0.007 between RT and 75°C incubated extracts). Importantly, the larvicidal effects of all these pre-incubated extracts are similar at 24h (**Figure 7.6**, p=0.1 between RT and 100°C pre incubated extract-mediated larval lethality). This heat resistant larvicidal activity of *Agave angustifolia* extract

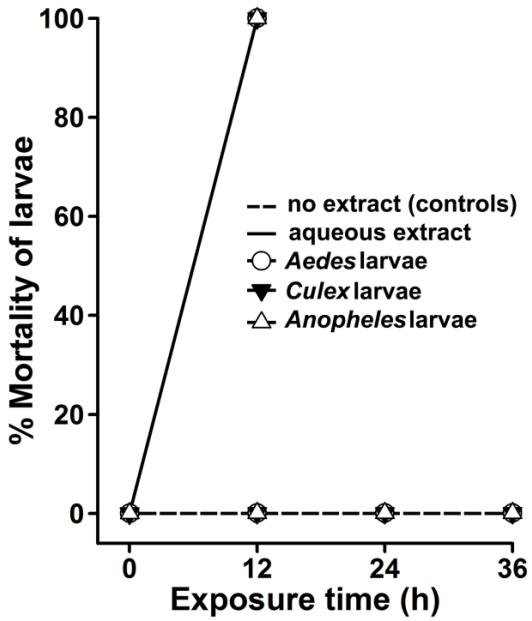

Figure 7.5: *Agave* aqueous extract effectively kills mosquito larvae. *A. aegypti*, *C. quinquefaciatus* or *A. stephensi* larvae were sham treated (no extract, controls) or exposed to 100 µg/ml aqueous extract of *Agave angustifolia*. The percentage mortality of larvae at each time point was calculated against the controls for each genus individually and represented as the mean ± SD of triplicates.

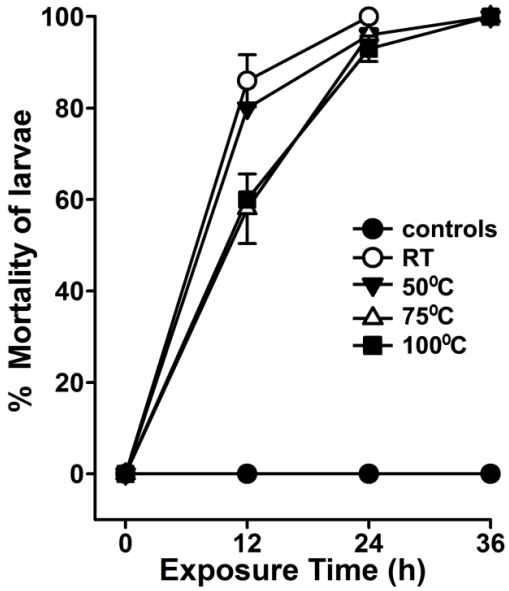

Figure 7.6: *Agave* aqueous extract-mediated larvicidal activity is highly thermostable. *A. aegypti* larvae were exposed to 100 µg/ml *Agave angustifolia* aqueous extracts that were pre-incubated at different temperatures for 1h. Percentage mortality of larvae was calculated at each time point against the sham treated controls and represented as the mean ± SD of triplicates.

may be useful to control the mosquito population in natural warm-hot conditions.

Agave angustifolia is generally a medium sized plant (~48 inches in height). Flowering occurs around 10 years of age or much later (Gilman, 1999). The plant we selected for larvicidal assays were approximately 44 inches in height and thus we considered them mature (**Figure 7.1B**). To determine the intrinsic larvicidal nature of *Agave angustifolia,* we compared the larval lethality in the aqueous extracts of juvenile and mature plants as represented in **Figure 7.1A** and **7.1B**. We found that 100 µg/ml aqueous extract of mature or juvenile plant killed 98 ± 1.4% and 93 ± 4% *A. aegypti* larvae, respectively at 12h (**Figure 7.7**, p=0.075). On the other hand,

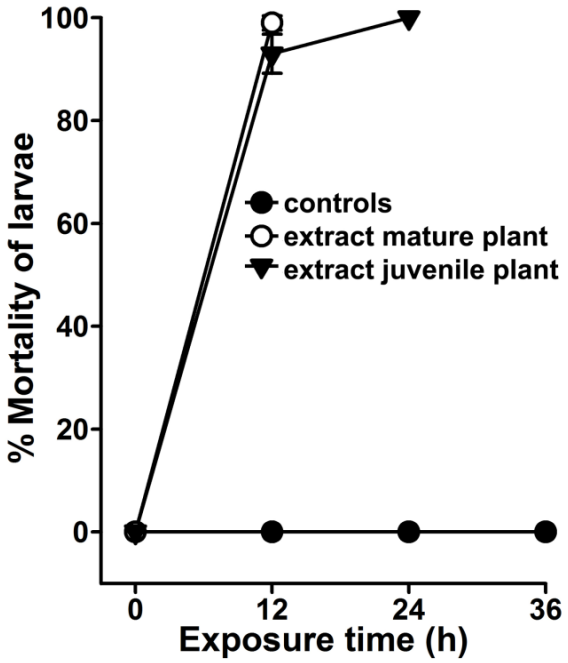

Figure 7.7: *Agave* larvicidal activity is independent of the plants vegetative growth. *A. aegypti* larvae were exposed to 100 µg/ml aqueous extract prepared from the leaves of a mature (~44 inches in height) or juvenile (~12 inches in height) *Agave angustifolia* plants. Percentage larval mortality at each time point was calculated against the sham treated controls and represented as the mean ± SD of triplicates.

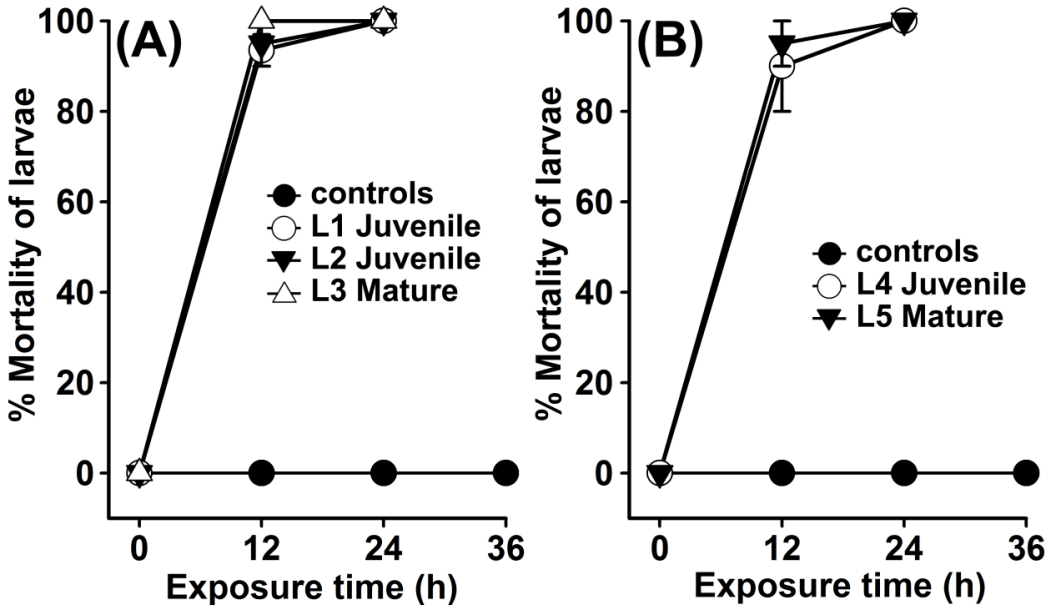

Figure 7.8: Larvicidal activity of *Agave* collected from different locations. Aqueous extracts were prepared from the leaves of mature and juvenile *Agave angustifolia* plants that were collected from five different locations (L) within the 400 hectare area of the university campus and nearby roadsides. **(A)** *A. aegypti* or (**B**) *A. stephensi* larvae were exposed to 100 µg/ml dose of each extract separately.

Percentage larval mortality at each time point was calculated against the sham treated controls and represented as the mean ± SD of triplicates.

we also analyzed the larvicidal activity in other mature and juvenile *Agave angustifolia* plants (height ranges from 4 to 50 inches) collected from different nearby locations and all revealed similar results (**Figure 7.8**). This indicates that the larvicidal nature of *Agave angustifolia* is not only inherited, it is also independent of its vegetative growth.

7.3.3 *Agave* larvicidal activity is induced exclusively during summer

We experienced a surprising outcome regarding the larvicidal nature of *Agave angustifolia*. Aqueous extracts prepared during summer (April-August, when outside temperature rises up to 45^{o}C or higher) from the plants that were growing in the open field demonstrated a dose-dependent larvicidal activity against *A. aegypti* larvae (**Figure 7.4A** and **Figure 7.5**). However, the aqueous extract prepared from the same plants revealed reduced and delayed larvicidal activity during winter (December-February, when the outside temperature falls between 4-10^{o}C or lower). Results depicted in **Figure 7.4B** revealed that 100 µg/ml aqueous extract killed 0 ± 0% *A. aegypti* larvae in 12h and likewise increased to 68 ± 2% at 36h of exposure. This larvicidal activity is significantly reduced as well as delayed in comparison to the summer activity (**Figure 7.4A** and **B**). These observations indicated that *Agave angustifolia* metabolite(s) mediating larvicidal activity in aqueous extract is/are induced by the environmental conditions, at least the higher temperature. This may be due to the specific physiological role of these metabolite(s) under given circumstances.

7.3.4 Manipulation of environmental temperature modulates *Agave* larvicidal activity and profiling of secondary metabolites

Our results indicated that environmental conditions seem to be influencing the larvicidal properties of *Agave angustifolia* (**Figure 7.4**). We hypothesized that during winter if *Agave angustifolia* plants are maintained under warm conditions, their larvicidal activity may be induced. We tested this fact after swapping juvenile plants ~12 inches in height (**Figure 7.1A**) growing in individual pots from outside cold winter environment to 37^{o}C in a plant growth chamber and compared their larvicidal activity to those growing outside. The aqueous extract from the plants maintained under warmer conditions revealed stronger lethality against *A. aegypti* larvae than the plants growing outside in winter (**Figure 7.9A**).

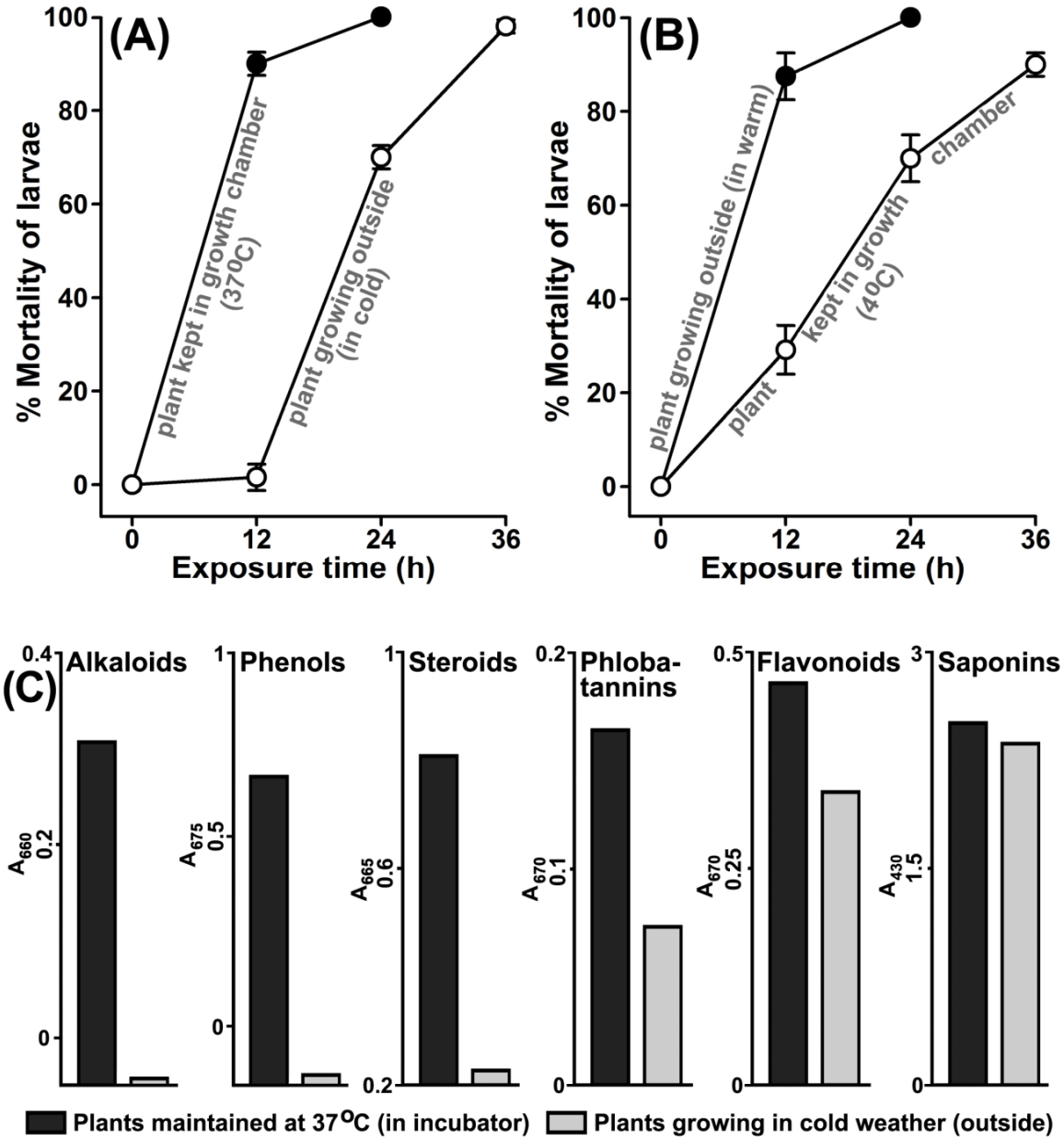

Figure 7.9: Manipulation of environmental temperature induces *Agave*-mediated larvicidal activity. The effect of environmental temperature on the induction of larvicidal activity in *Agave angustifolia* was analyzed against *A. aegypti* larvae. For that, the larvicidal activity in 100 µg/ml aqueous extract was compared from the plants that were growing or maintained in two different environmental conditions. The comparative larvicidal activities are shown here in those plants which were growing (**A**) outside in the cold environment during winter season and similar plants maintained at 37°C in a plant growth chamber or (**B**) outside in hot environment during the summer season and similar plants maintained at 4°C in a growth chamber as discussed in Material and Methods. The percentage mortality of larvae at each time point was calculated against the sham treated controls (not shown here) and represented as the mean ± SD of triplicates. (**C**) The relative levels of various secondary metabolites were compared in the aqueous extracts of *Agave angustifolia* plants maintained at 37°C in a plant growth chamber or growing in external environment during cold season as mentioned in the panel **A**. The values represent absorption maxima (A) in visible range for each metabolite separately.

Aqueous extract prepared from the plants that were maintained in a warm incubator killed 90 ± 3% larvae at 12h of exposure. However, the similar control plant growing

outside in the cold weather killed 1.6 ± 2.8% larvae in same time (p=<0.001). In addition, we also performed the similar experiment during summer and shifted the plants from outside hot to 4°C, keeping rest conditions similar to the natural environment, and performed larvicidal assays. The results illustrated in **Figure 7.9B** revealed that the plants growing outside in hot summer conditions killed 87 ± 5% and those maintained at lower temperature killed 29 ± 5% *A. aegypti* larvae at 12h (p=<0.001). This indicated that, at least, one of the abiotic stress factors (i.e. increased temperature) stimulates the production of those secondary metabolite(s) in *Agave angustifolia* that exhibit(s) larvicidal activity. Overall, these results demonstrated that the *Agave angustifolia* is equipped with active larvicidal metabolites mostly during summer however, the semi-natural warmer environment under the laboratory conditions can also replicate the same effect.

Our results confirmed that the larvicidal activity in *Agave angustifolia* is induced at least by environmental temperature (**Figure 7.9A** and **B**). Thus, we hypothesized that abiotic stress, i.e. temperature may alter the composition of metabolites and due to the production of specific compound(s) *Agave angustifolia* exhibits distinct larvicidal activity. To demonstrate this we analyzed and compared the levels of various secondary metabolites in those plants that are discussed in **Figure 7.9A**. The plant maintained in warm environment has elevated levels of several secondary metabolites such as flavonoids, phenols, alkaloids, phlobatannins and steroids in comparison to the plant growing at a low temperature (**Figure 7.9C**). In addition, when we analyzed these

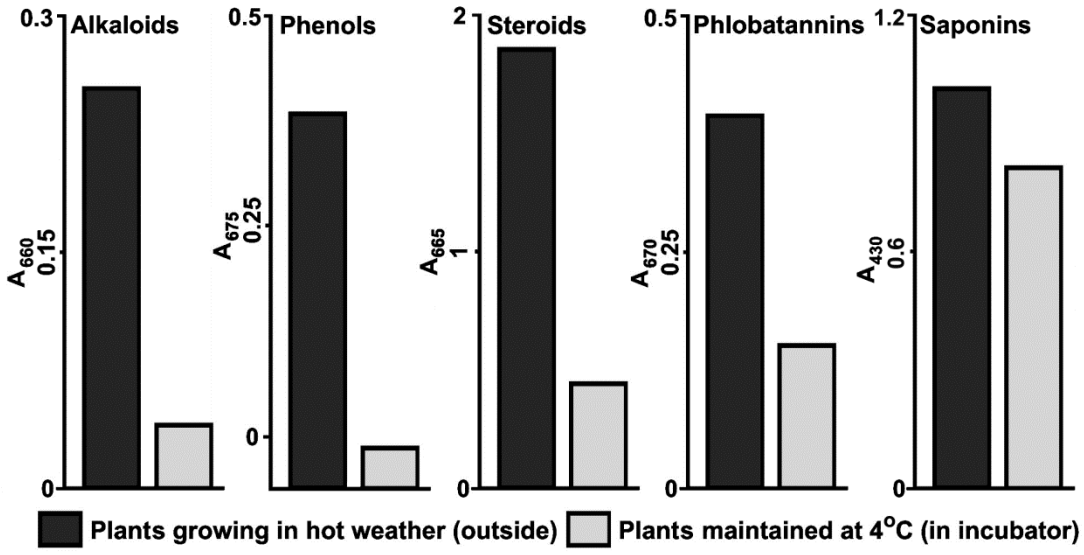

Figure 7.10: Secondary metabolite profiling of *Agave*. The relative levels of various secondary metabolites were compared in the aqueous extracts of identical *Agave angustifolia* plants maintained either at 4°C in a plant growth chamber or growing in the external environment during summer season as mentioned in Materials and Methods. The values represent absorption maxima (A) in visible range for each metabolite separately.

metabolites in plants as mentioned in **Figure 7.9B**, their levels also revealed similar patterns (**Figure 7.10**). These findings correlated an association between the external environment-induced production of secondary metabolites and larvicidal activity in *Agave angustifolia* aqueous extracts.

7.3.5 Agave dry leaf powder formulation also exhibits strong larvicidal activity

The larvicidal activity of *Agave angustifolia* is although inherited, but appears to be prominent exclusively during summer (**Figure 7.4**). This limited duration of available *Agave angustifolia* larvicidal activity in natural conditions impedes its utilization throughout the year. To overcome these limitations, we assumed that the leaf with larvicidal activity (**Figure 7.5**) could be dried and stored as powder for future usage. We prepared the powder from sun-, oven- or shade-dried leaves and after three months of shelf life, the larvicidal activity was analyzed in the powder or powder-free extract against *A. aegypti* larvae as mentioned in Materials and Methods. We found that the powder-free extract from sun-, oven- or shade-dried leaves exhibited 20 ± 1.4%, 0 ± 0% and 10 ± 0% larval mortality, respectively after 12h (**Figure 7.11**), which was remarkably less in comparison to the original leaf extract-mediated anti-larval activity (**Figure 7.5**). Furthermore, these extracts could increase the larval mortality to 60 ± 4%, 55 ± 4% and 45 ± 2.5%, respectively at 36h (**Figure**

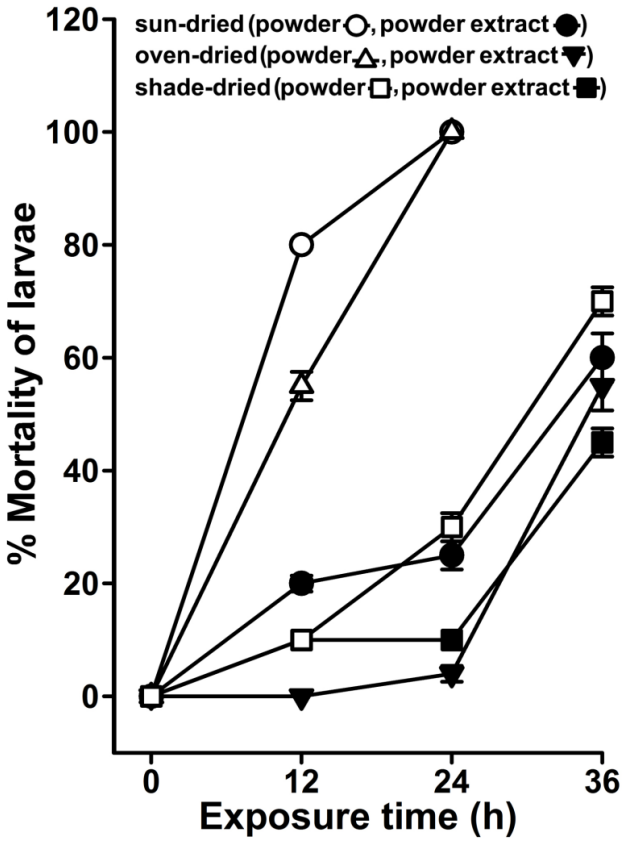

Figure 7.11: The larvicidal activity of *Agave* dried powder. *Agave angustifolia* leaves with active larvicidal activity were either sun-, oven- or shed-dried and the powder was prepared. The powder was stored at room temperature under moisture free conditions for three months (the shelf life of the powder). *A. aegypti* larvae were exposed to the powder-free aqueous extracts or powder directly added to the water in the amount equivalent to the fresh leaves exhibiting the larvicidal activity as mentioned in Figure 4. The percentage mortality of the larvae at each time point was calculated against sham-treated controls (not shown here) and represented as the mean ± SD of triplicates.

7.11). Interestingly, the sun- and oven-dried leaf powder itself killed 80 ± 0% and 55 ± 3.5% larvae, respectively in 12h that increased gradually to 100% mortality at 24h (**Figure 7.11**). However, the powder prepared from shade-dried leaves revealed minimum mortality (10 ± 0% to 70 ± 2.5%) with time (12 to 36h).

In conclusion, dried leaf powders have slightly delayed larvicidal activity against the original leaf extract. Interestingly, the dried leaf powder-mediated larval lethality is dependent on the method of drying the original leaf and sun-dried leaf powder could reveal stronger larvicidal effects among others (**Figure 7.11**). The inability of powder-free aqueous extract to kill larvae may be due to inadequate extraction of active larvicidal compounds from the powder due to the limitations of our extraction methods. Furthermore, the larvicidal activity in powders itself may be due to time-dependent leaching of larvicidal components into the water and that may explain those slightly delayed killing effects (**Figure 7.11**).

7.4 Discussion

Crude extracts prepared from the whole plant or specific parts of the plant such as leaf, stem, fruit and root have been reported to exhibit potent lethality against insect larvae (Bansal et al. 2012; Ghosh et al., 2012; Govindarajan, 2009) and hence, we termed them phyto-insecticides. These phyto-insecticides are biodegradable and reduce the environmental chemical burden as posed by the synthetic chemicals. In this study, we found that the crude extract prepared from *Agave angustifolia* by a simple, least labor-intensive and cost-effective method exhibits strong larvicidal activity against *A. aegypti*, *C. quinquefasciatus* and *A. stephensi* larvae within 12h (**Figure 7.5**). This is the minimum time reported for a plant crude extract to kill all the larvae of medically important mosquitoes and upholds a promising future to control vector population.

Larvicidal properties of natural compounds vary from one plant to another and may have a low degree of effectiveness only against selected genera of mosquitoes. The variations in the larvicidal efficacy of plant extracts are highly dependent on the type or the polarity of the solvent employed for extraction purpose (Ghosh et al., 2012). Therefore, the solvents with varying degree of polarity such as, hexane, petroleum ether, methanol, benzene, ethyl acetate, methanol, chloroform and acetone are generally used for this purpose (Ghosh et al., 2012; Govindarajan, 2009; Kumar et al., 2012; Rawani et al., 2010). The use of unrelated solvents for the preparation of plant crude extracts sometimes reveals that the extraction efficiency of one solvent is superior over the other solvents (Rawani et al., 2010; Singha and Chandra, 2011). Surprisingly,

we found that the crude extracts of *Agave angustifolia* in individual solvents of varying polarity (ethanol and hexane) have more pronounced larvicidal effect against *C. quinquefasciatus* than *A. aegypti* larvae (**Figure 7.2**). These findings support the previous studies where lethal doses of *Eichhornia crassipes* and *Artemisia nilagirica* plant extracts vary for two different genera of the mosquito (Jayanthi et al., 2012; Panneerselvam et al., 2012).

This may be due to the presence of diverged bioactive compounds in *Agave* or the varying solubility of the same compound in different solvents. In this condition, preparing the plant extract in a mixture of two or more solvents may enhance its mosquitocidal activity (Rawani et al., 2010; Singha and Chandra, 2011). In our experiments when we employed similar strategies to prepare *Agave angustifolia* extract by using a mixture of solvents, we did not find any additional effect on its larvicidal properties (**Figure 7.12**). This simply may be due to the limitations of our extraction methodology.

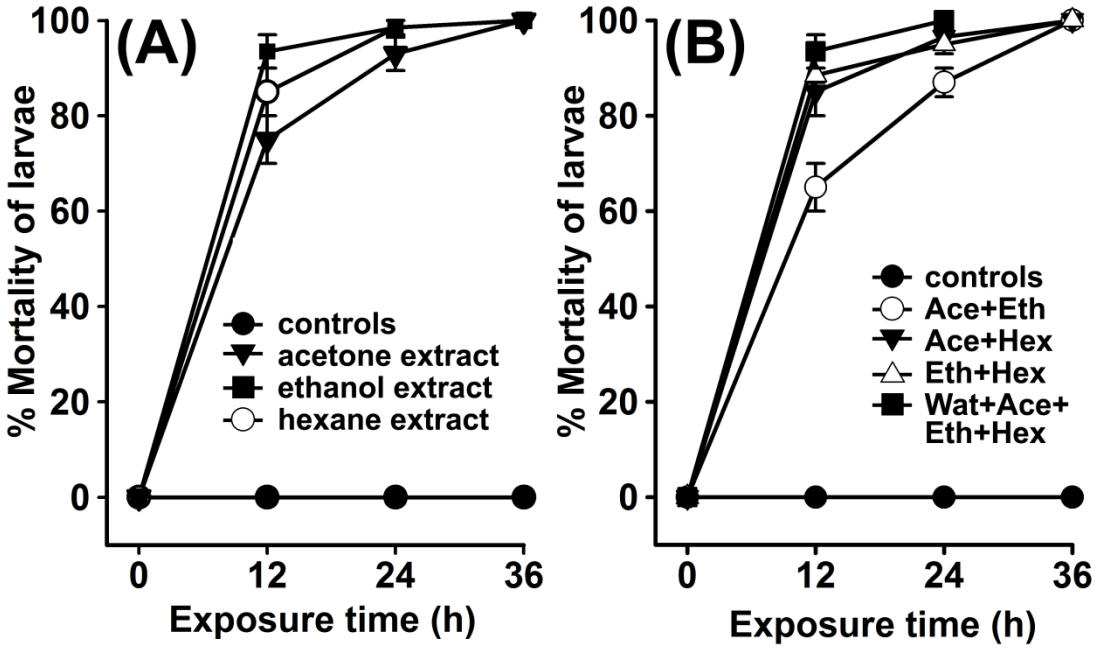

Figure 7.12: Larvicidal activity of *Agave* extract in the combinations of different organic solvents. The extracts of *Agave angustifolia* leaves were prepared either in **(A)** one particular organic solvent such as acetone, ethanol or hexane or (**B**) in the combination of two or more solvents in equal ratio as depicted in the figure**.** *A. aegypti* larvae were treated with 100 ppm dose of these organic extracts separately. The percentage of larval mortality was calculated against the sham treated controls and represented as the mean ± SD of triplicates. Abbreviations: **Ace**, Acetone; **Eth**, Ethanol; **Hex**, Hexane; **Wat**, Water.

In general, the organic solvents used for plant extraction might have a concern for 'cost of preparation' and may end up in escalating the chemical burden or toxicity in the natural environment as well. Their incompatibility to the aqueous environment is also

an associated concern. Therefore, we planned to analyze the larvicidal activity in a simply prepared aqueous extract of *Agave angustifolia*, which satisfies all the concerns related to organic solvent extractions. Interestingly, the aqueous extract of *Agave angustifolia* also exhibited a strong larvicidal activity against *A. aegypti*, *C. quinquefasciatus* and *A. stephensi* larvae (**Figure 7.5**). This is in contrast to some other reports where organic extracts from plants exhibit strong larvicidal activity however, their aqueous extracts remain inactive (Germinara et al., 2011).

While planning strategies to apply plant extracts for controlling the larval population, especially in warm countries, it may be worthwhile to identify those biolarvicides that exclusively withstand the environmental temperature. In other words, the discovery of temperature-resistant biolarvicides may be helpful in this direction. Although many of the plants have larvicidal activity in their aqueous extracts however, this activity is lost with time and/or increased temperature (Chansang et al., 2005; Pontual et al., 2012). On the contrary, we found that *Agave angustifolia* aqueous extract-mediated larvicidal activity was mostly retained in the crude extract after heat treatment (**Figure 7.6**), which may signifies its advanced usage in controlling mosquito populations in the natural environment of tropical countries. These findings also highlight that it will be important to investigate the mechanism by which *Agave angustifolia* acquires heat-resistant larvicidal activity.

The world of plants is unique in terms of producing different compounds or metabolites that may be directly linked to their stages of vegetative development, environmental conditions or geographical locations (Daniel et al., 2011). Previous reports suggested that the larvicidal efficacy of phytochemicals varies with plant age; young tissues have greater larvicidal activity than the older ones or sometimes may be *vice versa* (Ghosh et al., 2012). Thus, a consistency of larvicidal activity in the plant is an important concern in this field. We analyzed different sized *Agave angustifolia* plants, which denote their levels of maturity and vegetative growth, and found that the larvicidal activity is exhibited by all of them (**Figure 7.7** and **Figure 7.8**). These findings clearly indicated that the larvicidal nature of *Agave angustifolia* is an inherited feature and that is independent of its vegetative growth. These findings are not in agreement with the other reports where only the mature plants exhibited the larvicidal activity (Ghosh et al., 2012). In addition, geographical location of the plant also seems to be affecting its larvicidal properties. In case of *Annona squamosa* the plant leaves collected from different eco-zones possess various compositions of secondary metabolites and exhibit differential larvicidal activity (Daniel et al., 2011). However, when we collected *Agave*

angustifolia samples from different nearby areas, they resulted in similar larvicidal activity against mosquito larvae (**Figure 7.8**).

In addition, some published reports indicated that another species *Agave sisalana* also exhibited positive larvicidal activity (Nunes et al., 2014; Pizarro et al., 1999). In the first study, waste residues after sisal fiber separation from *Agave sisalana* leaves were found to be effective in killing *A. aegypti* or *C. quinquefasciatus* larvae within 24h. However, the effective lethal dose of these fiber residues against *A. aegypti* larvae was almost twice to that of *C. quinquefasciatus* larvae (Pizarro et al., 1999). In the second study, the liquid waste of *Agave sisalana* killed 100% *A. aegypti* larvae within 24h at 20 mg/ml concentration and the LC_{50} value was found to be 5.9 mg/mL (Nunes et al., 2014). Interestingly, a study was performed directly from the *Agave sisalana* leaves extracts and found that 2% dilution of the extract revealed 100% mortality against *A. stephensi* larvae however, 1% dilution exhibited same results in case of *C. quinquefasciatus* and *A. aegypti* larvae (Singh et al., 2014). It is also noteworthy to mention that the leaf extract prepared from one more species of *Agave*, *Agave americana* also revealed 100% mortality against 4th instar larvae of *Anopheles*, *Aedes* and *Culex* mosquitoes at a concentration of 0.08% within 24-48h (Dharmshaktu et al., 1987). In nutshell, all these studies indicated that although other species of *Agave* also exhibit larvicidal activity however, their larvicidal efficacy is variable against different mosquito larvae. Interestingly, our study revealed that a single dose (100 µg/ml or 0.01%) of *Agave angustifolia* extract killed *Aedes, Culex* and *Anopheles* larvae in a short duration of 12h (**Figure 7.5**).

The environmental conditions sometimes have a direct effect on plant physiology and behavior. Plants frequently encounter adverse abiotic conditions, such as salinity, drought, freezing and elevated environmental temperatures. Stress responses in plants are dynamic and engage complex crosstalk at different regulatory levels. Plants might overcome these stresses through avoidance or tolerance, which includes metabolic adjustment through alteration of compatible solutes or secondary metabolites (Krasensky and Jonak, 2012; Ramakrishna and Ravishankar, 2011). Our observations regarding the induction of *Agave angustifolia* larvicidal activity, exclusively during summer, might be an example of environmental abiotic stress. We believe that the plant might be producing some specific metabolites to counteract those stresses and some of these metabolites are also mediating larval lethality (**Figure 7.5** and **Figure 7.9**).

Variations in the temperature, an abiotic environmental factor, also alter the composition of plant metabolites. Studies show that the plant *Panax quinquefolius*

growing just at the difference of +5^{o}C contains a higher concentration of storage root ginsenosides than the ones growing at lower temperature (Jochum et al., 2007). Metabolic profiling of *Arabidopsis* indicated that 143 and 311 metabolites were altered in response to heat and cold shock, respectively. Interestingly, the comparison of these heat- and cold-shock responses revealed that the majority of heat-shock responses were shared with cold-shock responses (Kaplan et al., 2004). However, in case of *Agave angustifolia* this may not be true as the metabolites exhibiting strong larvicidal activity seems to be induced exclusively during summer but not in the winter (**Figure 7.4**).

Our study revealed that the levels of flavonoids, phenols, alkaloids, phlobatannins and steroids are higher in those *Agave angustifolia* plants that were maintained in warmer environments (**Figure 7.9C** and **Figure 7.10**). This profiling of secondary metabolites correlated the observed larvicidal activity in these plants (**Figure 7.9A** and **B**). These results are in agreement with other studies where several compounds such as terpenes, flavones, xanthones, steroids, resins, flavonoids, alkaloids, anthroquinones, anthocyanins, terpenoids, glycosides, phenols and saponins are mostly responsible for mosquitocidal activities either individually or in combinations (Farias et al.,2010; Ghosh et al., 2012; Kovendan et al., 2012; Nikkon et al., 2010). In our study, we did not find any significant difference in the levels of saponins in these plants (**Figure 7.9C** and **Figure 7.10**). Further studies are required to isolate and identify the active principles involved in *Agave angustifolia* -mediated larvicidal activity and their mode of action. Our group is actively engaged in that direction.

Larvicidal activity in *Agave angustifolia* is not perquisite for all seasons (**Figure 7.4**). However, the plant leaves with larvicidal activity may be stored in the form of dehydrated powder to avoid the fermentation of its active components, easy transportation and for future applications. Our study found that *Agave angustifolia* powder-free aqueous extract exhibited low larvicidal activity in comparison to the powder itself, which may be due to inadequate extraction of larvicidal metabolites in our preparations (**Figure 7.11**). In addition, powder-mediated larvicidal activity is highly dependent on the process of drying the wet leaves. This may be due to the quantitative/qualitative alteration of the active larvicidal metabolites during drying-mediated osmotic stresses as reported in other plants where air- or sun-drying markedly affected the levels of both primary and secondary metabolites (Dai et al., 2010; Mbah et al., 2012). We look forward for *Agave angustifolia* dry powder formulated preparations to enhance its potency and stability with minimal adverse effects on the environment. This

could help to design efficient strategies for *Agave angustifolia* extract-mediated mosquito controls.

7.5 Conclusion

In conclusion, the plants displaying larvicidal activity portray a noteworthy attention over the synthetic chemicals due to their biodegradable nature. *Agave angustifolia* aqueous extract that was prepared by the least labor-intensive and cost-effective method display a strong larvicidal activity against three major human disease vectors *A. aegypti*, *C. quinquefasciatus* and *A. stephensi* within a short exposure. Interestingly, the larvicidal activity of *Agave angustifolia* is heat-resistant and induced under the defined conditions therefore, it may be easily applicable at grass-root levels to control mosquito population.

Conclusions and Future Prospects

- Heme peroxidase HPX15 is characterized in Indian malaria vectors *A. stephensi* (AsHPX15) and *A. culicifacies* (AcHPX15). AsHPX15 has orthologs in 18 worldwide distributed species of *Anopheles* with 65-99% amino acid identity. As well as HPX15 does not have ortholog in other organisms, including arthropods such as, *Culex, Aedes* and *Drosophila*. Therefore, HPX15 is a lineage-specific heme peroxidase. *A. stephensi* HPX15 (AsHPX15) is 1941 bp long gene (three exons and two introns), which has binding sites for Ecdysone, STAT and Rel in its 5' UTR regulatory region and codes for a 597 amino acids long globular secretory protein. AsHPX15 is a blood induced midgut gene, may have role in development and immunity. Thus, due to the highly conserved nature of HPX15 protein among 19 anophelines, we propose that HPX15 might serve as a 'potent candidate' that can be used as a common target to manipulate mosquito vectorial capacity and blocking the transmission of malaria infection.

- Functional analysis of AsHPX15 through gene silencing approach reveals that disruption of gut barrier via HPX15 silencing lead to the activation of immune responses against *Plasmodium* and heavy bacterial load in *A. stephensi* midgut. As a result of immune activation, there is reduction in number of *Plasmodium* and bacteria. Nitric oxide synthase (NOS) is working as anti-plasmodial and -bacterial molecule after silencing the AsHPX15 gene. Thus, on the basis of our observation, we proposed a model that HPX15 silencing in *A. stephensi* may modulate the immune system in such a way that co-infection of *Plasmodium* along with exogenous bacteria, result in *Plasmodium* regulation through specific immune pathways. Due to uniqueness among anophelines and role in modulation of gut immunity make AsHPX15 as a potent target to control *Plasmodium* development inside the mosquito host.

- We have discovered that AsHPX15 is modulating gut immunity to regulate *Plasmodium* development in *A. stephensi*. Further, it is required to analyze the effect of AsHPX15 gene against field isolated *Plasmodium* strains.

- We have identified *Agave angustifolia* aqueous extract as potential larvicidal against all three disease vectors *Aedes*, *Culex* and *Anopheles* within short time period of 12h. Aqueous extract can be prepared by common man with the least labor-intensive and cost-effective method. Larvicidal activity is thermostable and dry leaf powder of plant also exhibit activity, this makes it suitable for transportation purpose. Further, in future this plant extract can be used for field trials at larger scale in aquatic ecosystem, so that potent larvicidal nature of *Agave angustifolia* can be used to eliminate vector population from disease prevalent areas.

- Active compound from water extract of *Agave angustifolia* can also be isolated to analyze their pronounced anti-larval effects.

References

References

Adak T, Kaur S, Singh OP. 1999. Comparative susceptibility of different members of the *Anopheles culicifacies* complex to *Plasmodium vivax*. Trans Roy Soc Trop Med Hyg 93:573-577.

Agaisse H, Perrimon N. 2004. The roles of JAK/STAT signaling in *Drosophila* immune responses. Immunol Rev 198:72–82.

Ahmed AM, Baggott SL, Maingon R, Hurd H. 2002. The costs of mounting an immune response are reflected in the reproductive fitness of the mosquito *Anopheles gambiae.* OIKOS 97:371–377.

Akagi K, Ueda H. 2011. Regulatory mechanisms of ecdysone-inducible Blimp-1 encoding a transcriptional repressor that is important for the prepupal development in *Drosophila*. Develop Growth Differ 53:697-703.

Aminake MN, Pradel G. 2013. Antimalarial drugs resistance in Plasmodium falciparum and the current strategies to overcome them. In Méndez-Vilas A, editor. Microbial pathogens and strategies for combating them: science, technology and education. Spain:Formatex Research Center 269-282.

Andersen SO. 2010. Insect cuticular sclerotization: a review. Insect Biochem Mol Biol 40: 166-178.

Azambuja P, Garcia ES, Ratcliffe NA. 2005. Gut microbiota and parasite transmission by insect vectors. Trends Parasitol 21:568-572.

Bahia AC, Dong Y, Blumberg BJ, Mlambo G, Tripathi A, BenMarzouk-Hidalgo OJ, Chandra R, Dimopoulos G. 2014. Exploring *Anopheles* gut bacteria for *Plasmodium* blocking activity. Environ Microbiol 16:2980-2994.

Bahia AC, Kubota MS, Tempone AJ, Araujo HR, Guedes BA, Orfano AS, Tadei WP, Rios-Velasquez CM, Han YS, Secundino NF, Barillas-Mury C, Pimenta PF, Traub-Cseko YM. 2011. The JAK-STAT pathway controls *Plasmodium vivax* load in early stages of *Anopheles aquasalis* infection. PLoS Negl Trop Dis 5: e1317.

Bansal SK, Singh KV, Sharma S, Sherwani MR. 2012. Laboratory observations on the larvicidal efficacy of three plant species against mosquito vectors of malaria, dengue/dengue hemorrhagic fever (DF/DHF) and lymphatic filariasis in the semi-arid desert. J Environ Biol 33:617-621.

Barik TK, Sahu B, Swain V. 2009. A review on *Anopheles culicifacies*: from bionomics to control with special reference to Indian subcontinent. Acta Trop 109:87-97.

Beard J. 2006. DDT and human health. Sci Total Environ 355:78–89.

Beier MS. Pumpuni CB, Beier JC, Davis JR. 1994. Effects of para-aminobenzoic acid, insulin, and .gentamycin on *Plasmodium falciparum* development in Anopheline mosquitoes (Diptera: Culicidae). J Med Entomol 31:561–565.

Billker O, Lindo V, Panico M, Etienne AE, Paxton T, Dell A, Rogers M, Sinden RE, Morris HR. 1998. Identification of xanthurenic acid as the putative inducer of malaria development in the mosquito. Nature 392:289-292.

Billker O, Shaw MK, Margos G, Sinden RE. 1997. The roles of temperature, pH and mosquito factors as triggers of male and female gametogenesis of *Plasmodium berghei* in vitro. Parasitology 115:1-7.

Blandin S, Shiao SH, Moita LF, Janse CJ, Waters AP, Kafatos FC, Levashina EA. 2004. Complement-like protein TEP1 is a determinant of vectorial capacity in the malaria vector *Anopheles gambiae*. Cell 116:661-670.

Boissière A, Tchioffo MT, Bachar D, Abate L, Marie A, Nsango SE, Shahbazkia HR, Awono-Ambene PH, Levashina EA, Christen R, Morlais I. 2012. Midgut Microbiota of the Malaria Mosquito Vector *Anopheles gambiae* and Interactions with *Plasmodium falciparum* Infection. PLoS Pathog 8: e1002742.

Bray SJ, Kafatos FC. 1991. Developmental function of Elf-1: an essential transcription factor during embryogenesis in *Drosophila*. Genes Dev 5:1672-1683.

Buchon N, Broderick NA, Poidevin M, Pradervand S, Lemaitre B. 2009. *Drosophila* intestinal response to bacterial infection: activation of host defense and stem cell proliferation. Cell Host Microbe 5:200-211.

Burge C, Karlin S. 1997. Prediction of complete gene structures in human genomic DNA. J Mol Biol 268:78-94.

Butler D. 2009. Initiative targets malaria eradication. Nature 462:19.

Cartharius K, Frech K, Grote K, Klocke B, Haltmeier M, Klingenhoff A, Frisch M, Bayerlein M,Werner T. 2005. MatInspector and beyond: promoter analysis based on transcription factor binding sites. Bioinformatics 21:2933–2942.

Chakraborty S, Ray S, Tandon N. 1998. Seasonal prevalence of *Anopheles stephensi* larvae and existence of two forms of the species in an urban garden in Calcutta City. Indian J Malariol 35:8-14.

Chansang U, Zahiri NS, Bansiddhi J, Boonruad T, Thongsrirak P, Mingmuang J, Benjapong N, Mulla MS. 2005. Mosquito larvicidal activity of aqueous extracts of long pepper (Piper retrofractum Vahl) from Thailand. J Vector Ecol 30:195-200.

Chavshin AR, Oshaghi MA, Vatandoost H, Pourmand MR, Raeisi A, Enayati AA, Mardani N, Ghoorchian S. 2012. Identification of bacterial microflora in the midgut of the larvae and adult of wild caught *Anopheles stephensi*: a step toward finding suitable paratransgenesis candidates. Acta Trop 121:129–134.

Chen A, Rogan WJ. 2003. Nonmalarial infant deaths and DDT use for malaria control. Emerg Infect Dis 9:960–964.

Cheng G, Liu Y, Wang P, Xiao X. 2016. Mosquito defense strategies against viral infection. Trends Parasitol 32:177-186.

Choumet V, Carmi-Leroy A, Laurent C, Lenormand P, Rousselle JC, Namane A, Roth C, Brey PT. 2007. The salivary glands and saliva of *Anopheles gambiae* as an essential step in the Plasmodium life cycle: a global proteomic study. Proteomics 7:3384-94.

Christophides GK, Zdobnov E, Barillas-Mury C, Birney E, Blandin S, Blass C, Brey PT, Collins FH, Danielli A, Dimopoulos G, Hetru C, Hoa NT, Hoffmann JA, Kanzok SM, Letunic I, Levashina EA, Loukeris TG, Lycett G, Meister S, Michel K, Moita LF, Müller HM, Osta MA, Paskewitz SM, Reichhart JM, Rzhetsky A, Troxler L, Vernick KD, Vlachou D, Volz J, von Mering C, Xu J, Zheng L, Bork P, Kafatos FC. 2002. Immunity-related genes and gene families in *Anopheles gambiae*. Science 298:159-165.

Cirimotich CM, Dong Y, Clayton AM, Sandiford SL, Souza-Neto JA, Mulenga M, Dimopoulos G. 2011a. Natural microbe-mediated refractoriness to *Plasmodium* infection in *Anopheles gambiae*. Science 332:855-858.

Cirimotich CM, Dong Y, Garver LS, Sim S, Dimopoulos G. 2010. Mosquito immune defenses against *Plasmodium* infection. Dev Comp Immunol 34:387-395.

Cirimotich CM, Ramirez JL, Dimopoulos G. 2011b. Native microbiota shape insect vector competence for human pathogens. Cell Host Microbe 10:307–310.

Cox S, Niskar AS, Narayan KM, Marcus M. 2007. Prevalence of self-reported diabetes and exposure to organochlorine pesticides among Mexican Americans: Hispanic Health and Nutrition Examination Survey, 1982–1984. Environ Health Perspect 115:1747–1752.

Cox-Singh J, Singh B. 2008. Knowlesi malaria: newly emergent and of public health importance? Trends Parasitol 24:406-410.

Crotti E, Rizzi A, Chouaia B, Ricci I, Favia G, Alma A, Sacchi L, Bourtzis K, Mandrioli M, Cherif A, Bandi C, Daffonchio D. 2010. Acetic Acid Bacteria, Newly Emerging Symbionts of Insects. Appl Environ Microbiol 76:6963–6970.

Dai H, Xiao C, Liu H, Tang H. 2010. Combined NMR and LC-MS analysis reveals the metabonomic changes in *Salvia miltiorrhiza* Bunge induced by water depletion. J Proteome Res 9:1460-75.

Daniel B, Innocent E, Mbwambo ZH, Musharraf SG. 2011. Comparison of mosquito larvicidal activity of *Annona squamosa* leaves growing in different eco-zones in Tanzania. Inter J. Pharma Bio Sci 2(B): 567-72.

Demirel I, Säve S, Kruse R, Persson K. 2013. Expression of suppressor of cytokine signalling 3 (SOCS3) in human bladder epithelial cells infected with uropathogenic *Escherichia coli*. APMIS 121:158-67.

Dharmshaktu NS, Prabhakaran PK, Menon PK. 1987. Laboratory study on the mosquito larvicidal properties of leaf and seed extract of the plant *Agave americana*. J Trop Med Hyg 90:79-82.

Dhawan R, Gupta K, kajla M, Kumar S, Gakhar SK, Kakani P, Choudhury TP, Gupta L. 2015. Molecular characterization of SOCS gene and its expression analysis on *Plasmodium berghei* infection in *Anopheles culicifacies.* Acta Trop 152:170–175.

Dillon RJ, Dillon VM. 2004. The gut bacteria of insects: nonpathogenic interactions. Annu Rev Entomol 49:71–92.

Dimopoulos G, Christophides GK, Meister S, Schultz J, White KP, Barillas-Mury C, Kafatos FC. 2002. Genome expression analysis of *Anopheles gambiae*: responses to injury, bacterial challenge, and malaria infection. Proc Natl Acad Sci U S A 99:8814-8819.

Dimopoulos G, Seeley D, Wolf A, Kafatos FC. 1998. Malaria infection of the mosquito *Anopheles gambiae* activates immune-responsive genes during critical transition stages of the parasite life cycle. EMBO J 17:6115-6123.

Dinglasan RR, Fields I, Shahabuddin M, Sacci JB Jr. 2003. Monoclonal antibody MG96 completely blocks *Plasmodium yoelii* development in *Anopheles stephensi.* Infect Immun 71:6995-7001.

Dondorp AM, Nosten F, Yi P, Das D, Phyo AP, Tarning J, Lwin KM, Ariey F, Hanpithakpong W, Lee SJ, Ringwald P, Silamut K, Imwong M, Chotivanich K, Lim P, Herdman T, An SS, Yeung S, Singhasivanon P, Day NP, Lindegardh N, Socheat D, White NJ. 2009. Artemisinin resistance in *Plasmodium falciparum* malaria. N Engl J Med 361:455-467.

Dong Y, Aguilar R, Xi Z, Warr E, Mongin E, Dimopoulos G. 2006. *Anopheles gambiae* immune responses to human and rodent *Plasmodium* parasite species. PLoS Pathog 2:e52.

Dong Y, Manfredini F, Dimopoulos G. 2009. Implication of the mosquito midgut microbiota in the defense against malaria parasites. PLoS Pathog 5:e1000423.

Dunford HB.1999. Heme Peroxidases. New York , John Wiley and Sons Inc. p.388.

Edeoga HO, Okwu DE, Mbaebie BO. 2005. Pytochemical constituents of some Nigerian medicinal plants. Afr J Biotech 4:685-688.

Eriksson P, Talts U. 2000. Neonatal exposure to neurotoxic pesticides increases adult susceptibility: a review of current findings. Neurotoxicology 21:37–47.

Farias DF, Cavalheiro MG, Viana MP, Queiroz VA, Rocha-Bezerra LC, Vasconcelos IM, Morais SM, Carvalho AF. 2010. Water extracts of Brazilian leguminous seeds as rich sources of larvicidal compounds against Aedes aegypti L. Ana Acad Bras Ciên 82:585-94.

Farrance CE, Rhee A, Jones RM, Musiychuk K, Shamloul M, Sharma S, Mett V, Chichester JA, Streatfield SJ, Roeffen W, Vegte-Bolmer MV, Sauerwein RW, Tsuboi T, Muratova OV, Wu Y, Yusibov V. 2011. A Plant-Produced Pfs230 Vaccine Candidate Blocks Transmission of *Plasmodium falciparum*. Clin Vaccine Immunol 18:1351–1357.

Fraiture M, Baxter RH, Steinert S, Chelliah Y, Frolet C, Quispe-Tintaya W, Hoffmann JA, Blandin SA, Levashina EA. 2009. Two mosquito LRR proteins function as complement control factors in the TEP1-mediated killing of *Plasmodium*. Cell Host Microbe 5:273–284.

Franke-Fayard B, Trueman H, Ramesar J, Mendoza J, van der Keur M, van der Linden R, Sinden RE, Waters AP, Janse CJ. 2004. A Plasmodium berghei reference line that constitutively expresses GFP at a high level throughout the complete life cycle. Mol Biochem Parasitol 137:23-33.

Frolet C, Thoma M, Blandin S, Hoffmann JA, Levashina EA. 2006. Boosting NF-κB-dependent basal immunity of *Anopheles gambiae* aborts development of *Plasmodium berghei*. Immunity 25:677–85.

Gaio Ade O, Gusmão DS, Santos AV, Berbert-Molina MA, Pimenta PF, Lemos FJ. 2011. Contribution of midgut bacteria to blood digestion and egg production in *Aedes aegypti* (diptera: culicidae) (L.). Parasit Vectors 4:105.

Garcia GE, Wirtz RA, Barr JR, Woolfitt A, Rosenberg R. 1998. Xanthurenic acid induces gametogenesis in *Plasmodium*, the malaria parasite. J Biol Chem 273:12003-12005.

Garver LS, Bahia AC, Das S, Souza-Neto JA, Shiao J, Dong Y, Dimopoulos G. 2012. *Anopheles* Imd pathway factors and effectors in infection intensity-dependent anti-*Plasmodium* action. PLoS Pathog 8:e1002737.

Garver LS, Dong Y, Dimopoulos G. 2009. Caspar controls resistance to *Plasmodium falciparum* in diverse anopheline species. PLoS Pathog 5:e1000335.

Germinara GS, Frontera AM, De Cristofaro A, Rotundo G. 2011. Insecticidal activity of different extracts from *Scrophularia canina* L. against *Culex pipiens* molestus Forskal (Diptera, Culicidae). J Environ Sci Health B 46:473-9. doi: 10.1080/03601234.2011.583858

Ghosh A, Chowdhury N, Chandra G. 2012. Plant extracts as potential mosquito larvicides. *Indian J Med Res* 135:581-598.

Ghosh A, Edwards MJ, Jacobs-Lorena M. 2000. The journey of the malaria parasite in the mosquito: hopes for the new century. Parasitol Today 16:196–201.

Ghosh SK, Tiwari S, Raghavendra K, Sathyanarayan TS, Dash AP. 2008. Observations on sporozoite detection in naturally infected sibling species of the *Anopheles culicifacies* complex and variant of *An. stephensi* in India. J Biosci 33: 333-336.

Gilman EF. *Agave angustifolia* fact sheet FPS-21. 1999. http://hort.ifas.ufl.edu/database/documents/pdf/shrub_fact_sheets/agaanga.pdf Accessed 22 Nov 2014.

Gonzalez-Ceron L, Santillan F, Rodriguez MH, Mendez D, Hernandez-Avila JE. 2003. Bacteria in midguts of field-collected Anopheles albimanus block Plasmodium vivax sporogonic development. J Med Entomol 40:371–374.

Govindarajan M. 2009. Bioefficacy of *Cassia fistula* Linn. (Leguminosae) leaf extract against chikungunya vector, *Aedes aegypti* (Diptera: Culicidae). Eur Rev Med Pharmacol Sci 13:99-103.

Gupta L, Molina-Cruz A, Kumar S, Rodrigues J, Dixit R, Zamora RE, Barillas-Mury C. 2009. The STAT pathway mediates late-phase immunity against *Plasmodium* in the mosquito *Anopheles gambiae*. Cell Host Microbe 5:498-507.

Gupta L, Noh JY, Jo YH, Oh SH, Kumar S, Noh MY, Lee YS, Cha SJ, Seo SJ, Kim I, Han YS. 2010. Apolipophorin-III mediates antiplasmodial epithelial responses in *Anopheles gambiae* (G3) mosquitoes. PLoS One 5:e15410.

Hampton MB, Kettle AJ, Winterbourn CC.1996. Involvement of superoxide and myeloperoxidase in oxygen-dependent killing of *Staphylococcus aureus* by neutrophils. Infect Immun 64:3512-3517.

Han Z.S, Ip YT. 1999. Interaction and specificity of Rel-related proteins in regulating *Drosophila* immunity gene expression. J Biol Chem 274:21355-21361.

Hemingway J, Ranson H. 2000. Insecticide resistance in insect vectors of human disease. Annu Rev Entomol 45:371–391.

Hillyer JF, Este´vez-Lao TY. 2010. Nitric oxide is an essential component of the hemocyte-mediated mosquito immune response against bacteria. Dev Comp Immunol 34:141–149.

Hughes AL. 2012. Evolution of the heme peroxisases of *Culicidae* (Diptera). Psyche 146387. Doi:10.1155/2012/146387.

Injera WE, Kabiru EW, Gicheru MM, Githure JI,. Beier JC. 2013. Immunopathological features developing in the mosquito midgut after feeding on *Anopheles gambiae* Mucin-1 /Interleukin-12 cDNA immunized mice. Int J Morphol 31:329-337.

Jacobs-Lorena M, Oo MM. 1996. The peritrophic matrix of insects. In: Beaty BJ, Marquardt WC, editors.The Biology of Disease Vectors. Niwot, CO:University Press of Colorado. p 318–332.

Jaramillo-Gutierrez G, Rodrigues J, Ndikuyeze G, Povelones M, Molina-Cruz A, Barillas-Mury C, 2009. Mosquito immune responses and compatibility between *Plasmodium* parasites and anopheline mosquitoes. BMC Microbiol 9:154-164.

Jayanthi P, Lalitha P, Aarthi N. 2012. Larvicidal and pupicidal activity of extracts and fractionates of *Eichhornia crassipes* (Mart.) Solms against the filarial vector *Culex quinquefasciatus* Say. Parasitol Res 111:2129-35.

Jochum GM, Mudge KW, Thomas RB. 2007. Elevated temperatures increase leaf senescence and root secondary metabolite concentrations in the understory herb *Panax quinquefolius* (Araliaceae). Am J Bot 94:819-26.

Kajla M, Gupta K, Gupta L, Kumar S. 2015a. A fine-tuned management between physiology and immunity maintains the gut microbiota in insects. Biochem Physiol 4:182.

Kajla M, Gupta K, Kakani P, Dhawan R, Choudhury TP, Gupta L, Gakhar SK, Kumar S. 2015b. Identification of an *Anopheles* Lineage-Specific Unique Heme Peroxidase HPX15: A plausible candidate for arresting malaria parasite development. J Phylogen Evolution Biol 3:160.

Kajla M, Kakani P, Choudhury TP, Gupta K, Dhawan R, Gakhar SK, Gupta L, Kumar S. 2014. Characterization of Anopheline unique peroxidase and its role in the regulation of *Plasmodium* development. Malar J 13:49.

Kajla M, Kakani P, Gupta K, Choudhury TP, Gupta L, Kumar S. 2016. Characterization and expression analysis of gene encoding hemeperoxidase HPX15 in major Indian malaria vector *Anopheles stephensi* (Diptera: Culicidae). Acta Tropica 158:107–116.

Kaplan F, Kopka J, Haskell DW, Zhao W, Schiller KC, Gatzke N, Sung DY, Guy CL. 2004. Exploring the temperature-stress metabolome of Arabidopsis. Plant Physiol 136:4159-68.

Kelly LA, Sternberg MJE. 2009. Protein structure prediction on the web: a case study using the Phyre server. Nat Protoc 4:363–371.

Kelly-Hope L, Ranson H, Hemingway J. 2008. Lessons from the past: managing insecticide resistance in malaria control and eradication programmes. Lancet Infect Dis 8:387-389.

Klebanoff SJ. 1970. Myeloperoxidase: contribution to the microbicidal activity of intact leukocytes. Science 169:1095-1097.

Klebanoff SJ. 1999. Myeloperoxidase. Proc Assoc Am Physicians 111:383-389.

Klein EY. 2013. Antimalarial drug resistance: a review of the biology and strategies to delay emergence and spread. Int J Antimicrob Agents 41:311– 317.

Kovendan K, Murugan K, Shanthakumar SP, Vincent S, Hwang JS. 2012. Larvicidal activity of *Morinda citrifolia* L. (Noni) (Family: Rubiaceae) leaf extract against *Anopheles stephensi*, *Culex quinquefasciatus* and *Aedes aegypti*. *Parasitol Res* 111:1481-1490.

Krasensky J, Jonak C. 2012. Drought, salt, and temperature stress-induced metabolic rearrangements and regulatory networks. J Exp Bot 63:1593-608.

Kuehn A, Pradel G. 2010. The coming-out of malaria gametocytes. J Biomed Biotechnol, 2010:976827.

Kumar S, Barillas-Mury C. 2005. Ookinete-induced midgut peroxidases detonate the time bomb in anopheline mosquitoes. Insect Biochem Mol Biol 35:721-727.

Kumar S, Gupta L, Han YS, Barillas-Mury C. 2004. Inducible peroxidases mediate nitration of *Anopheles* midgut cells undergoing apoptosis in response to *Plasmodium* invasion. J Biol Chem 279:53475–53482.

Kumar S, Molina-Cruz A, Gupta L, Rodrigues J, Barillas-Mury C. 2010. A peroxidase/dual oxidase system modulates midgut epithelial immunity in *Anopheles gambiae*. Science 327:1644–1648.

Kumar S, Warikoo R, Mishra M, Seth A, Wahab N. 2012. Larvicidal efficacy of the *Citrus limetta* peel extracts against Indian strains of *Anopheles stephensi* Liston and *Aedes aegypti* L. Parasitol Res 111:173-8.

Lehane MJ, Aksoy S, Levashina E. 2004. Immune responses and parasite transmission in blood-feeding insects. Trends Parasitol 20:433–439.

Lemaitre B, Kromer-Metzger E, Michaut L, Nicolas E, Meister M, Georgel P, Reichhart JM, Hoffmann JA. 1995. A recessive mutation, immune deficiency (imd), defines two distinct control pathways in the *Drosophila* host defense. Proc Natl Acad Sci U S A 92:9465–9469.

Lemaitre B, Nicolas E, Michaut L, Reichhart JM, Hoffmann JA. 1996. The dorsoventral regulatory gene cassette spatzle/Toll/cactus controls the potent antifungal response in *Drosophila* adults. Cell 86:973-983.

Lensen A, Mulder L, Tchuinkam T, Willemsen L, Eling W, Sauerwein R. 1998. Mechanisms that reduce transmission of *Plasmodium falciparum* malaria in semi immune and non-immune persons. J Infect Dis 177:1358–1363.

Li JS, Li J. 2006. Major chorion proteins and their crosslinking during chorion hardening in *Aedes aegypti* mosquitoes. Insect Biochem Mol Biol 36:954-964.

Lindh JM, Terenius O, Faye I. 2005. 16S rRNA gene-based identification of midgut bac-teria from field-caught *Anopheles gambiae* sensu lato and *A. funestus* mosquitoes reveals new species related to known insect symbionts. Appl Environ Microbiol 71:7217-7223.

Livak KJ, Schmittgen TD. 2001. Analysis of relative gene expression data using real-time quantitative PCR and the 2(-Delta Delta C(T)) Method. Methods 25:402-408.

Luckhart S, Li K, Dunton R, Lewis EE, Crampton AL, Ryan JR, Rosenberg R. 2003. Anopheles gambiae immune gene variants associated with natural *Plasmodium* infection. Mol Biochem Parasitol 128:83-86.

Luckhart S, Vodovotz Y, Cui L, Rosenberg R. 1998. The mosquito *Anopheles stephensi* limits malaria parasite development with inducible synthesis of nitric oxide. Proc Natl Acad Sci U S A 12:5700–5705.

Luna C, Hoa NT, Lin H, Zhang L, Nguyen HL, Kanzok SM, Zheng L. 2006. Expression of immune responsive genes in cell lines from two different Anopheline species. Insect Mol Biol 15:721-729.

Mace KA, Pearson JC, McGinnis W. 2005. An epidermal barrier wound repair pathway in *Drosophila* is mediated by grainy head. Science 308:381-385.

Maehr T, Vecino JL, Wadsworth S, Wang T, Secombes CJ. 2014. Four CISH paralogues are present in rainbow trout *Oncorhynchus mykiss*: Differential expression and modulation during immune responses and development. Mol Immunol 62:186-198.

Mahajan RC, Farooq U, Dubey ML, Malla N. 2005. Genetic polymorphism in *Plasmodium falciparum* vaccine candidate antigens. Indian J Pathol Microbiol 48: 429-438.

Marchler-Bauer A, Derbyshire MK, Gonzales NR, Lu S, Chitsaz F, Geer LY, Geer RC, He J, Gwadz M, Hurwitz DI, Lanczycki CJ, Lu F, Marchler GH, Song JS, Thanki N, Wang Z, Yamashita RA, Zhang D, Zheng C, Bryant SH. 2015. CDD: NCBI's conserved domain database. Nucleic Acids Res 43:D222-226.

Mathelier A, Zhao X, Zhang AW, Parcy F, Worsley-Hunt R, Arenillas DJ, Buchman S, Chen CY, Chou A, Ienasescu H, Lim J. 2013. JASPAR 2014: an extensively expanded and updated open-access database of transcription factor binding profiles. Nucleic Acids Res 42:D142–D147.

Matuschewski K. 2006. Getting infectious: formation and maturation of *Plasmodium* sporozoites in the *Anopheles* vector. Cell Microbiol 8:1547–1556.

Mbah BO, Eme PE, Paul AE. 2012. Effect of drying techniques on the proximate and other nutrient composition of *Moringa oleifera* leaves from two areas in Eastern Nigeria. Pak J Nut 11:1044-48.

Mehlotra RK, Lorry K, Kastens W, Miller SM, Alpers MP, Bockarie M, Kazura JW, Zimmerman PA. 2000. Random distribution of mixed species malaria infections in Papua New Guinea. Am J Trop Med Hyg 62:225-231.

Meister S, Agianian B, Turlure F, Relogio A, Morlais I, Kafatos FC, Christophides GK. 2009. *Anopheles gambiae* PGRPLC-mediated defense against bacteria modulates infections with malaria parasites. PLoS Pathog 5:e1000542.

Meister S, Kanzok SM, Zheng XL, Luna C, Li TR, Hoa NT, Clayton JR, White KP, Kafatos FC, Christophides GK, Zheng L. 2005. Immune signaling pathways regulating bacterial and malaria parasite infection of the mosquito *Anopheles gambiae*. Proc Natl Acad Sci U S A 102:11420-11425.

Michel K, Kafatos FC. 2005. Mosquito immunity against *Plasmodium*. Insect Biochem Mol Biol 35:677–689.

Michel T, Reichhart JM, Hoffmann JA, Royet, J. 2001. *Drosophila* Toll is activated by Gram-positive bacteria through a circulating peptidoglycan recognition protein. Nature 414:756-759.

Minard G, Mavingui P, Moro CV. 2013. Diversity and function of bacterial microbiota in the mosquito holobiont. Parasit Vectors 6:146.

Molina-Cruz A, DeJong RJ, Ortega C, Haile A, Abban E, Rodrigues J, Jaramillo-Gutierrez G, Barillas-Mury C. 2012. Some strains of *Plasmodium falciparum*, a human malaria parasite, evade the complement-like system of *Anopheles gambiae* mosquitoes. Proc Natl Acad Sci 109: E1975-62.

Motulsky HJ. 1999. Analyzing Data with GraphPad Prism. GraphPad Software Inc., San Diego, CA www.graphpad.com.

Mrema EJ, Rubino FM, Brambilla G, Moretto A, Tsatsakis AM, Colosio C. 2013. Persistent organochlorinated pesticides and mechanisms of their toxicity. Toxicol 307:74-88.

Nagpal BN, Sharma VP. 1995. Indian Anophelines. New Delhi:Oxford & IBH Publishing Co. Pvt. LTD., p. 416.

Nair S, Williams JT, Brockman A, Paiphun L, Mayxay M, Newton PN, Guthmann JP, Smithuis FM, Hien TT, White NJ, Nosten F, Anderson TJ. 2003. A selective sweep driven by pyrimethamine treatment in southeast Asian malaria parasites. Mol Biol Evol 20:1526–1536.

Narasimha M, Uv A, Krejci A, Brown NH, Bray SJ. 2008. Grainy head promotes expression of septate junction proteins and influences epithelial morphogenesis. J Cell Sci 121:747-752.

National Vector Borne Disease Control Program, (2010- 2014).Malaria situation in India. Available from: http://www. nvbdcp.gov.in/Doc/malaria-situation-March14. pdf, accessed on March 11, 2014.

Neafsey DE, Christophides GK, Collins FH, Emrich SJ, Fontaine MC, Gelbart W, Hahn MW, Howell PI, Kafatos FC, Lawson D, Muskavitch MA. 2013. The evolution of the *Anopheles* 16 genomes project. Genes Genome Genetics (G3) 3:1191-1194.

Nikkon F, Salam KA, Yeasmin T, Mosaddik A, Khondkar P, Haque ME. 2010. Mosquitocidal triterpenes from the stem of *Duranta repens*. Pharm Biol 48:264-8. doi: 10.3109/13880200903096570.

Noden BH, Vaughan JA, Pumpuni CB, Beier JC. 2011. Mosquito ingestion of antibodies against mosquito midgut microbiota improves conversion of ookinetes to oocysts for *Plasmodium falciparum*, but not *P. yoelii*. Parasitol Int 60:440-6.

Noedl H, Se Y, Sriwichai S, Schaecher K, Teja-Isavadharm P, Smith B, Rutvisuttinunt W, Bethell D, Surasri S, Fukuda MM, Socheat D, Chan Thap L. 2010. Artemisinin resistance in Cambodia: a clinical trial designed to address an emerging problem in Southeast Asia. Clin Infect Dis 51:e82-89.

Nunes F, Guimarães L, Lacerda D, Mascarenhas S, Braga V. 2014. Larvicidal activity of *Agave sisalana* against *Aedes aegypti* mosquito, the dengue vector. BMC Proc 8:5. doi:10.1186/1753-6561-8-S4-P5

Ohno S.1970. Evolution by gene duplication. New York: Springer-Verlag.

Oliveira GA, Lieberman J, Barillas-Mury C. 2012. Epithelial nitration by a peroxidase/NOX5 system mediates mosquito antiplasmodial immunity. Science 335:856–859.

Osta MA, Christophides GK, Vlachou D, Kafatos FC. 2004. Innate immunity in the malaria vector *Anopheles gambiae*: comparative and functional genomics. J Exp Biol 207:2551-2563.

Pace CN, Scholtz JM. 1998. A helix propensity scale based on experimental studies of peptides and proteins. Biophys J 75:422-427.

Panneerselvam C, Murugan K, Kovendan K, Mahesh KP. 2012. Mosquito larvicidal, pupicidal, adulticidal, and repellent activity of *Artemisia nilagirica* (Family: *Compositae*) against *Anopheles stephensi* and *Aedes aegypti*. Parasitol Res 111:2241-51.

Passardi F, Bakalovic N, Teixeira FK, Margis-Pinheiro M, Penel C, Dunand C. 2007. Prokaryotic origins of the non-animal peroxidase superfamily and organelle-mediated transmission to eukaryotes. Genomics 89:567-579.

Payne D. 1987. Spread of chloroquine resistance in *Plasmodium falciparum*. Parasitol Today 3:241–246.

Persson T, Andersson P, Bodelsson M, Laurell M, Malm J, Egesten A. 2001. Bactericidal activity of human eosinophilic granulocytes against *Escherichia coli*. Infect Immun 69: 3591-3596.

Péterfi Z, Geiszt M. 2014. Peroxidasins: novel players in tissue genesis. Trends Biochem Sci 39:305-307.

Petersen TN, Brunak S, von Heijne G, Nielsen H. 2011. SignalP 4.0: discriminating signal peptides from transmembrane regions. Nat Methods 8:785–786.

Peterson ME, Chen F, Saven JG, Roos DS, Babbitt PC, Sali A. 2009. Evolutionary constraints on structural similarity in orthologs and paralogs. Protein Sci 18:1306-1315.

Phyo AP, Nkhoma S, Stepniewska K, Ashley EA, Nair S, McGready R, Ier Moo C, Al-Saai S, Dondorp AM, Lwin KM, Singhasivanon P, Day NP, White NJ, Anderson TJ, Nosten F. 2012. Emergence of artemisinin-resistant malaria on the western border of Thailand: a longitudinal study. Lancet 379:1960-1966.

Piven NM, Barredo-Pool FA, Borges-Arga´ez IC, Herrera-Alamillo MA, Mayo-Mosqueda A, Herrera-Herrera JL, Robert ML. 2001. Reproductive biology of henequen (*Agave fourcroydes*) and its wild ancestor *Agave angustifolia (*Agavaceae). I. Gametophyte development. Am J Bot 88:1966-1976.

Pizarro AP, Oliveira Filho AM, Parente JP, Melo MT, dos Santos CE, Lima PR. 1999. Utilization of the waste of sisal industry in the control of mosquito larvae. Rev Soc Bras Med Trop 32:23-9.

Pontual EV, Napoleão TH, Dias de Assis CR, de Souza Bezerra R, Xavier HS, Navarro DM, Coelho LC, Paiva PM. 2012. Effect of Moringa oleifera flower extract on larval trypsin and acethylcholinesterase activities in Aedes aegypti. Arch Insect Biochem Physiol 79:135-52.

Povelones M, Waterhouse RM, Kafatos FC, Christophides GK. 2009. Leucine-rich repeat protein complex activates mosquito complement in defense against *Plasmodium* parasites. Science 324:258–261.

Pradel G. 2007. Proteins of the malaria parasite sexual stages: expression, function and potential for transmission blocking strategies. Parasitology 134:1911-1929.

Pumpuni CB, Beier MS, Nataro JP, Guers LD, Davis JR. 1993. *Plasmodium falciparum*: inhibition of sporogonic development in *Anopheles stephensi* by Gram-negative bacteria. Exp Parasitol 77:195–199.

Pumpuni CB, DeMaio J, Kent M, Davis JR, Beier JC. 1996. Bacterial population dynamics in three anopheline species: the impact on *Plasmodium* sporogonic development. Am J Trop Med Hyg 54:214–218.

Ramakrishna A, Ravishankar GA. 2011. Influence of abiotic stress signals on secondary metabolites in plants. Plant Signal Behav 6:1720-1731.

Ramirez JL, Dimopoulos G. 2010. The Toll immune signaling pathway controls conserved anti-dengue defenses across diverse *Aedes aegypti* strains and against multiple dengue virus serotypes. Dev Comp Immunol 34:625-629.

Ramiro RS, Alpedrinha J, Carter L, Gardner A, Reece SE. (2011). Sex and Death: The effects of innate immune factors on the sexual reproduction of Malaria Parasites. PLoS Pathog 7:e1001309.

Rani A, Sharma A, Rajagopal R, Adak T and Bhatnagar RK.2009. Bacterial diversity analysis of larvae and adult midgut microflora using culture-dependent and culture-independent methods in lab-reared and field-collected *Anopheles stephensi*-an Asian malarial vector. BMC Microbiol 9:96.

Rao BA, Sweet WC, Subba Rao AM. 1938. Ova measurements of *Anopheles stephensi* type and *Anopheles stephensi* var. *mysorensis*. J Malar Inst India 1:261-266.

Rawani A, Ghosh A, Chandra G. 2010. Mosquito larvicidal activities of *Solanum nigrum* L. leaf extract against *Culex quinquefasciatus* Say. Parasitol Res 107:1235-40.

Rayms-Keller A, McGaw M, Oray C, Carlson JO, Beaty BJ. 2000. Molecular cloning and characterization of a metal responsive *Aedes aegypti* intestinal mucin cDNA. Insect Mol Biol 9:419–426.

Reese MG. 2001. Application of a time-delay neural network to promoter annotation in the *Drosophila melanogaster* genome. Comput Chem 26:51-56.

Riehle MM, Xu J, Lazzaro BP, Rottschaefer SM, Coulibaly B, Sacko M, Niare O, Morlais I, Traore SF, Vernick KD. 2008. *Anopheles gambiae* APL1 is a family of variable LRR proteins required for Rel1-mediated protection from the malaria parasite, *Plasmodium berghei*. PLoS One 3:e3672.

Roper C, Pearce R, Bredenkamp B, Gumede J, Drakeley C, Mosha F, Chandramohan D, Sharp B. 2003. Antifolate antimalarial resistance in southeast Africa: a population-based analysis.Lancet 361:1174–81.

Saitou N, Nei M. 1987. The neighbor-joining method: a new method for reconstructing phylogenetic trees. Mol Biol Evol 4:406-425.

Salazar CE, Mills-Hamm D, Kumar V, Collins FH. 1993. Sequence of a cDNA from the mosquito *Anopheles gambiae* encoding a homologue of human ribosomal protein S7. Nucleic Acids Res 21:4147.

Shahabuddin M, Cociancich S, Zieler H. 1998. The search for novel malaria transmission blocking targets in the mosquito midgut. Parasitol Today. 14:493-497.

Shahi M, Hanafi-Bojd AA, Iranshahi M, Vatandoost H, Hanafi-Bojd MY. 2010. Larvicidal efficacy of latex and extract of *Calotropis procera* (Gentianales: Asclepiadaceae) against

Culex quinquefasciatus and *Anopheles stephensi* (Diptera: Culicidae). J Vector Borne Dis 47:185-8.

Shaw WR, Teodori E, Mitchell SN, Baldini F, Gabrieli P, Rogers DW, Catteruccia F. 2014. Mating activates the heme peroxidase HPX15 in the sperm storage organ to ensure fertility in *Anopheles gambiae*. Proc Natl Acad Sci U S A 111:5854–5859.

Shi G-Q, Yu Q-Y, Zhang Z. 2012. Annotation and evolution of the antioxidant genes in the silkworm, *Bombyx mori*. Arch Insect Biochem Physiol 79:87-103.

Simon N, Lasonder E, Scheuermayer M, Kuehn A, Tews S, Fischer R, Zipfel PF, Skerka C, Pradel G. 2013. Malaria parasites co-opt human factor H to prevent complement-mediated lysis in the mosquito midgut. Cell Host Microbe 13:29-41.

Sinden RE, Billingsley PF. 2001. *Plasmodium* invasion of mosquito cells: Hawk or dove? Trends Parasitol 17:209–212.

Sinden RE. 1999. *Plasmodium* differentiation in the mosquito. Parassitologia 41:139-148.

Singh RK, Mittal PK, Kumar G, Dhiman RC. 2014. Evaluation of mosquito larvicidal efficacy of leaf extract of a cactus plant, *Agave sisalana.* J Entomol Zoo Stud 2:83-86.

Singha S, Chandra G. 2011. Mosquito larvicidal activity of some common spices and vegetable waste on *Culex quinquefasciatus* and *Anopheles stephensi*. Asian Pac J Trop Med 4:288-293.

Sinka ME, Bangs MJ, Manguin S, Rubio-Palis Y, Chareonviriyaphap T, Coetzee M, Mbogo CM, Hemingway J, Patil AP, Temperley WH Gething PW, Kabaria CW, Burkot TR, Harbach RE, Hay SI. 2012. A global map of dominant malaria vectors. Parasit Vectors 5:69.

Smith RC, Rodríguez JV, Jacobs-Lorena M. 2014. The *Plasmodium* bottleneck: malaria parasite losses in the mosquito vector. Mem Inst Oswaldo Cruz 109:644-661.

Sologub L, Kuehn A, Kern S, Przyborski J, Schillig R, Pradel G. 2011. Malaria proteases mediate inside-out egress of gametocytes from red blood cells following parasite transmission to the mosquito. Cell Microbiol 13:897-912.

Sritunyalucksana K, Wongsuebsantati K, Johansson MW, Söderhäll K. 2001. Peroxinectin, a cell adhesive protein associated with the proPO system from the black tiger shrimp, *Penaeus monodon*. Dev Comp Immunol 25:353-363.

Subbarao SK, Adak T, Vasnatha K, Joshi H, Raghavandra K, Cochrane AH, Nussenzweig RS, Sharma VP. 1988. Susceptibility of *Anopheles culicifacies* species A and B to *Plasmodium vivax* and *Plasmodium falciparum* as determined by immunoradiometric assay. Trans R Soc Trop Med Hyg 82:394-397.

Subbarao SK. 1998. Anopheline Species Complexes in South-East Asia. WHO.Technical Publication. 18:82.

Swevers L, Iatrou K. 2003. The ecdysone regulatory cascade and ovarian development in lepidopteran insects: insights from the silkmoth paradigm. Insect Biochem Mol Biol 33:1285–1297.

Tamura K, Peterson D, Peterson N, Stecher G, Nei M, Kumar S. 2011. MEGA5 molecular evolutionary genetics analysis using maximum likelihood, evolutionary distance, and maximum parsimony methods. Mol Biol Evol 28:2731-2739.

Telang A, Frame L, Brown MR. 2007. Larval feeding duration affects ecdysteroid levels and nutritional reserves regulating pupal commitment in the yellow fever mosquito *Aedes aegypti* (Diptera: Culicidae). J Exp Biol 210:854-864.

The RTS,S Clinical Trials Partnership. 2014. Efficacy and Safety of the RTS,S/AS01 Malaria Vaccine during 18 Months after Vaccination: A Phase 3 Randomized, Controlled Trial in Children and Young Infants at 11 African Sites. PLoS Med 11(7): e1001685.

Touré AM, Mackey AJ, Wang ZX, Beier JC. 2000. Bactericidal effects of sugar-fed antibiotics on resident midgut bacteria of newly emerged anopheline mosquitoes (Diptera: Culicidae). J Med Entomol 37:246–249.

Upton L M, Povelones M, Christophides GK. 2015. *Anopheles gambiae* blood Feeding Initiates an Anticipatory Defense Response to *Plasmodium berghei*. J Innate Immun 7:74-86.

Vargas-Ponce O, Zizumbo-Villarreal D, Mart í nez-Castillo J, Coello-Coello J, Colunga-GarcíaMarín P. 2009. Diversity and structure of landraces of *Agave* grown for spirits under traditional agriculture: A comparison with wild populations of *A. Angustifolia* (Agavaceae) and commercial plantations of *A. Tequilana*. Am J Bot 96:448-457.

Vijay S, Rawat M, Adak T, Dixit R, Nanda N, Srivastava H, Sharma JK, Prasad GB, Sharma A. 2011. Parasite killing in malaria non-vector mosquito *Anopheles culicifacies* species B: implication of nitric oxide synthase upregulation. PloS one 6:e18400.

Vizioli J, Bulet P, Hoffmann JA, Kafatos FC, Müller HM, Dimopoulos G. 2001. Gambicin: a novel immune responsive antimicrobial peptide from the malaria vector *Anopheles gambiae.* Proc Natl Acad Sci USA 98:12630-12635.

Vlachou D, Schlegelmilch T, Christophides GK, Kafatos FC. 2005. Functional genomic analysis of midgut epithelial responses in *Anopheles* during *Plasmodium* invasion. Curr Biol 15:1185–1195.

Wang J, Slungaard A. 2006. Role of eosinophil peroxidase in host defense and disease pathology. Arch Biochem Biophys 445:256-260.

Wang Y, Gilbreath TM, Kukutla P, Yan G, Xu J. 2011. Dynamic Gut Microbiome across Life History of the Malaria Mosquito *Anopheles gambiae* in Kenya. PLoS ONE 6:e24767.

Warr E, Das S, Dong Y, Dimopoulos G. 2008. The Gram-negative bacteria-binding protein gene family: its role in the innate immune system of *Anopheles gambiae* and in anti-*Plasmodium* defence. Insect Mol Biol 17:39-51.

Wass MN, Kelley LA, Sternberg MJ. 2010. 3D LigandSite: predicting ligand- binding sites using similar structures. Nucleic Acids Res 38:W469–W473.

Waterhouse RM, Kriventseva EV, Meister S, Xi Z, Alvarez KS, Bartholomay LC, Barillas-Mury C.2007. Evolutionary Dynamics of Immune-Related Genes and Pathways in Disease-Vector Mosquitoes. Science. 316:1738-1743.

White NJ. 2004. Antimalarial drug resistance. J Clin Invest 113:1084–1092.

White NJ. 2008. *Plasmodium knowlesi*: the fifth human malaria parasite. Clin Infect Dis 46:172–173.

WHO. 2015: “World malaria report: 2015,” in WHO Global Malaria Programme. (Geneva: World Health Organization).

Wiegmann BM, Trautwein MD, Kim JW, Cassel BK, Bertone MA, Winterton SL, Yeates DK. 2009. Single-copy nuclear genes resolve the phylogeny of the holometabolous insects. BMC biology 7:34-47.

Wirth CC, Pradel G. 2012. Molecular mechanisms of host cell egress by malaria para-sites. Int J Med Microbiol 302:172-178.

Wormald S, Hilton DJ. 2004. Inhibitors of cytokine signal transduction. J Biol Chem 279:821–824.

Wotton RS, Chaloner DT, Yardley CA, Merritt RW. 1997. Growth of *Anopheles* mosquito larvae on dietary microbiota in aquatic surface microlayers. Med Vet Entomol 11:65-70.

Yang T, Liu N. 2013. Permethrin resistance profiles in a field population of mosquitoes, *Culex quinquefasciatus* (Diptera: Culicidae). J Med Entomol 50:585-93.

Zámocký M, Hofbauer S, Schaffner I, Gasselhuber B, Nicolussi A, Soudi M, Pirker KF, Furtmüller PG, Obinger C. 2015. Independent evolution of four heme peroxidase superfamilies. Arch Biochem Biophys 574:108-119.

Zhang M, Xiao ZZ, Sun L. 2011. Suppressor of cytokine signaling 3 inhibits head kidney macrophage activation and cytokine expression in *Scophthalmus maximus*. Dev Com Immunol 35:174–181.

List of Publications in Cited Journals (SCI)

1. **Kajla M**, Kakani P, Gupta K, Choudhury TP, Gupta L, Kumar S. 2016. Characterization and expression analysis of gene encoding heme peroxidase HPX15 in major Indian malaria vector *Anopheles stephensi* (Diptera: Culicidae). **Acta Tropica**. 158:107–116. doi:10.1016/j.actatropica.2016.02.028

2. **Kajla M**, Bhattacharya K, Gupta K, Banerjee U, Kakani P, Gupta L, Kumar S. 2016. Identification of temperature Induced Larvicidal Efficacy of *Agave angustifolia* against *Aedes*, *Culex* and *Anopheles* Larvae. **Frontiers in Public Health.** 3:286. doi: 10.3389/fpubh.2015.00286.

3. **Kajla M,** Gupta K, Kakani P, Dhawan R, Choudhury TP, Gupta L, Gakhar SK, Kumar S. 2015. Identification of an *Anopheles* Lineage-Specific Unique Heme Peroxidase HPX15: A Plausible Candidate for Arresting Malaria Parasite Development. **Phylogenetics & Evolutionary Biology.** 3:160. doi:10.4172/2329- 9002.1000160.

4. **Kajla M,** Gupta K, Gupta L, Kumar S**.** 2015. A Fine-Tuned Management between Physiology and Immunity Maintains the Gut Microbiota in Insects. **Biochemistry & Physiology.** 4:182. doi: 10.4172/2168-9652.1000182.

5. **Kajla M,** Kakani P, Choudhury TP, Gupta K, Dhawan R, Gakhar SK, Gupta L, Kumar S. 2014. Characterization of anopheline unique peroxidase and its role in regulation of *Plasmodium* development. **Malaria Journal**. 13 (suppl 1):P49.

6. Dhawan R, Gupta K, **Kajla M**, Kumar S, Gakhar SK, Kakani P, Choudhury TP and Gupta L. 2015. Molecular characterization of SOCS gene and its expression analysis on *Plasmodium berghei* infection in *Anopheles culicifacies*. **Acta Tropica.** 152:170–175.

7. Gupta K, Dhawan R, **Kajla M**, Kumar S, Jnanasiddhy B, Singh NK, Dixit R, Bihani A, Gupta L. 2016. Molecular Identification of *Aedes aegypti* mosquitoes from Pilani region of Rajasthan, India. **Journal Vector Borne Diseases**. 53:149-155.

List of Publications in Pipeline

1. **Kajla M**, Choudhury TP, Kakani P, Gupta K, Dhawan R, Gupta L, Kumar S. 2016. Silencing of *Anopheles stephensi* Heme Peroxidase HPX15 Activates Diverse Immune Pathways to Regulate the Growth of Midgut Bacteria.

2. **Kajla M**, Kakani P, Choudhury TP, Gupta K, Dhawan R, Gupta L, Kumar S. 2016. *Anopheles stephensi* heme peroxidase HPX15 modulates midgut epithelial immunity against *Plasmodium.*

List of Publications in International and National conferences

1. **Kajla M**, Kakani P, Choudhury TP, Gupta K, Dhawan R, Gupta L and Kumar S. HPX15 modulates immune response against gut bacteria of Anopheles stephensi. BITS Conference on Gene and Genome Regulation (BCGGR 2016). February 18-20, 2016 BITS Pilani, Pilani Campus, India.

2. Kakani P, Yadav A, **Kajla M**, Choudhury TP, Gupta K, Dhawan R, Gupta L and Kumar S. Comparative analysis of two duplicated heme-peroxidase AsHPX10 and AsHPX11 genes in Anopheles stephensi having high divergent mRNA expression. BITS Conference on Gene and Genome Regulation (BCGGR 2016). February 18-20, 2016 BITS Pilani, Pilani Campus, India.

3. Choudhury TP, **Kajla M**, Kakani P, Gupta K, Dhawan R, Gupta L and Kumar S. Exploring the role of Anopheles stephensi heme peroxidase in mosquito innate immunity. BITS Conference on Gene and Genome Regulation (BCGGR 2016). February 18-20, 2016 BITS Pilani, Pilani Campus, India.

4. Choudhury TP, **Kajla M**, Kakani P, Gupta K, Dhawan R, Gupta L and Kumar S. Exploring the role of Anopheles stephensi heme peroxidase in mosquito innate immunity. 6th World Congress on Biotechnology. October 05-07, 2015 New Delhi, India. J Biotechnol Biomater DOI: 10.4172/2155-952X.C1.044.

5. Kakani P**, Kajla M,** Gupta K, Dhawan R, Choudhury TP Gupta L and Kumar S. Characterization of *Anophelines* Peroxidase- Role in Development and Immunity against Blood- borne antigens. VIIIth National conference of Indian Academy of Tropical Parasitology TROPACON-2014, 20th – 22nd Nov, 2014, RMRC, Dibrugarh, Assam, India.

6. Choudhury TP**, Kajla M,** Gupta K, Dhawan R, Kakani P**,** Gupta L and Kumar S. Exploring the role of *Anopheles stephensi* Heme Peroxidase in Mosquito Innate Immunity. VIIIth National conference of Indian Academy of Tropical Parasitology TROPACON-2014, 20th – 22nd Nov, 2014, RMRC, Dibrugarh, Assam, India.

7. Vaswani D**, Kajla M,** Kakani P, Dhawan R, Gupta K, Choudhury TP**,** Gupta L and Kumar S. Characterization of Inhibitory Effects of Herbal Extracts on *Aedes aegypti* Egg Chorion Melanization and Hardening. VIIIth National conference of Indian Academy of Tropical Parasitology TROPACON-2014, 20th – 22nd Nov, 2014, RMRC, Dibrugarh, Assam, India.

8. Dhawan R, Soam A, Gupta K, **Kajla M**, Kakani P, Choudhury TP, Kumar S, Gupta L. Role of Mosquito Immunity against Parasite Development: An Expedition of Potent Immune Molecules of *Anopheles* Mosquitoes. VIIIth National conference of Indian Academy of Tropical Parasitology TROPACON-2014, 20th – 22nd Nov, 2014, RMRC, Dibrugarh, Assam, India.

9. Gupta L, Gupta K, Dhawan R, Kumar S, Kakani P, **Kajla M**, and Choudhury TP. *Anopheles* STAT pathway duplication and its role in immunity against *Plasmodium*. VIIIth National conference of Indian Academy of Tropical Parasitology TROPACON-2014, 20th – 22nd Nov, 2014, RMRC, Dibrugarh, Assam, India.

10. Kumar S, Kakani P, **Kajla M**, Gupta K, Choudhury T.P, Dhawan R, and Gupta L. Compartment-specific immune responses in malaria vector determine the vectorial capacity. 25th National Congress of Parasitology on "Global Challenges in the Management of Parasitic Diseases (GCMPD), Central Drug Research Institute (CDRI), OP 27, 16-18th Oct. 2014, Lucknow, UP, India.

11. Gupta K, Dhawan R, **Kajla M**, Choudhury T. P, Kakani P, Kumar S and Gupta L**.** Genomic diversity of STAT (Signal Transducer and Activator of Transcription) gene in different *Anopheles* mosquito species. 25th National Congress of Parasitology on "Global Challenges in the Management of Parasitic Diseases (GCMPD), Central Drug Research Institute (CDRI), YS 2, 16-18th Oct. 2014, Lucknow, UP, India

12. **Kajla M**, Kakani P, Choudhury TP, Gupta K, Dhawan R, Gupta L, Gakhar SK , Gupta L , Kumar S. Characterization of *Anopheline* unique peroxidase and its role in regulation of *Plasmodium* development. Challenges in Malaria Research: Core science and innovation. Organized by BioMed Central, The Open Acess Publisher, September 22-24, 2014 at **Oxford University, Oxford, UK**.

13. Gupta L**,** Gupta K, Dhawan R, **Kajla M**, Bihani A, Kumar S**.** Duplication of evolutionary conserved STAT transcription factor in *Anopheles stephensi* and its role in mosquito immunity. Host-Parasite Interactions, Biology of. Gordon Research Conference, 8- 13 June 2014 Salve Regina University in New port, RI, United States.

14. **Kajla M**, Gupta K, Dhawan R, Kakani P, Gupta L, Kumar S. Characterization of *Anopheles* midgut immune peroxidase and their role in regulation of *Plasmodium* development.XII th International conference on Vector and Vector Borne Diseases (Vector borne diseases challenges in 21st century: Their Global Impact and Strategic Management), 16-18 September 2013, Udaipur, Rajasthan, India. (**Recipient of first best poster award**).

15. **Kajla M**, Gupta K, Dhawan R, Kakani P, Gupta L, Kumar S. Characterization of *Anopheles stephensi* Organic Anion Transporter. National symposium on Fight against Malaria Prospects and Prospective (FAMMP-2013), 9th March, 2013, Maharshi Dayanand University, Rohtak, Haryana, India.

16. Gupta L **,** Dhawan R , Gupta K, **Kajla M**, Gakhar S K, Kumar S. ROS Detoxification enzymes in *Anopheles culicifacies* and their role in *Plasmodium* development. American Society of Tropical Medicine and Hygiene (**ASTMH**), 62nd Annual Meeting, 13-17 Nov 2013, Washington DC, USA.

17. Kumar S, **Kajla M**, Bhattacharya K, Banerjee UK, Gupta L. Phytochemicals: naturally-occurring eco-friendly larvicides. XII International Conference on Vector and Vector-Borne Diseases (Vector borne diseases challenges in 21st century, Udaipur, Sep 16-18. 2013

18. Gupta L, Kumar S, Gupta K, Dhawan R, **Kajla M**. Mosquito Immune signaling pathway and its role in *Plasmodium* development. In XXIV National Congress of Parasitology, 27-29 April 2013, RMRCT, Jabalpur, M.P., India.

19. Gupta K, Dhawan R, **Kajla M**, Kumar S**,** Gupta L. *Anopheles stephensi* STAT pathway: Exploring its effects on *Plasmodium* development. In XXIV National Congress of Parasitology, 27-29 April 2013, RMRCT, Jabalpur, M.P. India.

20. Dhawan R, Gupta K, **Kajla M**, Kumar S, Gakhar SK, Gupta L. Proving ground for sequence divergence of suppressor of Cytokine signaling (SOCS) in *Anopheles culicifacies*. XXI^{V} National Congress of Parasitology, 27-29 April 2013, RMRCT, Jabalpur, M.P. India.

21. Gupta K, Dhawan R, **Kajla M**, Sharma Y, Kumar S and Gupta L. Molecular and Phylogenetic Analysis of Immune genes in *Anopheles stephensi isolated* from Rajasthan region. National symposium on Fight against Malaria Prospects and Prospective (FAMMP-2013), 9th March, 2013, Maharshi Dayanand University, Rohtak, Haryana, India.

22. Dhawan R, Gupta K, **Kajla M**, Kumar S, Gakhar SK, Gupta L. Suppressor of Cytokine Signaling (SOCS): Characterization in *Anopheles culicifacies* mosquitoes. National symposium on Fight against Malaria Prospects and Prospective (FAMMP-2013), 9th March, 2013, Maharshi Dayanand University, Rohtak, Haryana, India.

23. Gupta L, Gupta K, **Kajla M**, Dhawan R, Kumar S. The mosquito STAT pathway and its role in *Plasmodium* development. In symposium on molecular basis of vector-pathogen interactions (S 1301), XXIV International Congress of Entomology (ICE), 2012. Daegu, South Korea.

24. Kumar S, Gupta L, **Kajla M**, Gupta K, Singh NK. Modulation of mosquito immunity during *Plasmodium* development. In Symposium on Molecular basis of vector-pathogen interactions (S 1301), XXIV International Congress of Entomology (ICE), 2012. Daegu, South Korea.

25. **Kajla M**, Bhattacharya K, Jnanasiddhy B, Banerjee U, Kumar S, Gupta L. Screening and characterization of novel natural compounds for Mosquito larvicidal activity. CTBPR, 12-13 March, 2011. BITS-Pilani Rajasthan.

26. **Kajla M**, Banerjee U, Bhattacharya K, Jnanasiddhy B, Gupta L, Kumar S. Characterization of mosquito larvicidal activity in xerophytic plants from Rajasthan region. XII symposium on vector and vector borne diseases 15-17th october 2011, Regional Medical Research Centre for Tribals, Jabalpur, India**.**

Biography of Prof. Sanjeev Kumar

Prof. Sanjeev Kumar is presently the Associate Dean, SRCD, BITS-Pilani and Associate Professor, Department of Biological Sciences, BITS, Pilani, Rajasthan. He received his Ph.D. degree in 1999 from Banaras Hindu University, Varanasi, UP, India. He has been a Research Fellow (a Federal Full time equivalent) at Laboratory of Malaria and Vector Research, National Institutes of Health (NIH), Rockville, MD, USA. He has been also a Post Doctoral Fellow in the Department of Microbiology, Immunology and Pathology, Colorado State University, Fort Collins, CO, USA. He has been an INSERM foreign scientist in the Lymphoid cell differentiation and gene recombination laboratory, INSERM-CNRS Centre d'Immunologie Marseille-Luminy (CIML), Marseille, France. He has been awarded with various achievements and fellowships. He has been involved in the research and teaching for more than 15 years. His area of interest includes understanding the cellular and molecular biology of mosquito (malaria vector) innate immune responses during *Plasmodium* (malaria parasite) infection and Importance of peroxidases against *Plasmodium* and bacteria. He is also involved in the Identification of plant secondary metabolites and biopesticides to control vector population. He has published various research articles in peer reviewed international journals. He has been PI for the projects funded by DST, DBT and ICMR.

Distinguished Publications in:

1. **Kumar S**, Molina-Cruz A, Gupta L, Rodrigues J, Barillas-Mury C. **2010**. A Peroxidase/Dual Oxidase system modulates midgut epithelial immunity in *Anopheles gambiae*. **Science**. 327:1644-1648.

2. **Kumar S**, Gupta L, Han YS, Barillas-Mury C. **2004**. Inducible peroxidases mediate nitration of *Anopheles* midgut cells undergoing apoptosis in response to *Plasmodium* invasion. **Journal of Biological Chemistry**. 279:53475-53482.

3. **Kumar S,** Christophides GK, Cantera R, Charles B, Han YS, Meister S, Dimopoulos G, Kafatos FC, Barillas-Mury C. **2003**. The role of reactive oxygen species on *Plasmodium* melanotic encapsulation in *Anopheles gambiae*. **Proceedings of the National Academy of Sciences (PNAS) USA**. 100:14139-14144.

4. Gupta L, Molina-Cruz A, **Kumar S**, Rodrigues J, Dixit R, Zamora RE, Barillas-Mury C. **2009**. The STAT pathway mediates late-phase immunity against *Plasmodium* in the mosquito *Anopheles gambiae*. **Cell Host and Microbes** 5:498-507.

5. Kamhawi S, Ramalho-Ortigao M, Pham VM, **Kumar S**, Lawyer PG, Turco SJ, Barillas-Mury C, Sacks DL, Valenzuela JG. **2004**. A role for insect galectins in parasite survival: *Leishmania major* persists in its vector *Phlebotomus papatasi* through binding to PpGalec. **Cell**. 119: 329-341.

6. DeJong, RJ, Miller LA, Molina-Cruz A, Gupta L, **Kumar S**, Barillas-Mury C. **2007**. Reactive oxygen species detoxification by catalase is a major determinant of fecundity in the mosquito *Anopheles gambiae*. **Proceedings of the National Academy of Sciences (PNAS) USA**. 104:2121-2126.

Biography of Mithilesh Kajla

Mithilesh Kajla completed B.Sc. Biotechnology from Banasthali Vidyapith, Banasthali, Rajasthan in 2006 and M.Sc. Biotechnology in 2008 from Rajasthan Agricultural University (RAU) Bikaner, Rajasthan. She worked as JRF at Central Salt and Marine Chemicals Research Institute (CSMCRI), Bhavnagar, Gujarat (CSIR lab). She received 92 percentile in GATE 2009. She has cleared various national and state level examinations like CSIR/UGC-LS (NET) and RPSC-SET in 2013. She has been enrolled as Ph.D. student at Birla Institute of Technology and Science (BITS), Pilani, since Jan 2010. Her area of interest includes understanding the Importance of peroxidases in innate immune responses against *Plasmodium* and bacteria in *Anopheles*. She has been also involved in the identification of plant secondary metabolites to control vector population. She has published various research articles in well renowned international journals. She also received the first best poster award on "Characterization of *Anopheles* midgut immune peroxidase and their role in regulation of *Plasmodium* development" in XII International conference on Vector and Vector Borne Diseases, 2013 organized by NVBD Udaipur, Rajasthan, India. She has published 7 research articles, out of these 5 are in first author.